Universidad del País Vasco Euskal Herriko Unibertsitatea
BILBOKO INGENIARITZA ESKOLA
ESCUELA DE INGENIERÍA DE BILBAO

MASTER'S DEGREE IN

TELECOMMUNICATIONS ENGINEERING

MASTER'S THESIS

CHARACTERIZATION OF GRID IMPEDANCE VARIATIONS AND THEIR INFLUENCE ON NB-PLC IN THE FREQUENCY RANGE 10-500 kHz

Student *Jon González Ramos*
Co-director *Igor Fernández Pérez*
Co-director *Itziar Angulo Pita*
Department *Communications Engineering*
Academic Course *2020-2021*

Bilbao, 10th June 2021

Abstract

PLC *(Power Line Communications)* is a technology that uses the electrical grid as a means of communication. Although it has many advantages, as that the electrical grid is already deployed, the noises introduced by the different equipment connected to the network and the changing impedance of the grid can affect the communications. For that reason, in this work, the grid impedance is characterized and its influence on PLC is analyzed. The study is based on the calculation of two parameters: the attenuation suffered by the PLC signal and the FER-SNR curves that set the quality of communications. The objective of the project is achieved considering two kind of loads. On the one hand, static loads, that show resonances in some frequencies, but a constant impedance frequency responses over time and, on the other hand, dynamic loads, that present short-term impedance variations within the mains cycle.

Keywords: Power Line Communications, PRIME, grid impedance, transmission losses, EMC filters, short-term impedance variations.

Resumen

PLC *(Power Line Communications)* es una tecnología que utiliza la red eléctrica como medio de transmisión. Aunque tiene muchas ventajas, como que la red eléctrica ya está desplegada, los ruidos introducidos por los diferentes equipos conectados a la red y la impedancia cambiante de la misma pueden afectar a las comunicaciones. Por ello, este trabajo se centra en la caracterización de la impedancia de la red y en el análisis de su influencia en PLC. El estudio se basa en el cálculo de dos parámetros: la atenuación sufrida por la señal y las curvas FER-SNR que fijan la calidad de las comunicaciones. El objetivo del proyecto se consigue considerando dos tipos de cargas. Por un lado, las cargas estáticas, que presentan resonancias en algunas frecuencias, pero una respuesta frecuencial en impedancia constante en el tiempo y, por otro lado, las cargas dinámicas, que presentan variaciones de impedancia a corto plazo dentro del ciclo de la red.

Palabras clave: Power Line Communications, PRIME, impedancia de la red, pérdidas de transmisión, filtros EMC, variaciones de impedancia a corto plazo.

Laburpena

PLC *(Power Line Communications)* sare elektrikoa transmisio-bide gisa erabiltzen duen teknologia bat da. Nahiz eta abantaila asko eduki, hala nola sare elektrikoa dagoeneko zabalduta egotea, sarera konektatutako ekipoek sortutako zarata-elektromagnetikoek eta sarearen inpedantzia aldakorrak komunikazioei eragin diezaiekete. Horregatik, lan hau sarearen inpedantziaren karakterizazioan eta honek PLCn duen eraginan oinarritzen da. Azterlana bi parametroren kalkuluan oinarritzen da, seinaleak jasandako atenuazioan eta komunikazioen kalitatea ezartzen duten FER-SNR kurbetan, hain zuzen. Proiektuaren helburua bi karga elektriko mota kontuan hartuta lortzen da. Alde batetik, karga estatikoak, maiztasun batzuetan erresonantziak dituztenak, baina inpedantziaren maiztasun-erantzun konstantea dutenak denboran zehar, eta, bestetik, karga dinamikoak, epe laburrean inpedantzia-aldaketak dituztenak sarearen zikloaren barruan.

Gako-hitzak: Power Line Communications, PRIME, sare elektrikoaren inpedantzia, transmisio-galerak, EMC iragazkiak, epe laburreko inpedantzia-aldaketak.

Table of Contents

List of Figures

List of Tables

List of Acronyms

AC	Alternate Current
AGC	Automatic Gain Control
ARIB	Association of Radio Industries and Businesses
AWGN	Additive White Gaussian Noise
BB-PLC	Broadband PLC
BN	Base Node
CENELEC	Comité Européen de Normalisation Électrotechnique
CFR	Channel Frequency Response
DC	Direct Current
DPSK	Differential Phase Shift Keying
EUT	Equipment under Test
EMC	Electromagnetic Compatibility
EMI	Electromagnetic Interference
EVM	Error Vector Magnitude
FCC	Federal Communications Commission
FEC	Forward Error Correction
FER	Frame Error Ratio
FFT	Fast Fourier Transform
FWR	Full-Wave Rectifier
HDR	High Data Rate
HF	High Frequency
HWR	Half-Wave Rectifier
IGBT	Insulated Gate Bipolar Transistor
LDR	Low Data Rate
LISN	Line Impedance Stabilization Network
LPTV	Linear Periodic Time-Variant
LV	Low-Voltage
NB-PLC	Narrowband Power Line Communications
OFDM	Orthogonal Frequency Division Multiplexing
PLC	Power Line Communications

PPDU	Physical Protocol Data Unit
PRIME	PoweRline Intelligent Metering Evolution
RF	Radio Frequency
RSSI	Received Signal Strength Indicator
SCR	Silicon Control Rectifiers
SLF	Super Low Frequency
SN	Service Node
SNR	Signal to Noise Ratio
SS	Spread Spectrum
TC	Transformation Centre
TSR	Tratamiento de la Señal y Radiocomunicaciones
ULF	Ultra Low Frequency
UNB-PLC	UltraNarrowband PLC
VFH	Very High Frequency

1. Introduction

PLC (Power Line Communications) is a technology that uses the electrical grid as a transmission medium for communication signals. Its main advantage is the great extension of a network that it is already deployed, so that the costs of new network infrastructures are avoided. However, the electrical grid is not optimized for data transmission. The noise generated by the different devices connected to it together with the changing impedance of the medium can considerably degrade the communications [1].

PLC can be classified taking into account different criteria. Depending on the frequency range used, three technologies are considered: UltraNarrowband PLC, Narrowband PLC and Broadband PLC. This work is focused on Narrowband PLC, used by the electrical operators for communicating smart meters. In Europe, the allocation of this technology is currently limited to CENELEC (Comité Européen de Normalisation Électrotechnique) A band (3 – 95 kHz), whereas in other countries, it works up to 500 kHz. The transmission on higher frequency bands provides more bandwidth available, and less expected interferences than in lower frequencies.

This work focuses on PLC PRIME (PoweRline Intelligent Metering Evolution), a technology based on OFDM (Orthogonal Frequency Division Multiplexing) [2]. PRIME technology, nowadays an international standard known as ITU G.9904 [2], was developed by PRIME Alliance, chaired by Iberdrola. In the first version, PRIME v1.3.6, the basic characteristics of the technology were specified. The version 1.4 includes some improvements, such as robust modes and the possibility of using higher frequency channels, up to 500 kHz, leading to greater flexibility and higher data rates.

The main objective of this work is to analyze the impact of the grid impedance variations on NB – PLC according to PRIME version 1.4. For that purpose, different loads are studied under laboratory conditions. First, the influence of the introduction of EMC (Electromagnetic Compatibility) filters is discussed. These devices, which are used for electromagnetic interference suppression, show important frequency-dependent impedance variations, but these variations are constant over time. Second, the effects of different devices that present short-time impedance variations within the fundamental period are studied.

2. State of the art

2.1. Power Line Communications

Power Line Communications carry data signals on a conductor that is also used simultaneously for electric power transmission or electric power distribution to consumers. PLC can be classified considering different criteria: the type of electrical signal transmitted, DC (Direct Current) or AC (Alternate Current); the voltage of the signal (low, medium or high voltage); and, finally, the frequency band for transmission. The latter classification considers UNB-PLC (UltraNarrowband PLC), NB-PLC (Narrowband PLC) and BB-PLC (Broadband PLC) [1].

UNB-PLC, which operates in the frequency range between 30 Hz and 3 kHz, i.e., the SLF (Super Low Frequency) and ULF (Ultra Low Frequency) bands, allows a low bit rate of bps and a range of hundreds of kilometers. Its main use is focused on high-voltage teleprotection.

NB-PLC (3-500 kHz) are divided into LDR (Low Data Rate) and HDR (High Data Rate). The bitrate supported for LDR is in the order of kbps, whereas for HDR is up to 500 kbps. Telemetry and services in home networks and Smart Grids are the main applications, because of the low attenuation suffered in frequencies below 500 kHz [3]. The maximum range is of several kilometers, which can be extended by signal repeaters. NB-PLC use SS (Spread Spectrum) or OFDM modulations for trying to avoid potential degradations in communications related to the attenuation suffered by the signal, impedance variations or noise generated and introduced by different equipment connected to the grid.

Finally, BB-PLC, which use the HF (High Frequency) and VHF (Very High Frequency) bands (1.8-250 MHz), allow bitrates up to hundreds of Mbps with a similar range to NB-PLC. Similarly to NB-PLC, Broadband PLC use SS or OFDM modulations. It is considered a cost-effective alternative to xDSL broadband services. Home network services and carrier services are the most spread applications of this technology.

2.1.1. NB-PLC frequency allocation

The frequency allocation of Narrowband PLC depends on the geographical area. FCC (Federal Communications Commission) and FCES, in the United States of America and Canada respectively, allocate the frequency range between 0 kHz and 535 kHz to this technology. In Japan, ARIB (Association of Radio Industries and Businesses) defines the 10 – 450 kHz band, whereas in China its use is restricted to 3 – 500 kHz. Finally, in Europe, CENELEC, in addition to specifying the in-band and out-of-band voltage emission limits, allocates the frequency range between 3 kHz and 148.5 kHz, divided into the following four sub-bands [1].

- CENELEC A (3 – 95 kHz): used for monitoring and control of low voltage distribution applications.
- CENELEC B (95 – 125 kHz): used for any application. It does not require any access protocol.
- CENELEC C (125 – 140 kHz): used for homework systems. Uses CSMA/CD as access protocol.
- CENELEC D (140 – 148.5 kHz): main applications are security and alarm systems.

CENELEC allows a maximum power of 5 mW and bitrates up to 144 kbps with coverage distances of, approximately, 500 m. The bandwidth is only 86 kHz, which is very small compared to the bandwidth allocated by the FCC in the USA.

Figure 1 shows the frequency bands allocated by FCC and CENELEC, and Table 1 gathers a summary of the frequency bands allocated for each region and the corresponding standards organization.

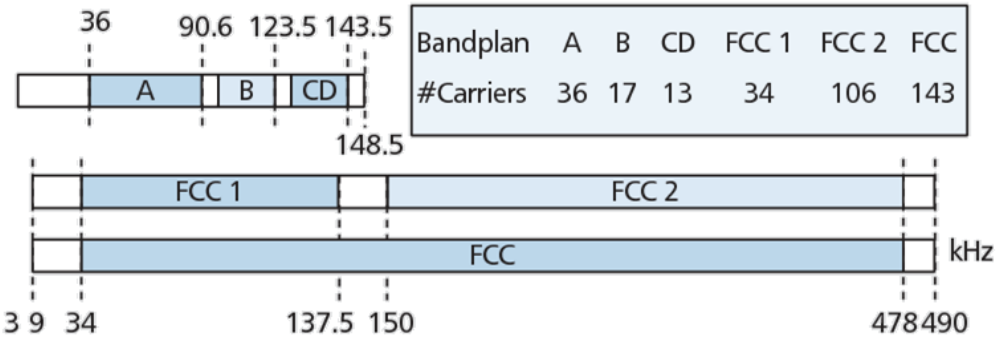

Figure 1. FCC and CENELEC frequency allocation [1]

Region	Organization	Frequency band (kHz)
Europe	CENELEC	3 – 148.5
Japan	ARIB	10 – 450
China	EPRI	3 – 500
USA	FCC	0 – 535
Canada	FCES	0 – 535

Table 1. Allocated frequency bands by the different organizations in the different regions

2.1.2. PLC PRIME v1.4

PLC PRIME is a technology designed for narrowband data transmission. Frequencies below 40 kHz show different problems in LV (low-voltage) networks: the colored noise is always present in the power grid due to the sum of different low-power noise sources, and a grid load less than 1 Ω might be seen by the transmitter [2]. For this reason, PLC PRIME v1.4 uses the frequency band between 41.992 kHz and 471.6796875 kHz, divided into eight independent channels. Channel 1 corresponds to the frequency band defined by the protocol version 1.3.6. Figure 2 shows the eight channels and their correspondence with the bands standardized by CENELEC in Europe, ARIB in Japan and FCC in the United States.

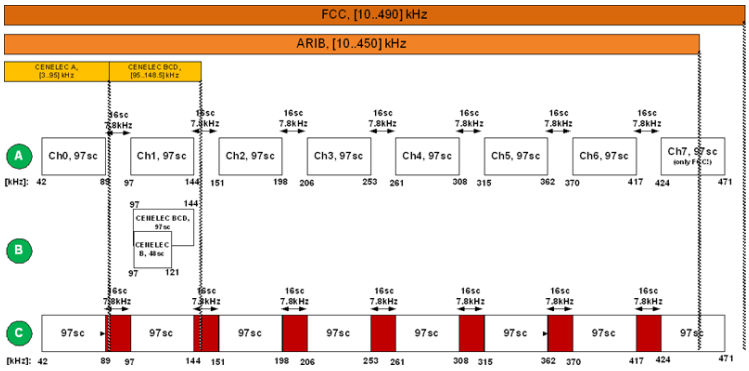

Figure 2. Channel frequency bands of PRIME v1.4

The physical layer of PLC PRIME is composed of a traditional OFDM layer, a cyclic prefix, orthogonally differentially coded subcarriers, a convolutional encoder, the preamble, the header and the payload [3].

OFDM modulation is chosen because of its ability to adapt to very common and unpredictable frequency selective channels and to achieve high spectral efficiencies with simple transceiver implementations. In addition, it is very robust to impulsive noise, due to the extended cyclic prefix and the use of FEC (Forward Error Correction). OFDM modulation is used, with 97 equally spaced subcarriers transmitted in 2240 μs symbols (102 μs are assigned to the cyclic prefix).

This technology uses DPSK (Differential Phase Shift Keying), offering three different constellations: DBPSK (binary), DQPSK (quaternary) and D8SPK (eight symbols). Version 1.3.6 considers these three modulations and the corresponding ones with FEC, i.e., DBPSK_C, DQPSK_C and D8PSK_C. Version 1.4, in addition to those mentioned for version1.3.6, allows the use of robust modulations, R_DBPSK and R_DQPSK, which introduce a repetition code with a factor of four.

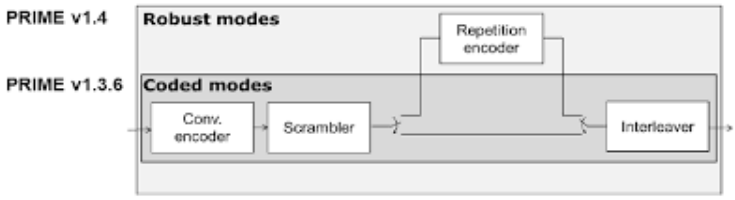

Figure 3. Coded and Robust modes for PRIME v1.3.6 and v1.4 [2]

Three frame types are considered: type A, type B and type BC. Type A, which is compatible with PRIME v1.3.6, starts with a preamble of 2.048 ms, followed by a number of OFDM symbols of 2.24 ms duration each. The first two symbols correspond to the frame header and are always sent using DBPSK with FEC, as repetition codes are not available. The remaining M symbols carry the payload, which may be modulated using DBPSK, DQPSK or D8PSK modulation, depending on the configuration selected by the MAC layer. This selection will be made on the basis of the number of errors in transmissions to the same receiver or using SNR (Signal to Noise Ratio) feedback. Thus, it is a dynamic configuration where the system itself chooses whether or not to use error correction codes. The number of symbols M included in the payload is indicated in the initial header, with a maximum value of 63. The structure of the type A frame is shown in Figure 4.

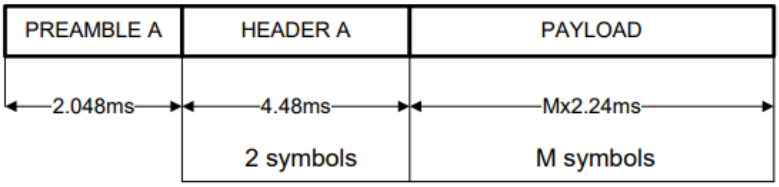

Figure 4. Structure of the type A frame [2]

The bit stream of the header and the payload and the location of the different pilot and data subcarriers of the type A frame are shown in Figure 5 and Figure 6.

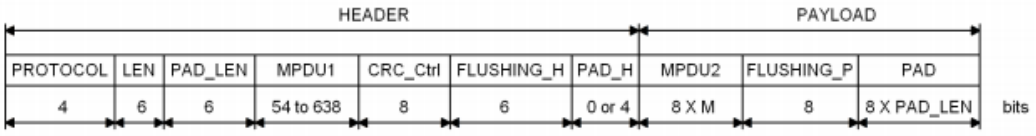

Figure 5. Bit stream of the header and the payload of a type A frame [2]

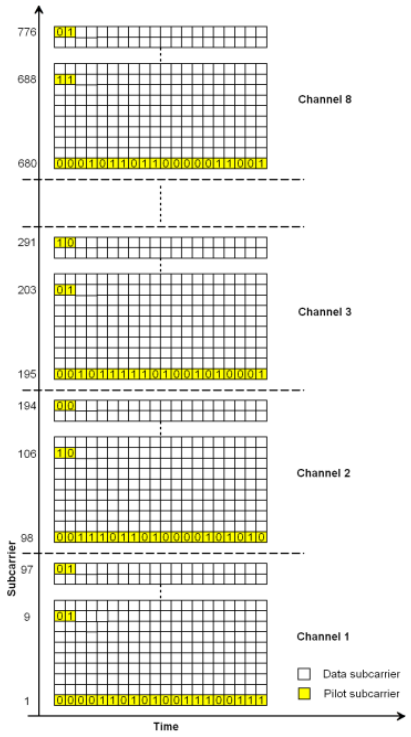

Figure 6. Location of the pilot and the data subcarriers in the different PRIME channels for a type A frame [2]

The type B frame, with a different structure from the type A frame as shown in Figure 7, starts with a preamble of 8.192 ms, four times longer than in type A frame. The symbol duration is 2.24 ms. The header consists of four OFDM symbols modulated with DBPSK, with FEC and repetition codes enabled. The number of symbols for the payload must be less than 252. Therefore, the length of the type B frame is much longer than a type A frame.

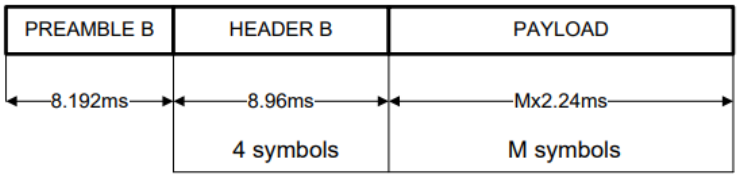

Figure 7. Structure of the type B frame [2]

The bit stream of the header and the payload and the location of the different pilot and data subcarriers of the type B frame are shown in Figure 8 and Figure 9.

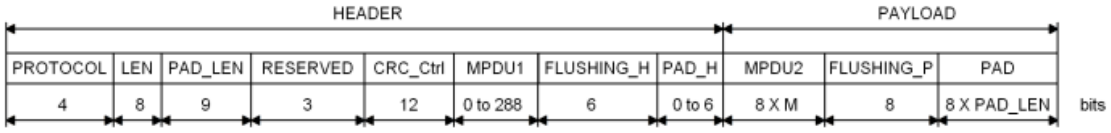

Figure 8. Bit stream of the header and the payload of a type B frame [2]

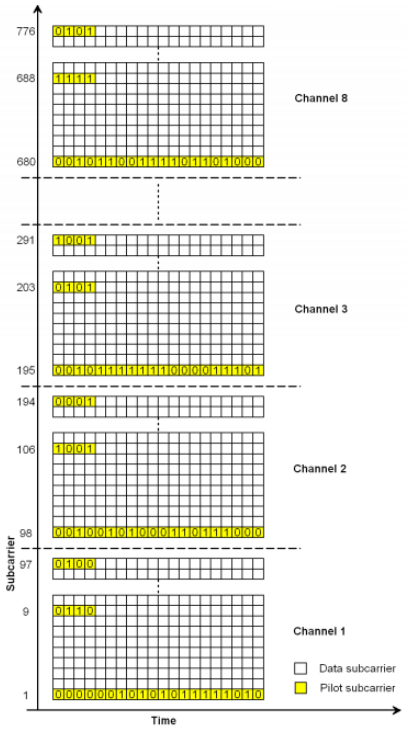

Figure 9. Location of the pilot and the data subcarriers in the different PRIME channels for a type B frame [2]

Since PRIME v1.4 is an extension of v1.3.6, it is necessary for the equipment to implement the new version to be able to operate in v1.3.6 homogeneous networks, v1.4 homogeneous networks and heterogeneous networks. In the latter, some of the devices connected to the network work with version 1.4 (they have robust modulations and type B frames), while others work with v1.3.6. This is the main reason for defining the BC frame, shown in Figure 10.

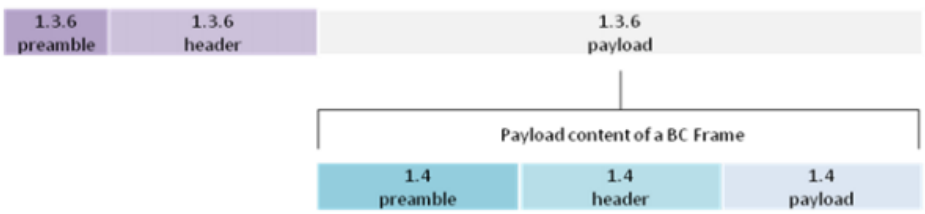

Figure 10. Structure of the type BC frame [2]

2.2. Characterization of the electrical grid as a transmission medium

As explained before, the electrical grid is not prepared for data transmission, as the power line cables are not originally designed to be used in communications and their characteristics change over time and frequency [4]. Besides, the PLC channel is affected in terms of impedance variation, attenuation, variable position of notches, signal distortions, channel capacity and noises introduced by the different equipment connected to the power grid [5] [6].

Connected unmatched and time variant equipment loads have a considerable impact on the PLC channel, as it is mainly dependent on the load characteristics. For that reason, an in-depth analysis of the equipment load impedance is necessary for a correct design of PLC systems [7]. In [7] and [8], it is shown that the access impedance is one of the major factors affecting in PLC. Moreover, in the frequency range 30-500 kHz, these access impedances are frequency dependent and time variant in some cases. Therefore, it is necessary to characterize the behavior of loads in time and frequency domains.

It is important to mention that, traditionally, only the long-term impedance variations, due to the connection or disconnection of the electric devices connected to the power grid, have been taken into account. However, some other works such as [9] show that there are also short-time impedance variations, periodic with the fundamental frequency, which involve a periodic time-varying channel frequency response.

Furthermore, in [6] and [10], it is stated that the electronic devices are the main sources of noise in the in-home PLC, especially when they are connected in the same power network of the receiver, due to the impedance changes that they introduce into the grid. If the load shows a short-time impedance variation, the noise is considered as cyclostationary. The results presented in the noise measurement campaign carried out in France [11], where noises at various locations and at different times are considered, show that the cyclostationary noise is dominant, because of the high number of loads connected to the electrical grid.

The impedance variations introduced by the different equipment modify the PLC channel frequency response. The highest attenuations are due to the switching ON/OFF equipment (sudden changes in loads) and the addition of new lines or customers [5]. Nevertheless, there is not an in-depth study where the PLC channel characteristics are analyzed. In [12], a statistical characterization of the channel is gathered for NB-PLC, whereas [13] and [14] analyze the frequency band between 30 kHz and 10 MHz. In all of them, experimental indoor low-voltage channel environments are considered for the study.

Therefore, it is fundamental to characterize the grid as a transmission medium in terms of frequency-dependent grid impedance, which is related to the channel frequency response and the noise due to NIEs (Non-Intentional Emissions).

For this purpose, some measurement campaigns have been carried out all around the world. In [15], the low voltage grid access impedance from 35 kHz to 500 kHz has been measured in three different scenarios, two urban and a rural, in the Basque Country (Spain). In each area, the grid impedance at the TCs (Transformer Station) and at a set of access points was analyzed, concluding that the urban distribution could be modeled as

a particular scenario of short cable sections and numerous homes. In [16], an urban/suburban area with low riser apartment buildings in China is considered, where apart from the access impedance, the attenuation and the NIEs in three buildings were measured in the frequency range 30-500 kHz. The results lead to conclude that the three phases show very low impedances. Besides, no long-term impedance variations are observed, obtaining similar impedance results in the measurements carried out at different times.

However, in field measurements it is not possible to differentiate the individual effects of the different loads connected to the grid, only the result of the combination of all of them. For that reason, this work aims at analyzing the influence of different kinds of loads in a controlled environment, so that their effect on attenuation and the quality of communications can be analyzed. Two types of impedances have been considered: static loads, which show resonances at some frequencies but a constant impedance frequency-response over time, and dynamic loads, which present short-time impedance variations within the 50 Hz fundamental cycle.

2.2.1. Static loads: EMC filters

Power electronics is a key technology for the efficient conversion, control and conditioning of electric energy from the source to the load. For the last decades, a wide adoption of energy-efficient power converters has been observed in several application fields such as buildings and lighting, power supplies, smart electricity grid (including integration of distributed renewable energy sources and electric vehicle), and industrial drives [17], [18].

However, the use of energy-efficient power converters implies some associated issues, including EMI (Electromagnetic Interference). Typical sources of interference are, for example, IGBT (Insulated Gate Bipolar Transistor) inverters for motor control and switched power supplies. Both devices generate voltages and currents with steep edges in their operation. For frequencies at hundreds of kHz, the interference is spread the same way as the power supply voltage, i.e., current flows in the loop formed by the phase and neutral conductors. Such noise is called differential-mode noise [19].

The use of passive filters is one of the most spread solutions for electromagnetic interference suppression [20]. An optimally-designed mains filter can perform a double function. First, the filter protects an electronic control circuit from voltage spikes in the mains supply, which may be generated, for example, by electromechanical switches and relays. Simultaneously, the same filter also acts in the opposite direction, attenuating the interference generated in the unit towards the power supply line.

However, the use of EMC filters might also lead to an undesired effect on NB-PLC signals. Due to the parallel and/or series resonances of EMC filters, notching effects can affect communication signals, which are more likely to be disturbed when the output impedance of the filter is low in comparison with the impedance of the grid [21].

It is well known that common low voltage electrical cables are designed with low impedance in order to reduce the losses associated with energy delivery. Moreover, the connection of electrical devices to the grid results in an access impedance that is dependent on location and variable in time [22], [23]. The introduction of EMC filters,

thus, might become an additional source of impedance mismatch between NB-PLC equipment and the electrical networks.

2.2.2. Dynamic loads: Short-time impedance variations

In [24], several measurements have been carried out in the low voltage distribution grid, connecting the measurement equipment as close as possible to the house connection box. The results show that, as described in [16], the grid access impedance is not variable in the long term, that is, it is stable over long periods of time. However, the behavior of some devices is not linear and varies within the period of the fundamental frequency [6], [9], due to the switching operations. These impedances are known as LPTV (Linear Periodic Time-Variant) loads.

Although in some field measurements these kind of impedances have been found, most of the loads that are connected to the electrical grid do not present short-time impedance variations, due to the EMC filters embedded in the circuitry of the modern electronic devices [6]. LPTV loads can be divided into two types taking into account their behavior during the mains cycle. The first group is composed of those loads whose impedance exhibits two different states and abrupt transitions between them, usually due to the SCR (Silicon Control Rectifiers). Low-power lamps, light dimmers, electric shavers and electric blankets show this type of impedance behavior. They vary within the 20 ms cycle with a repetition rate of 100 Hz. The second group, where monitors, microwave ovens, vacuum cleaners or coffee machines can be found, presents smoother time variations in the impedance behavior. In this case, the repetition rate is 50 Hz [9].

Therefore, it is important to mention that some studies have been carried out identifying which devices show a short-time variant impedance and how they affect PLC channel characteristics. However, the potential effects on the quality of NB-PLC have not been analyzed yet.

3. Objectives

The main objective of this work is to analyze the impact of grid impedance variations on NB-PLC according to PRIME v1.4. In order to achieve this main objective, a number of partial objectives have been defined:

- To define and validate a methodology to analyze the impact of impedance variations on PRIME PLC, considering the frequency bands defined in v1.4.
- To select and characterize electrical devices that introduce static and short-time impedance variations in the grid in the frequency band of interest.
- To analyze the attenuation suffered by the PRIME PLC signals due to loads with static and time-varying impedance characteristics in the different frequency bands.
- To evaluate the potential quality degradation of PRIME PLC due to changes in the channel frequency response caused by loads with static and time-varying impedance characteristics.

4. Methodology

4.1. General description and metrics

The main objective of this work is to analyze the influence of the impedance variations on NB-PLC, using both static loads and loads whose impedances vary within the cycle of the fundamental frequency. For that purpose, two indicators have been calculated.

First, signal attenuation due to the load under test is obtained. This attenuation is calculated as the difference of the modulus of the channel frequency response when the corresponding load is connected to the setup and the modulus of the channel frequency response when no load is connected.

Second, FER (Frame Error Rate), i.e., the ratio of frames received with errors to total frames received, is calculated and then represented as a function of SNR in the receiver. A frame is defined as a set of OFDM symbols and Preamble, which constitute a single PPDU (Physical Protocol Data Unit) [2]. SNR indicates how many dB is the signal power higher than the noise. This parameter can be modified in two different ways: varying the signal power level and varying the noise power level. In this work, only the power of the signal is reduced, keeping a fixed level of background noise. The SNR threshold for a FER of 5% is calculated for comparison purposes, as this FER is the acceptability limit for narrowband PLC [25].

4.2. Measurement setup

The methodology is based on controlled trials in a laboratory scenario by means of hardware equipment and software for post-processing of the recorded data. As shown in Figure 11, the setup is composed of: three LISN (Line Impedance Stabilization Network), which are in charge of isolating the setup from the power grid; different attenuators; a PLC evaluation kit, which includes a transmitter and a receiver; and a signal generator to include a fixed level of AWGN (Additive White Gaussian Noise).

The transmitter and the receiver are connected at the EUT (Equipment Under Test) port of the first and third LISN, respectively, whereas the RF ports are interconnected in order to provide a communication path for the NB-PLC signals. The different loads to be evaluated are connected at either point A, point B or point C in order to test the influence of a device connected near to the transmitter, in the communication channel or near to the receiver, respectively.

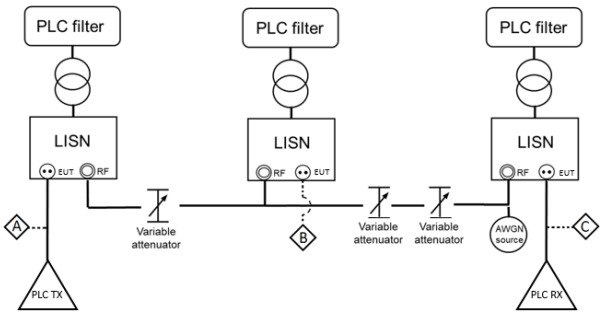

Figure 11. Measurement setup

4.2.1. LISN

As previously mentioned, the setup is composed of three LISNs. The main function of a LISN is to provide a precise impedance to the power input of the EUT. It also prevents the high-frequency noise of the power source from coupling into the system and provides a RF (radio frequency) noise measurement port. In our trials, the RF port acts as the communication channel for the NB-PLC signals.

In the measurement setup, the electric supply of the LISNs includes a PLC filter to avoid external communication signals to interfere with the tests, and a transformer for safety purposes. The LISN model used in the setup, whose characteristic impedance is 2 Ω, was designed according to the definition included in the PRIME specification [2]. Figure 12 shows the spectral variation of the actual characteristic impedance of the LISN, measured by the impedance measurement system described in Section 4.3.3.

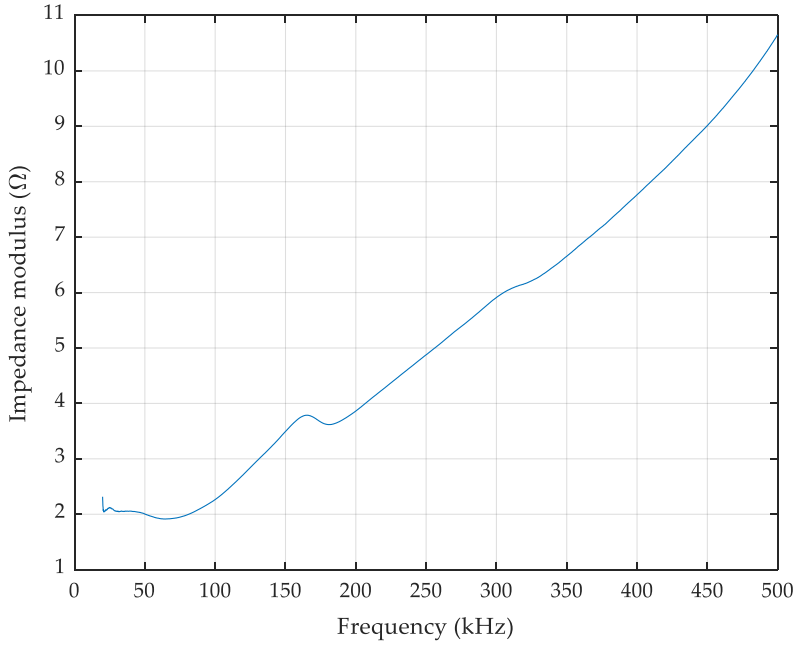

Figure 12. Measured impedance modulus of the LISN model for the frequency band of interest

4.2.2. Microchip PL360G55CF-EK evaluation kit

PLC according to PRIME v1.4 standard are established by means of a Microchip PL360G55CF-EK evaluation kit, composed of two transceivers, in such a way that one is configured to act as a transmitter and the other acts as the receiver in a point-to-point link. Each device has two cables: a micro A/B-type USB cable, to connect the board to a laptop that acts as a controller and that powers it, and a power cord cable, which allows the board to be connected to the point of frame transmission-reception.

Figure 13. Microchip PL360G55CF-EK evaluation kit

These devices can be configured by means of three different programs. First, PLC Sniffer, which is designed to sniff out packets from the different devices connected to the same network. Second, Microchip PRIME Manager, which also offers the Sniffer option and enables the assignment of the SN (Service Node) or BN (Base Node) function to each board. Finally, Microchip PLC PHY Tester Tool establishes PLC PRIME and G3-PLC communications and provides information about the reception quality. Only the data to start one of the three previously mentioned software can be loaded into the board at a time. The loading process is done by the terminal emulator "Tera Term".

Throughout this work, Microchip PLC PHY Tester Tool is used. The parameters to be configured in the Microchip PLC PHY Tester Tool are detailed below. First, those to be selected only in the transmitter are indicated, and then those to be chosen in the same way in the transmitter and the receiver. The configurations selected for the laboratory trials are detailed in Section 4.6.1.

The Microchip transmitter offers different options for the following parameters: *Channel, Frame Type, Modulation Scheme, Attenuation Level* and *Transmission Mode.*

- The *Channel* parameter allows to select one of the eight PRIME v1.4 channels.
- The *Frame Type* configuration offers the following options: *Type A/PRIME v1.3.6, Type B* (version 1.4) and *Type BC* (backwards compatible frame).
- If Frame Type A is selected (PRIME version 1.3.6), six options for *Modulation Scheme* are available: DBPSK, DQPSK and D8PSK without and with FEC. For Type Frame B, eight options for *Modulation Scheme* are available: DBPSK, DQPSK and

D8PSK with and without FEC, R_DBPSK and R_DQPSK (which include FEC and a repetition by four).

- The *Attenuation Level*, represented in dB, is variable between 0 and 21 dB.
- *Transmission Mode* is related to the output impedance of the transmitter. This field has four options: *Low, Very Low, High* and *Auto*. In addition, for each of the impedance options, the possibility of activating the AGC (Automatic Gain Control) is permitted. Its function is to maintain constant the output signal amplitude, regardless of variations in the input signal. Thus, the dynamic range is considerably reduced.

Figure 14 presents the software's interface where the previously mentioned parameters have to be configured.

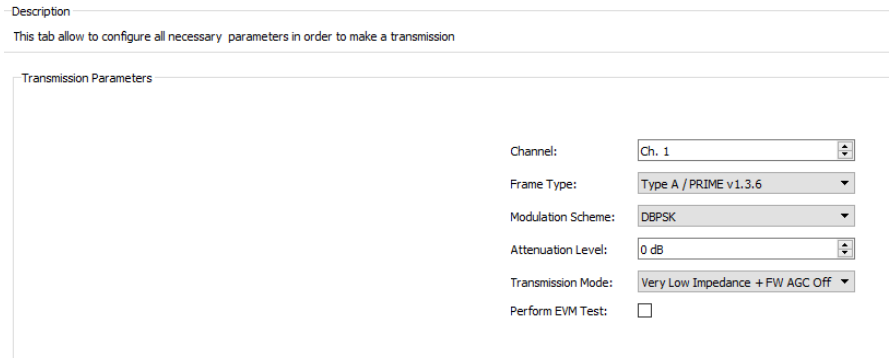

Figure 14. Parameters to be configured in the transmitter

Apart from the parameters to be configured in the transmitter, there are some parameters to be set in the transmitter and in the receiver. If, due to an error, the two devices were not equally configured, communication would not be correctly established.

- *Time Interval (ms)*, in milliseconds, specifies the separation between two frames.
- *Number of Frames* specifies the number of frames that the transmitter must send.
- *Message* specifies the data to be sent in the frames.

The following figure shows the parameters to be selected, in the same way, in the transmitter and the receiver.

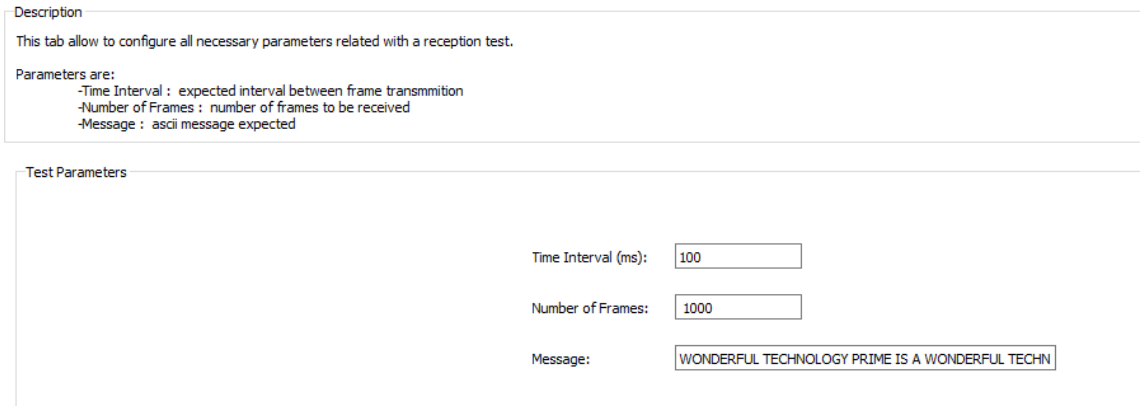

Figure 15. Parameters to be modified in the same way in the transmitter and in the receiver

The receiver, for each of the frames, shows information that allows to evaluate the quality of the communications. For that purpose, five parameters are used: *RSSI* (Received Signal Strength Indicator), *SNR* (Signal to Noise ratio), *EVM* (Error Vector Magnitude), the *received message* and *Payload Integrity*.

- *RSSI* represents the received signal level in dBuV. It varies according to the configuration of the transmitted signal, attenuation and impedance mismatching effects.
- *SNR* measures how many dB is the signal power higher than the noise power. Therefore, its value increases if the power of the transmitted signal is increased or if the power of the noise is decreased. However, Microchip devices calculate SNR as the inverse value of the EVM plus 3 dB, as specified in PRIME 1.4 standard [2]. EVM, normally used to evaluate the performance of a transmitter, indicates the difference between the ideal points and the real points in the IQ constellation.
- The *received message* field shows the message decoded for each of the received frames.
- *Payload Integrity* indicates whether the frame has been correctly received or not (*Ok* or *No Ok*).

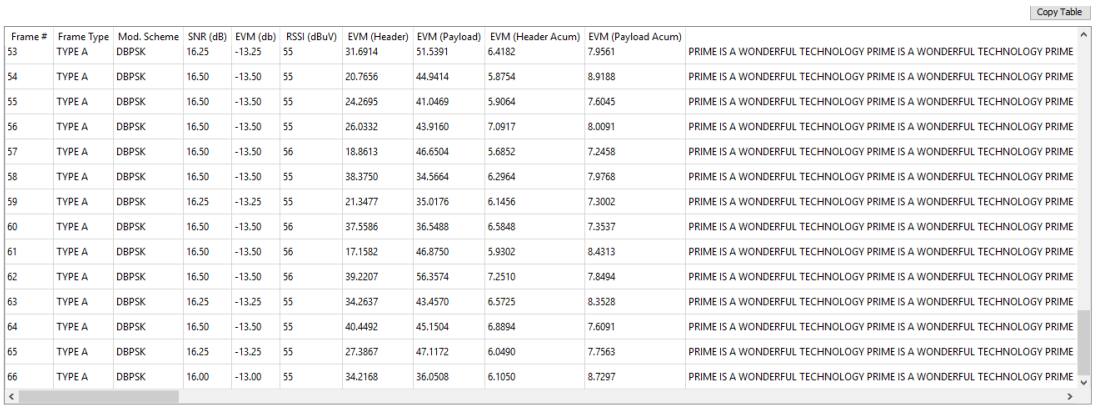
Copy Table

Frame #	Frame Type	Mod. Scheme	SNR (dB)	EVM (db)	RSSI (dBuV)	EVM (Header)	EVM (Payload)	EVM (Header Acum)	EVM (Payload Acum)	
53	TYPE A	DBPSK	16.25	-13.25	55	31.6914	51.5391	6.4182	7.9561	PRIME IS A WONDERFUL TECHNOLOGY PRIME IS A WONDERFUL TECHNOLOGY PRIME
54	TYPE A	DBPSK	16.50	-13.50	55	20.7656	44.9414	5.8754	8.9188	PRIME IS A WONDERFUL TECHNOLOGY PRIME IS A WONDERFUL TECHNOLOGY PRIME
55	TYPE A	DBPSK	16.50	-13.50	55	24.2695	41.0469	5.9064	7.6045	PRIME IS A WONDERFUL TECHNOLOGY PRIME IS A WONDERFUL TECHNOLOGY PRIME
56	TYPE A	DBPSK	16.50	-13.50	55	26.0332	43.9160	7.0917	8.0091	PRIME IS A WONDERFUL TECHNOLOGY PRIME IS A WONDERFUL TECHNOLOGY PRIME
57	TYPE A	DBPSK	16.50	-13.50	56	18.8613	46.6504	5.6852	7.2458	PRIME IS A WONDERFUL TECHNOLOGY PRIME IS A WONDERFUL TECHNOLOGY PRIME
58	TYPE A	DBPSK	16.50	-13.50	55	38.3750	34.5664	6.2964	7.9768	PRIME IS A WONDERFUL TECHNOLOGY PRIME IS A WONDERFUL TECHNOLOGY PRIME
59	TYPE A	DBPSK	16.25	-13.25	55	21.3477	35.0176	6.1456	7.3002	PRIME IS A WONDERFUL TECHNOLOGY PRIME IS A WONDERFUL TECHNOLOGY PRIME
60	TYPE A	DBPSK	16.50	-13.50	56	37.5586	36.5488	6.5848	7.3537	PRIME IS A WONDERFUL TECHNOLOGY PRIME IS A WONDERFUL TECHNOLOGY PRIME
61	TYPE A	DBPSK	16.50	-13.50	56	17.1582	46.8750	5.9302	8.4313	PRIME IS A WONDERFUL TECHNOLOGY PRIME IS A WONDERFUL TECHNOLOGY PRIME
62	TYPE A	DBPSK	16.50	-13.50	56	39.2207	56.3574	7.2510	7.8494	PRIME IS A WONDERFUL TECHNOLOGY PRIME IS A WONDERFUL TECHNOLOGY PRIME
63	TYPE A	DBPSK	16.25	-13.25	55	34.2637	43.4570	6.5725	8.3528	PRIME IS A WONDERFUL TECHNOLOGY PRIME IS A WONDERFUL TECHNOLOGY PRIME
64	TYPE A	DBPSK	16.50	-13.50	55	40.4492	45.1504	6.8894	7.6091	PRIME IS A WONDERFUL TECHNOLOGY PRIME IS A WONDERFUL TECHNOLOGY PRIME
65	TYPE A	DBPSK	16.25	-13.25	55	27.3867	47.1172	6.0490	7.7563	PRIME IS A WONDERFUL TECHNOLOGY PRIME IS A WONDERFUL TECHNOLOGY PRIME
66	TYPE A	DBPSK	16.00	-13.00	55	34.2168	36.0508	6.1050	8.7297	PRIME IS A WONDERFUL TECHNOLOGY PRIME IS A WONDERFUL TECHNOLOGY PRIME

Figure 16. Parameters related to communication quality provided by the receiver

4.2.3. Signal generator Keysight 33500B Series

The trials carried out should not be affected by the characteristics of noise. If no additional source of noise was included to the setup, the only source of noise would be the internal noise of the receiver, i.e., the noise which is generated internally within the receiver. This kind of noise cannot be characterized and it might have frequency-dependent characteristics. Moreover, under real scenarios, the level of noise of the LV network is always higher than the internal noise of the receiver, which is considered to be negligible. Therefore, in order to provide a fixed, low level of noise, and flat in terms of frequency, AWGN is injected into the RF port of the third LISN. The level of injected AWGN is higher than the internal noise of the receiver, so that the tests are not affected by the noise of the communication device.

In order to inject AWGN noise, a Matlab file including random samples is loaded into a Keysight 335000B Series signal generator and steadily reproduced.

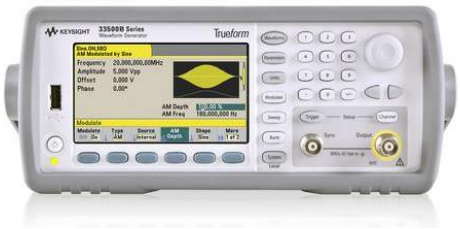

Figure 17. Keysight 33500B Series signal generator

4.2.4. Attenuators

In this work, as mentioned above, the level of background noise is kept fixed. For that reason, it is necessary to decrease the signal level to obtain the different points that make up the FER-SNR curves by means of external attenuators. In our scenario, three variable attenuators are connected to the RF outputs of the LISNs. The first one, between A and B, and the second one, between B and C, are 110 dB attenuators (a 100 dB roulette with a 10 dB increment and a 10 dB roulette with a 1 dB increment). The last one, connected between B and C, introduces a maximum attenuation of 1 dB with steps of 0.1 dB. The variable attenuator located between the first and the second LISN is fixed at 3 dB, except when it is not possible to reach a FER of 5%. In that case, a 2 dB attenuation is selected.

The two first attenuators, called 50DR-001, and the third one, AS-SMA-2.5-2-1, are presented in Figure 18.

Figure 18. Attenuators 50DR-001 (left) and AS-SMA-2.5-2-1 (right)

4.3. Measurement systems

4.3.1. Channel Frequency Response measurement system for static channel conditions

The equipment and methodology for the channel frequency response measurements for static channel conditions are based on the system presented in [26]. The system described here is an improved version of the previous system, where an ad-hoc signal is injected instead of a NB-PLC signal. Therefore, the characterization is performed for the whole frequency range of interest, without frequency gaps.

The channel frequency response measurement system calculates the transmission losses, in modulus and phase, between two electrical points, P1 and P2. The channel frequency response is calculated as the difference between the level of the signal injected at point P1 and the level of the signal measured at point P2 as a function of frequency. Between these two points, there can be a controlled environment, as the one presented in this work, or a section of the real low voltage network. Figure 19 shows the measurement system for the channel frequency response.

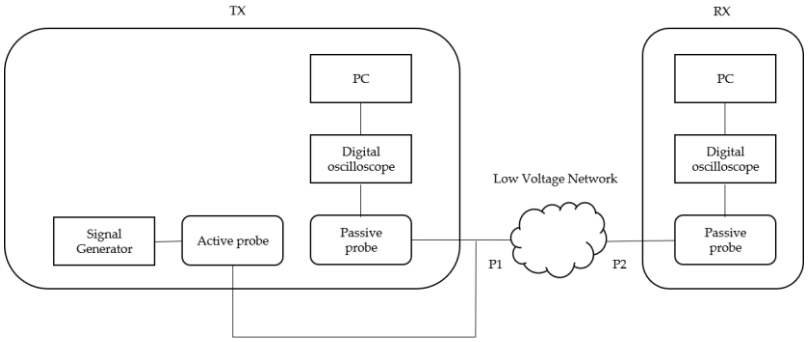

Figure 19. Measurement system for the assessment of the channel frequency response for static channel conditions

The system is composed of three voltage probes, two of them connected at point P1, and one at point P2. One of the probes connected at point P1 is an active probe [27], which is responsible for injecting a sweep in the frequency range 5 – 530 kHz and for filtering the 50 Hz signal of the network, so that it does not affect the signal generator. The second probe located at point P1 is a passive probe, which decouples the injected signal from the grid in order to measure its actual level. Finally, the probe located at point P2 decouples the received signal. Voltage measurements are digitized with two high-resolution oscilloscopes with a sampling resolution of 16 bits. A dedicated software in the laptop configures and processes the oscilloscope recordings following these three main steps: signal windowing, Fourier analysis and attenuation assessment.

First, a sliding windowing in time is applied to the recorded voltage values. More precisely, a rectangular window with a 1/50 s duration is used with 93% of overlapping between consecutive windows. Afterwards, a FFT (Fast Fourier Transform) is performed using the above-mentioned parameters. Besides, data processing procedure includes a

Signal to Noise ratio adjustment when the power of the recorded signal is not 10 dB higher than the recorded noise power.

4.3.2. Channel Frequency Response measurement system for variable channel conditions

The channel frequency response measurement system for variable channel conditions calculates the time-varying transmission losses, in modulus and phase, between two electrical points, P1 and P2, during a cycle of the fundamental frequency. As the previously explained measurement system, the channel frequency response is calculated as the difference between the level of the injected signal at P1 and the received signal at P2. Figure 20 shows the channel frequency response measurement system during the cycle of the fundamental frequency.

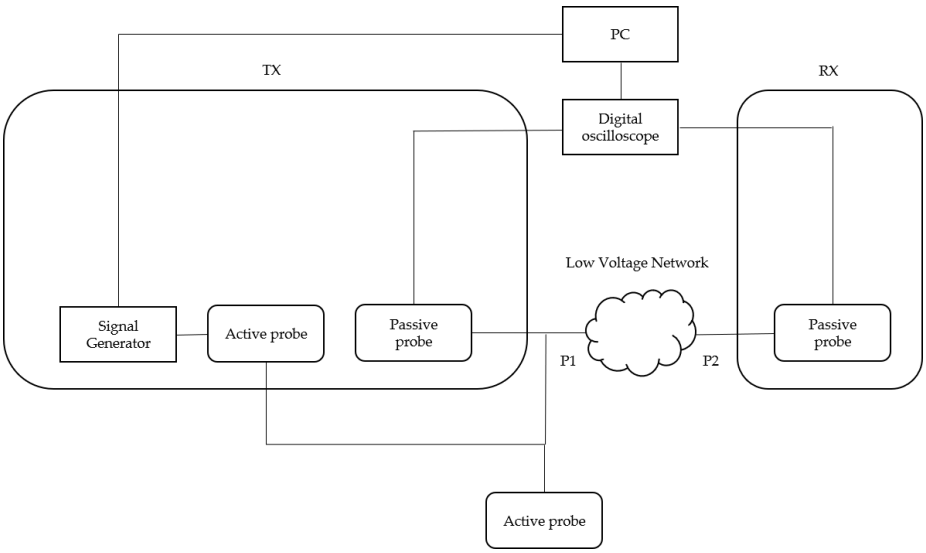

Figure 20. Measurement system for the assessment of the channel frequency for variable channel conditions

The system is composed of four voltage probes: three of them connected in P1, and one in P2. One of these probes is used for measuring the 50 Hz reference signal, in order to be able to analyze 20 ms intervals.

The signal generator, controlled by means of a Matlab script, is the responsible for transmitting bursts of 90 ms from 6 kHz to 507 kHz with 3 kHz steps. In order to stablish a guard period so that the frequencies are not mixed, a gap of 10 ms between two consecutive bursts is fixed. From each 90 ms burst, the first and the last 20 ms are disregarded and only 20 ms are taken into account. In order to know the beginning of these 20 ms to be analyzed, the instant where a maximum of the signal is located and 5 ms are added, so that a zero of the signal is taken.

For the signal post-processing, a sliding windowing with a 1/3000 s duration and an overlapping of 75 % between consecutive windows is applied, so that the frequency resolution is 3 kHz.

4.3.3. Impedance measurement system for static channel conditions

The impedance measurement system, shown in Figure 21, calculates the impedance as the ratio between a voltage and a current over a well-characterized reference impedance.

In order to do so, a signal generator is responsible for injecting a sweep of 10 Vpp with a duration of 1 s, covering the whole frequency band between 5 kHz and 530 kHz. The signal generator is connected to a current probe, which injects the transmitted signal into the circuit by means of the magnetic field induced in the wire.

As it is shown in Figure 21, a 560 nF capacitor is connected to the branch of the circuit where the signal is injected. Therefore, it can withstand the 50 Hz and a low impedance is seen at the frequencies of interest.

The impedance measurement system calculates the impedance as the ratio between the voltage V and the current I_3 shown in Figure 21. It has to be mentioned that the network voltage $V_N$is negligible with respect to the injected signal at the frequency band of interest. The other two current probes allow to measure the currents $I_1$and I_2. Thus, applying the Kirchhoff's first law, I_3 is obtained. Since the network impedance to be measured is in parallel with a well-characterized reference impedance, composed of a resistor (100 Ω) and a capacitor (560 nF) in series, the voltage across both impedances is the same. Therefore, the voltage V can be calculated as the product of the impedance composed of the resistor and capacitor, previously measured with a precision LCR meter in the whole analyzed frequency band, and the current I_2.

Three channels of the oscilloscope are used. The channel A is connected to the second probe, where I_1 current is measured, while the channel B is connected to the third probe, where I_2 is measured. The channel C is connected to the signal generator, in order to stablish synchronization between both equipment, so that a faster processing is achieved.

For the signal processing, a sliding windowing with a 20 ms duration and a 2 ms separation between consecutive Gaussian windows is applied.

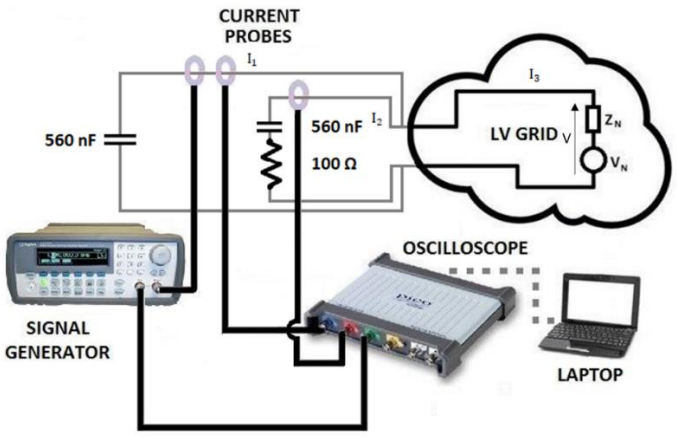

Figure 21. Impedance measurement system for static channel conditions

4.3.4. Impedance measurement system for variable channel conditions

The impedance measurement system shown in Figure 22 allows to measure short-time impedance variations. It is very similar to the impedance measurement system presented in Figure 21, where the impedance was calculated as the ratio between the voltage V and the current I_3. The only difference lies in that the signal generator is controlled by means of a Matlab script, instead of using the *Sweep* option. As explained in Section 4.3.2, bursts of 90 ms from 6 kHz to 507 kHz with 3 kHz steps are injected into the circuit, analyzing only one fundamental period of the signal, that is, 20 ms. The same process followed in the channel frequency response measurement system for variable channel conditions is used for determining the beginning of the 20 ms interval.

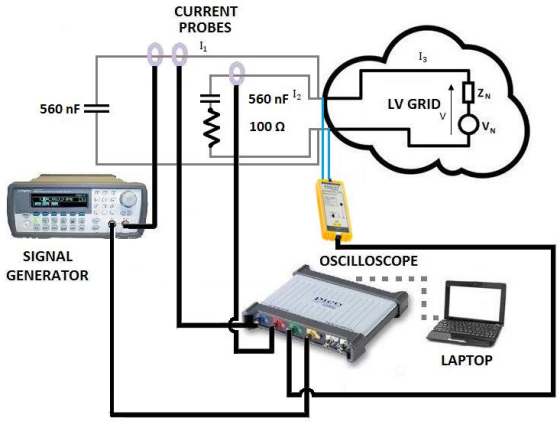

Figure 22. Impedance measurement system for variable channel conditions

4.3.5. Non-Intentional Emissions measurement system

The NIEs measurement system, shown in Figure 23, is based on a voltage probe connected to the electrical point where the noise will be measured. The digital oscilloscope, controlled by a laptop, is the responsible for recording the signal. Subsequently, a signal processing is performed, according to the CISPR 16-1-1 standard [28].

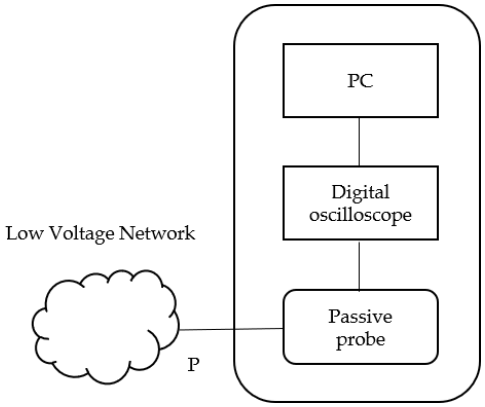

Figure 23. Measurement system for Non-Intentional Emissions

4.4. Loads under test

4.4.1. EMC filters

In this work, four EMC filters have been used, designed according to IEC 60939 – Passive filters for suppressing electromagnetic interference [29], whose characteristics are shown in Table 2. The schematics and component values are shown in Figure 24 and Table 3. The references of these filters are 5500.2044, 5500.2052, 5500.2055 and 5500.2060 [30].

	Description	Rated current	Leakage current	Applications
5500.2044	2-stage line filter, high attenuation	6 A	< 0.5 mA (standard version)	Suitable for use in equipment according to IEC/UL 62368-1
5500.2052	2-stage line filter, very high attenuation, broadband	2 A	0.25 mA (standard version)	Suitable for use in equipment according to IEC/UL 62368-1 Especially suitable for use in switching power supplies e.g. in electronic designs with high repetitive switching frequency
5500.2055	2-stage line filter, very high attenuation, broadband	6 A	1.4 mA (industrial version)	Suitable for use in equipment according to IEC/UL 62368-1 Especially suitable for use in switching power supplies e.g. in electronic designs with high repetitive switching frequency
5500.2060	2-stage line filter, very high symmetrical and asymmetrical attenuation	6 A	0.25 mA (standard version)	Suitable for use in equipment according to IEC/UL 62368-1 Especially designed for industrial applications such as: Frequency Converters, Stepper Motor Drives, UPS-Systems, Inverters Especially suitable for use in switching power supplies

Table 2. Characteristics of the four EMC filters [30]

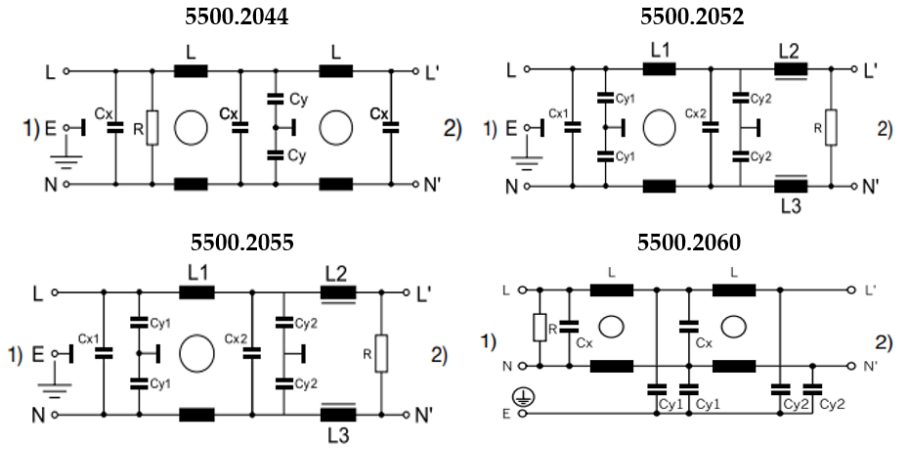

Figure 24. Schematics of the four EMC filters: 5500.2044 (upper left), 5500.2052 (upper right), 5500.2055 (bottom left), 5500.2060 (bottom right)

EMC filter	L (mH)	R (MΩ)	Cx (µF)	Cy (µF)	Cx1 (µF)	Cx2 (µF)	Cy1 (µF)	Cy2 (µF)	L1 (mH)	L2 (mH)	L3 (mH)
2044	2 x 0.8	0.5	100	4.7	-	-	-	-	-	-	-
2052	-	1	-	-	0.1	0.47	1.5	1	2 x 10	0.4	0.4
2055	-	1	-	-	0.1	0.68	10	4.7	2 x 6	0.5	-
2060	2 x 0.8	1	0.1	1.5	-	-	1.5	1	-	-	-

Table 3. Components of the four EMC filters [30]

The four EMC filters show a wide range of impedance values along the PLC frequency band, mainly due to the resonance effects they cause at specific frequencies. Their frequency-dependent impedance, in terms of magnitude and phase, are presented in the figures below. These impedances are obtained offline, that is, without connecting the filters to the measurement setup using the impedance measurement system described in Section 4.3.3.

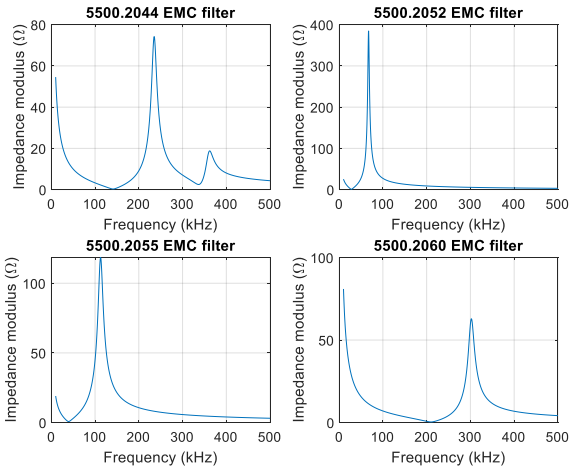

Figure 25. Modulus of the four EMC filters under study

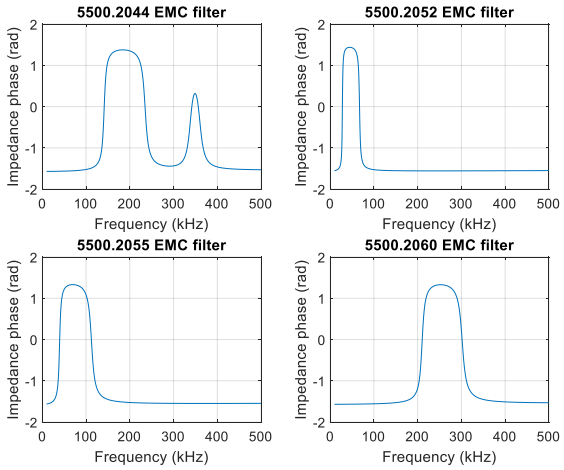

Figure 26. Phase of the four EMC filters under study

4.4.2. Time-variant loads

Many electronics devices connected to the electrical grid consist of a rectifier circuit with a DC link capacitor [31]. During the recharge period of the capacitor, it gets connected to the network, modifying the impedance seen from the measurement point. The diode opens and closes every half cycle of the fundamental cycle. Thus, the network impedance is changed twice between two different states, as shown in Figure 27.

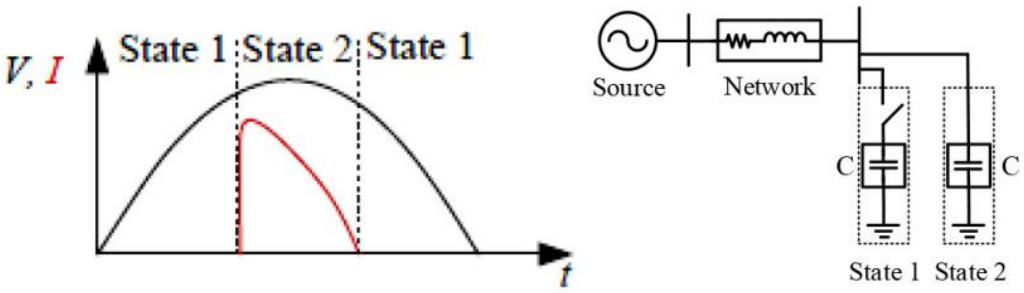

Figure 27. Different states and equivalent circuit of a rectifier circuit [31]

Depending on the rectifier configuration, i.e., whether a single diode or a diode bridge is used, the current pulse appears one or two times during the 20 ms fundamental period. If the rectifier is composed of a four diode bridge, that is, a FWR (Full-wave rectifier), the current pulse appears every half cycle, 100 Hz frequency, when two of the four diodes are in conduction state [6]. The Figure 28 shows the equivalent circuit and the output rectified waveform of the FWR.

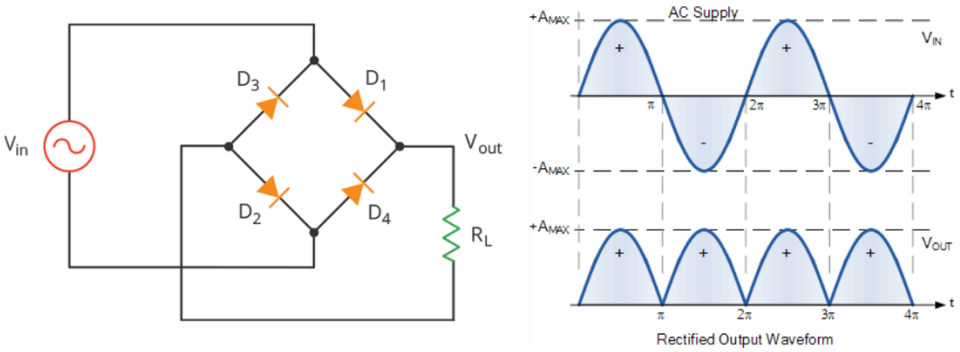

Figure 28. Equivalent circuit and output rectified waveform of a Full-wave rectifier

If a unique diode is used, HWR (Half-wave rectifier), the current pulse appears once every positive or negative cycle of the signal (50Hz), when the diode is conducting [6]. Figure 29 shows the equivalent circuit and the output rectified waveform of a Half-wave rectifier.

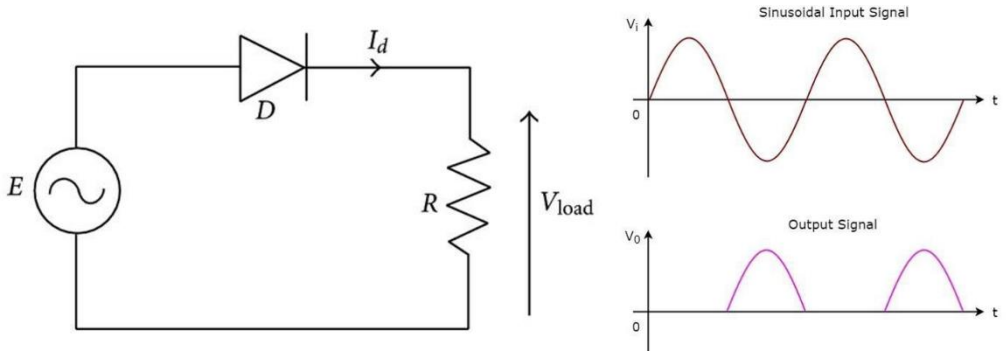

Figure 29. Equivalent circuit and output rectified waveform of a Half-wave rectifier

In order to study the influence of time-variant impedances, first, a selection of equipment that includes rectifiers in its circuitry is needed. However, as presented in [6], the number of loads that show a short-time impedance variation is lower than expected, due to the noise suppression capacitors and EMC filters embedded in the household electronic devices. In this way, unwanted harmonics on the input current are minimized. The modulus and phase of the impedances that fulfill time-variant conditions are shown in Section 6.1.3: a set of LEDs, a safety razor, a hair removal razor, hair clippers, the charger of a Nokia mobile phone and an alarm clock. In Annex III – Time-variant loads an impedance database of the different electronic devices measured is shown.

4.5. Methodology validation

This section presents the different tests carried out to determine the appropriate scenario of measurements to achieve the previously mentioned objectives.

4.5.1. Validation of the attenuation measurements system

The characterization of the attenuation suffered by the PLC signal due to the introduction of the different loads to the setup is one of the partial objectives of the work. For that purpose, the attenuation is measured in two different ways, using the channel frequency response measurement system designed in TSR (Tratamiento de la Señal y Radiocomunicaciones) and the RSSI offered by the Microchip receiver board, in order to have a reliable measurement system.

On the one hand, using the channel frequency response measurement system, the CFR (Channel Frequency Response) without a filter and for the four filters available is measured. Results are obtained by connecting the filters on the EUT port of LISN 1 (A), LISN 2 (B) and LISN 3 (C). The attenuation of each filter is calculated as the difference of the channel frequency response when a filter is connected and the channel frequency response in a configuration where no filter is connected.

$$\text{Filter attenuation} = \text{CFR with filter connected} - \text{CFR without filter connected}$$

On the other hand, using the configuration selected in the previous section, i.e. a LISN impedance of 2 Ω and a Low output transmitter impedance, the RSSI in the different channels is measured, when no filter is connected and when each filter is introduced into the setup. The attenuation is obtained for each of the configurations, as the

difference between the RSSI with and without filter. Initially, results were obtained for channels 1, 2, 4 and 8 with the AGC configuration activated. However, due to the possible influence of this parameter on the results, the measurements were repeated for all PRIME channels without AGC.

$$\text{Filter attenuation} = \text{RSSI with filter connected} - \text{RSSI without filter connected}$$

The results obtained by both methods are superimposed, in order to compare them in a simpler way. It is important to mention that no external attenuators are used in either case.

The following two figures present the modulus of the channel frequency response when no filter is connected to the measurement system and the attenuation of the 5500.2044 connected at A using both methods. In addition, the table shows the average attenuation and standard deviation within each channel (using the CFR measurement system) and the attenuation obtained through the RSSI for this same configuration.

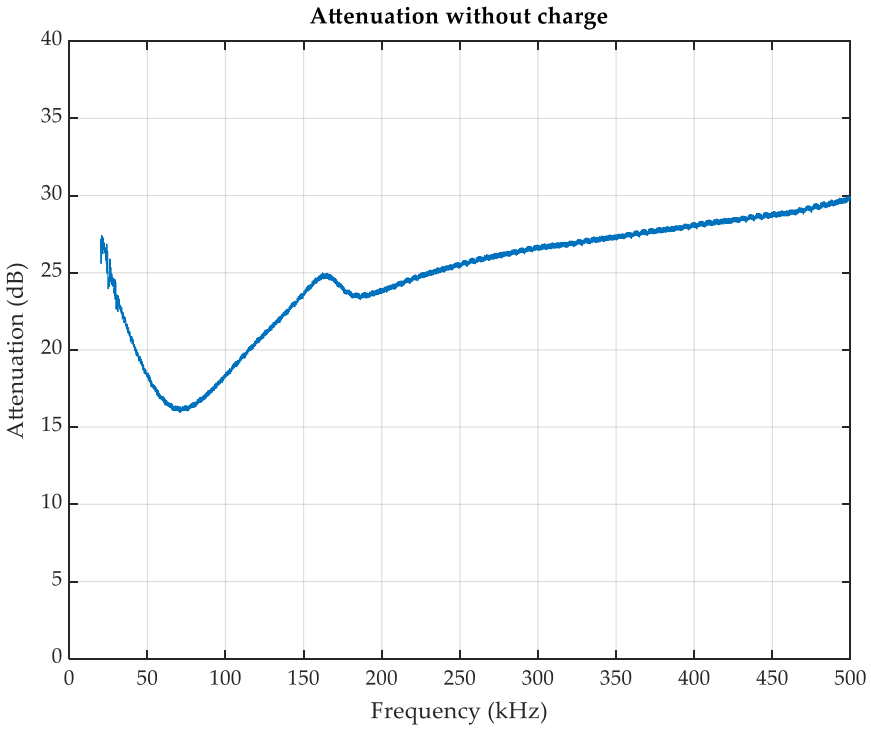

Figure 30. Attenuation of the whole system without charge connected

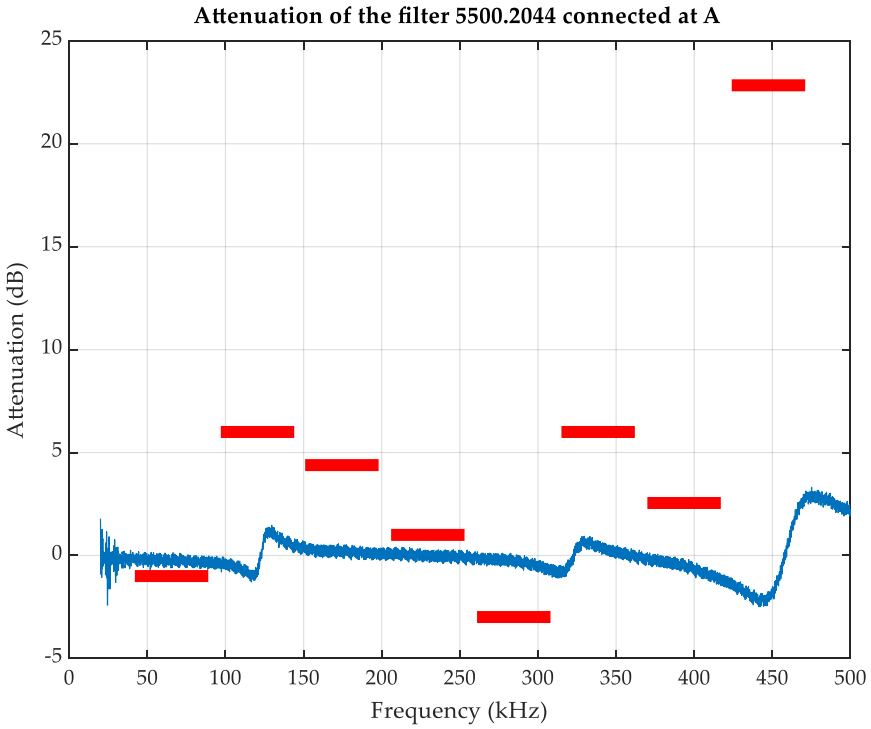

Figure 31. Attenuation of the 5500.2044 filter connected at A using both attenuation measurements system

Channel	Mean Attenuation (dB)	Standard deviation (dB)	Attenuation using RSSI (dB)
CH 1	-0,25	0,18	-1,00
CH 2	0,01	0,76	6,00
CH 3	0,19	0,18	4,39
CH 4	0,00	0,17	1,00
CH 5	-0,32	0,23	-2,99
CH 6	0,16	0,42	6,00
CH 7	-0,56	0,33	2,55
CH 8	-0,76	1,62	22,84

Table 4. Mean attenuation and standard deviation of each channel using the attenuation measurement system and the RSSI when filter 5500.2044 is connected at A

As the results show, the attenuations measured using the different methods are not similar. Therefore, taking into account that the attenuation measured by the RSSI offers only a constant value for each channel and that the measurement system allows us to conclude that the attenuation varies with frequency even within the same channel, the results presented during this work will be obtained by the channel frequency response system developed in TSR. These variations within each frequency channel are of real interest in our analysis.

4.5.2. Validation of the attenuators

Although the Microchip boards have an attenuation parameter for the transmitted signal, it was decided not to use it and to connect three attenuators at the RF port of the different LISNs. Their characterization is important in order to ensure that any possible degradation of the FER-SNR curves is exclusively due to the introduction of EMC filters or variant loads within the 50 Hz cycle. Therefore, it is necessary to know the real attenuation introduced by the attenuators and the possible impedance variations produced by them.

The analysis of the possible influence on the setup is carried out by comparing, firstly, the attenuation provided by the channel frequency response measurement system when the attenuators are not connected and when they are connected but no attenuation is introduced. In addition, the possible variations in the channel produced by modifying the attenuation level are studied. The trials presented in this section do not include the connection of any load to the system.

The following figure shows the channel frequency response measured without attenuators and with the attenuators at 0 dB.

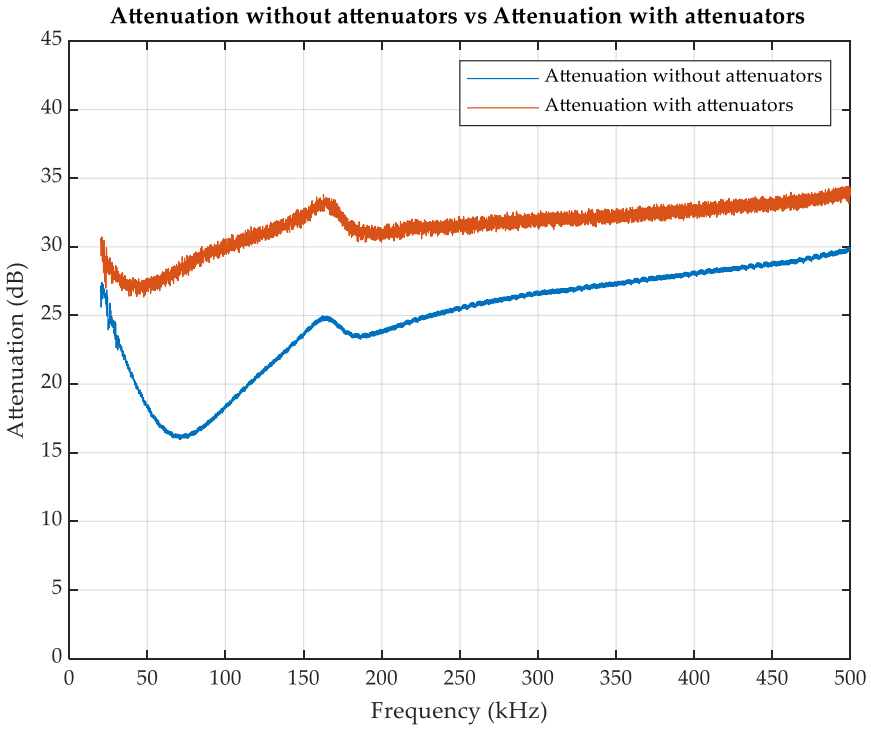

Figure 32. System channel frequency response with and without attenuators when no load is connected

Consequently, the introduction of the attenuators in the system leads to an increase in attenuation, shown in Figure 33.

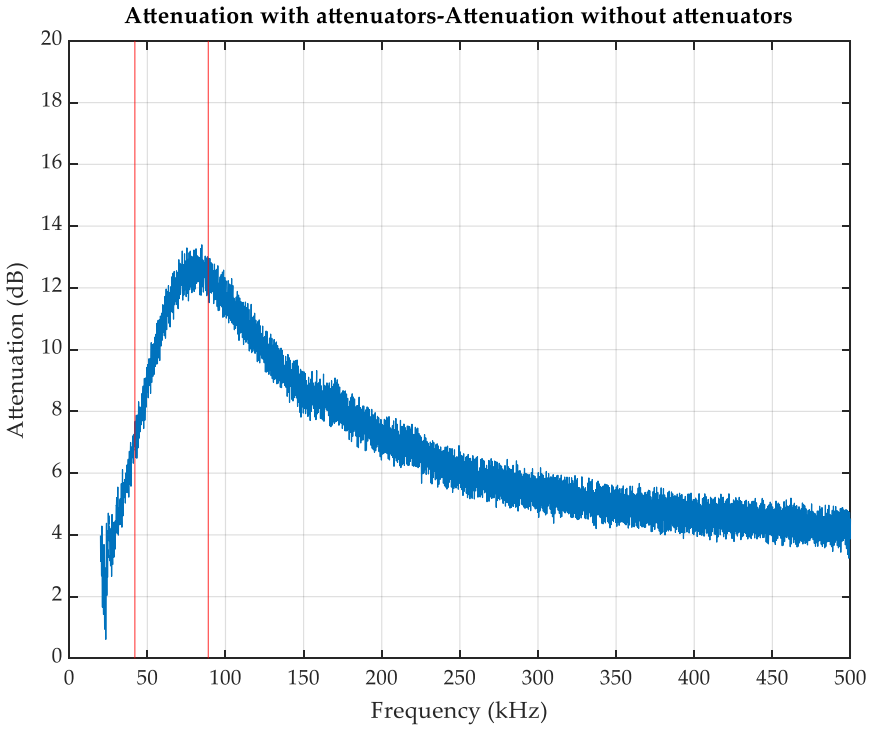

Figure 33. Difference between the attenuation measured in the system with and without attenuators

The vertical lines indicate the beginning (42 kHz) and the ending (89 kHz) of the channel 1 of PRIME, where, as it can be seen, the attenuation is highly variable within the channel. Therefore, the frequency response of the channel is affected by the introduction of the attenuators in the system.

The distortion, calculated as the difference of the maximum and the minimum attenuation within a frequency channel, is shown in the next table.

Attenuation with attenuators-Attenuation without attenuators			
Channel	**Minimum Att.**	**Maximum Att.**	**Distortion (dB)**
CH 1	6.48	13.40	6.91
CH 2	8.29	12.58	4.28
CH 3	6.68	9.32	2.65
CH 4	5.28	7.77	2.49
CH 5	4.57	6.54	1.97
CH 6	4.20	5.92	1.72
CH 7	3.77	5.55	1.78
CH 8	3.61	5.22	1.61

Table 5. Medium distortion within each PRIME frequency channel

Figure 34 shows the difference in system attenuation if the attenuation value introduced is varied. For example, the orange curve represents the difference when the attenuation is 5 dB (3 dB the first, 2 dB the second and 0 dB the third attenuator) and

when it is at 4 dB. In principle, in this case, a horizontal line at 1 dB should be expected. However, the attenuation difference is approximately 4 dB in the whole frequency band.

The attenuation suffered by the signal does not introduce variations in the FER-SNR curves, as long as it is flat over the frequency range, as it happens in this case. Therefore, if the attenuators introduce attenuations different from those selected, it only means that a different point of the curve will be obtained.

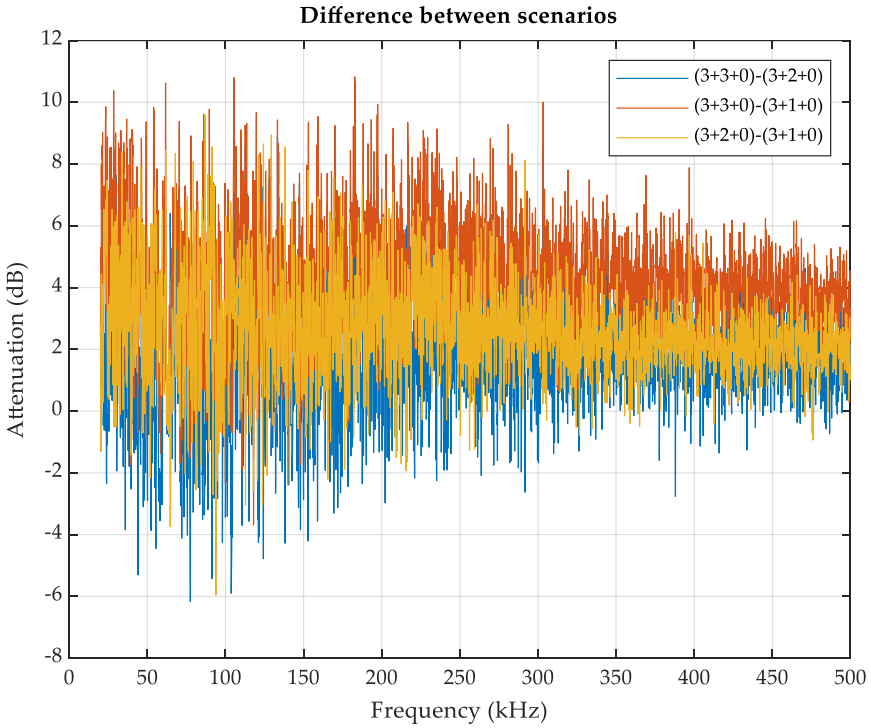

Figure 34. Difference in attenuation due to the variations in the attenuators

Thus, it can be concluded that only the introduction of the attenuators, not the variation of their attenuation value, introduces changes in the channel frequency transfer function. However, these may not be critical enough to affect communications. To check this, the FER-SNR curves are represented with and without attenuators at 0 dB, in order to observe whether they introduce degradations. In this second case, the different points of the curve are obtained by fixing the attenuation of the Microchip Evaluation Kit at 21 dB and varying the amplitude of the white Gaussian noise introduced with the signal generator.

Table 6 shows the SNR for a FER of 5 %, in a configuration without attenuators and when they are connected but no attenuation is introduced. In this way, the possible variations obtained can be quickly and easily appreciated. For most of the measured configurations, SNR values for a 5 % of FER are not available. For that reason, they are obtained by a linear approximation using the following formula.

$$y_x = y_0 + \frac{x - x_0}{x_1 - x_0} \cdot (y_1 - y_0)$$

In the formula, x corresponds to the 5 % FER obtained (0.05 when entered in it) and x_0 and x_1 are the FER value immediately below and above available to the 5 % FER. y_x corresponds to the SNR associated to the FER of 5 % and y_0 and y_1 to the SNR values associated to x_0 and x_1.

SNR (dB) for FER = 5 %		
Channel	**With Att.**	**Without Att.**
CH 1	11.02	10.98
CH 2	11.94	10.34
CH 3	10.51	10.09
CH 4	9.93	10.68
CH 5	10.18	10.22
CH 6	10.52	10.53
CH 7	10.01	9.95
CH 8	11.00	10.59

Table 6. Comparative of the SNR thresholds for a FER of 5 % without attenuators and with attenuators at 0 dB

If all eight channels are taken into account, the maximum difference is 1.59 dB. However, none of the modules of the Microchip boards are prepared to transmit on channel 2. Therefore, if channel 2 is disregarded, the difference would decrease to 0.75 dB, which could be due to the fact that the trials carried out are based on hardware. Thus, it could be concluded that the introduction of the attenuators in the system does not influence the communications.

4.6. Summary of performed tests

4.6.1. Configuration of the transmitter and receiver

As described in Section 4.2.2, the Microchip transmitter offers different options for the following parameters: *Channel, Frame Type, Modulation Scheme, Attenuation Level* and *Transmission Mode.* Apart from the parameters to be configured in the transmitter, there are some parameters to be set in the transmitter and in the receiver: *Time Interval (ms)*, *Number of Frames* and *Message.*

The *Channel* parameter allows you to select one of the eight PRIME v1.4 channels. However, as mentioned above, the specifications of the Microchip boards, as shown in the following figure, indicate that the module of the board is not prepared to transmit on channel 2.

Board Name	Description	Frequency Band (kHz)	Branch	Electrical Isolation	PRIME Channel	G3-PLC Band	Applicable Regulation
PLCOUP011-ISO	Dual PRIME / G3 for CENELEC A and FCC bands	35 - 91 151-472	Double	Yes	1, 3, 4, 5, 6, 7 and 8	G3 CENELEC A and FCC	CENELEC EN 50065

Figure 35. PRIME channels supported by each communication module of the Microchip boards [32]

For the *Frame Type* configuration, in all the trials, *Type B* is selected, the one used in version 1.4 of the PRIME specification, since version 1.3.6. is not originally defined to work in the frequency band up to 500 kHz.

Regarding *Modulation Scheme,* different options are selected for the laboratory trials, in order to test their robustness for the different channel conditions.

The *Attenuation Level* is set to 0 dB, because external attenuators placed in the measurement setup are used when the transmitted signal level has to be reduced, as the external attenuators are capable of offering higher values of attenuation (110 dB + 110 dB + 1 dB).

Finally, *Transmission Mode* is related to the output impedance of the transmitter. This field has four options: *Low, Very Low, High* and *Auto.* This parameter involves considerable variations in the level of the actually transmitted signal. Therefore, its influence in the established communications is studied in detail.

In order to analyze how the configuration of the transmitter output impedance affects the received signal level, the RSSI is measured in different configurations, varying the transmitter output impedance as High, Low or Very Low. The Auto option offered by the boards is not used.

The transmitter and the receiver are connected to the EUT port of the LISN 1 and the LISN 3, respectively. In this scenario, no external attenuators are used and a DBPSK modulation, frame Type B, 256 byte message, time interval of 100 ms and a transmission of 1000 frames are selected. In addition, AGC is activated.

In order to obtain the average RSSI in each configuration, the RSSI measured in dBuV associated to each frame is converted to linear, averaged and transformed back to logarithmic. The standard deviation is directly calculated with the logarithmic values of each frame.

The obtained results are presented below.

Transmission Mode	PRIME channel	Mean RSSI (dBuV)	St. Deviation RSSI
High	1	94.00	0.07
Low	1	102.00	0.00
Very low	1	102.00	0.00
High	2	93.01	0.13
Low	2	101.00	0.00
Very low	2	101.00	0.00
High	4	93.99	0.17
Low	4	100.08	0.27
Very low	4	100.26	0.43
High	8	86.01	0.19
Low	8	98.00	0.00
Very low	8	97.99	0.11

Table 7. Mean and standard deviation of the RSSI for different impedance configurations of the transmitter and for different PRIME channels

On the one hand, the received signal is much lower if a High impedance is used. However, there is practically no difference between selecting a Low or Very Low impedance. Consequently, considering the results, it is decided to use a configuration with Low output impedance.

With respect to *Time Interval (ms),* modulation schemes with higher robustness require more time to correctly decode the received frames. In case the time indicated is not enough, the reception process is timed out and the frame is lost. In this work, for the least robust modulations used, that is, DBPSK, DQPSK_C and DBPSK_C, a value of 100 ms is indicated. R_DQPSK, by contrast, needs at least a 200 ms interval, while R_DBPSK requires 300 ms.

For configuring *Number of Frames,* it should be taken into account that, according to [33], the number of sent messages shall be at least 500 for each measurement of FER. In our case, for a certain measurement setup and signal configuration, 1000 frames are sent from the transmitter. The minimum FER that can be taken as a reference is two orders of magnitude higher than the inverse of the number of frames transmitted, i.e., 0.1 (10 %). However, as it can be seen on following sections, in all the curves represented in this work the threshold for 0.05 (5 %) are taken, as this FER is the acceptability limit for narrowband PLC [25].

Finally, the *Message* parameter is a 256 bytes length message, as specified in [25].

5. Results - Static loads

Regarding the channel frequency response measurements, first, the channel frequency response when no device under test is connected is measured as a reference, covering the whole frequency range of interest. Then, with the objective of evaluating the influence of the location of the filters, the channel frequency response is measured when each EMC filter is connected in the EUT port of each of the three LISNs. The trials are carried out for the two configurations of the EMC filters: an open-circuit configuration, i.e., when no external load is connected to the filter in L'-N' [34] [35], and a loaded configuration, when a passive load composed of a 50 resistor connected in series with a 560 nF capacitor is connected in L'-N'.

In regard to the potential effects of EMC filters on NB-PLC systems, and starting from a reference in which no device under test is connected to the setup, the FER-SNR curves are represented for seven communication channels as defined by PRIME v1.4 specification. Then, FER-SNR curves are obtained for the four EMC filters under test connected at Points A, B and C and for the two configurations mentioned above.

Finally, five modulations from PRIME v1.4 specification are considered in order to analyze their robustness against channel variability: DBPSK, DBPSK_C, DQPSK_C, R_DBPSK and R_DQPSK.

5.1. Impedance variations due to the EMC filters

Figure 36 and Figure 37 show the impedance measured at the EUT port of the first LISN when the different filters are connected at this same point in the open-circuit configuration. For that purpose, the impedance measurement system described in 4.3 has been used [26].

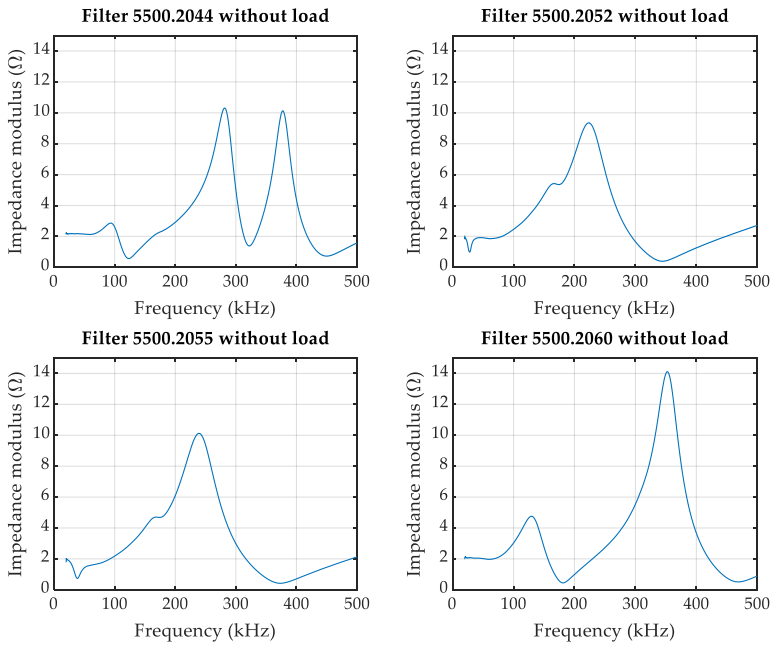

Figure 36. Impedance modulus of the four EMC filters connected to the setup

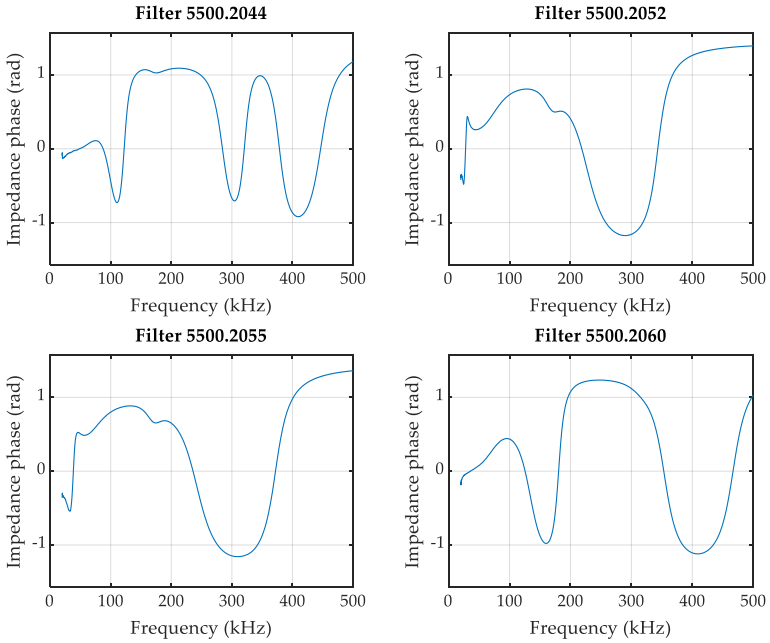

Figure 37. Impedance phase of the four EMC filters connected to the setup

Similarly, Figure 38 and Figure 39 show the impedance of each EMC filter when connecting L-N ports to the setup and L'-N' to the load.

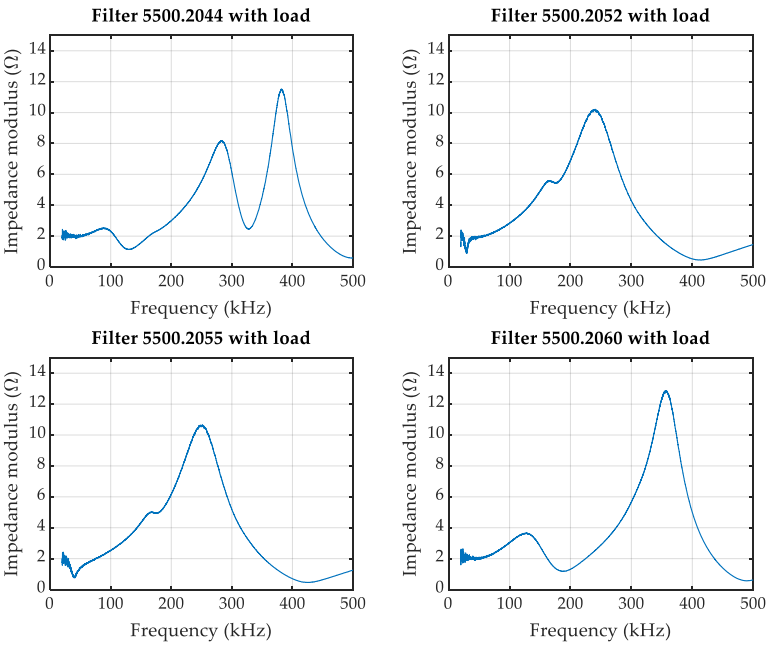

Figure 38. Impedance modulus of the four EMC filters connected to the setup, when a load is connected in L'-N'

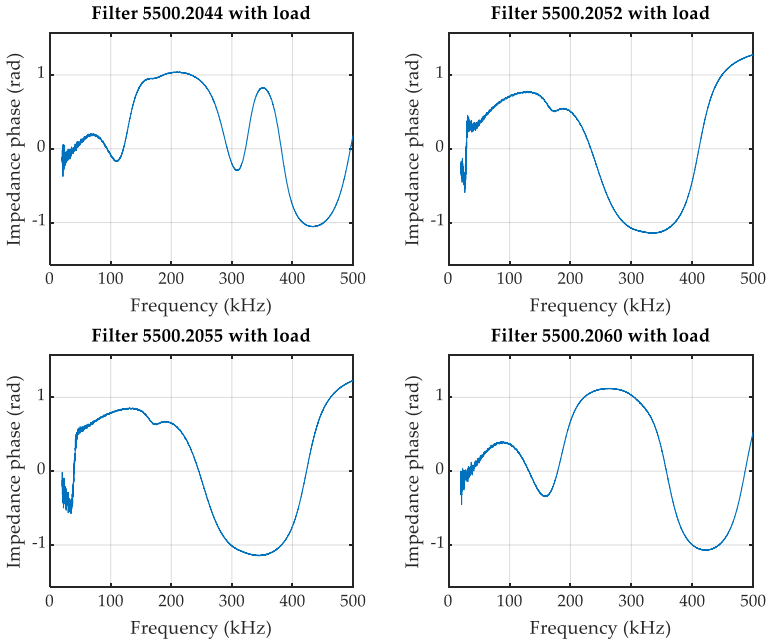

Figure 39. Impedance phase of the four EMC filters connected to the setup, when a load is connected in L'-N'

As it can be seen, the EMC filters introduce important impedance variations within the frequency band of interest for both configurations (with and without load). The variations shown in Figure 36 are the result of the combination of the impedance of each EMC filter and the components of the LISN (Figure 12), as it is noticeable if compared to the offline impedance measurement of the filters found in the Section 4.4.1 and in [35].

Table 8 and Table 9 gather the mean value and the standard deviation of the impedance measured when the EMC filters are connected to the setup, calculated for seven communication channels defined in [2], for the open-circuit and the loaded configurations respectively. The statistical characterization of the impedance is provided as an estimation in order to relate the characteristics of the impedance with the attenuation suffered by the PLC signal and the potential degradation of the communications on each communication channel.

	Impedance modulus of 5500.2044 (Ω)		**Impedance modulus of 5500.2052 (Ω)**		**Impedance modulus of 5500.2055 (Ω)**		**Impedance modulus of 5500.2060 (Ω)**	
Channel	**Mean**	**Standard Deviation**	**Mean**	**Standard Deviation**	**Mean**	**Standard Deviation**	**Mean**	**Standard Deviation**
CH 1	2.35	0.50	1.91	0.11	1.58	0.23	2.08	0.16
CH 3	2.33	0.40	5.43	0.49	4.82	0.44	1.06	0.61
CH 4	4.66	0.90	9.39	0.75	9.15	1.19	2.11	0.49
CH 5	8.27	2.21	4.86	1.35	5.33	1.61	4.69	0.92
CH 6	3.11	1.69	1.57	0.49	1.55	0.53	11.26	2.27
CH 7	6.89	2.85	0.44	0.08	0.49	0.09	5.06	2.09
CH 8	0.94	0.43	1.04	0.20	1.17	0.20	0.99	0.40

Table 8. Mean and standard deviation of the modulus of the impedance measured when EMC filters are connected to the setup

	Impedance of 5500.2044 + load (Ω)		Impedance of 5500.2052 + load (Ω)		Impedance of 5500.2055 + load (Ω)		Impedance of 5500.2060 + load (Ω)	
Channel	Mean	Standard Deviation	Mean	Standard Deviation	Mean	Standard Deviation	Mean	Standard Deviation
CH 1	2.21	0.18	2.15	0.20	1.75	0.35	2.24	0.22
CH 3	2.28	0.36	5.65	0.39	5.07	0.36	1.62	0.47
CH 4	4.34	0.74	9.32	0.81	9.02	1.28	2.17	0.45
CH 5	7.09	0.98	5.86	1.43	7.08	1.69	4.65	0.87
CH 6	3.74	1.31	2.21	0.56	2.68	0.66	10.28	1.99
CH 7	8.66	2.29	0.67	0.20	0.86	0.28	6.35	2.25
CH 8	2.10	0.76	0.78	0.17	0.63	0.14	1.57	0.56

Table 9. Mean and standard deviation of the impedance measured when EMC filters are connected to the setup, connecting a load in L'-N'

5.2. Attenuation due to the EMC filters

As a result of the impedance variations introduced by the EMC filters, the resulting channel frequency response also varies. In this section, the attenuation introduced by each of the EMC filters is analyzed. For this purpose, using the measurement system explained before, the channel frequency response is calculated when a filter is connected and in absence of it. The signal attenuation due to the filter is defined as the difference between both channel frequency responses. Figure 40 shows the signal attenuation due to the four EMC filters when connected at points A, B and C in the open-circuit configuration.

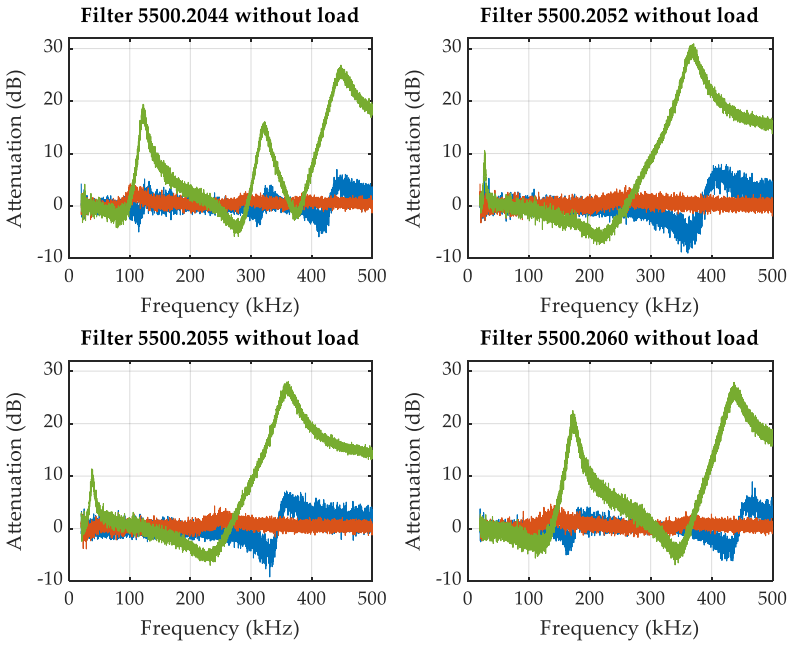

Figure 40. Attenuation due to EMC filters under study in open-circuit configuration. Blue lines indicate that the filter is connected at point A, red lines indicate connection point B, and green lines indicate connection point C

As shown in Figure 40, the attenuation introduced by the filters greatly depends on the point of connection. Attenuation measured when the filter is connected at points A or B is very low, being practically 0 dB when connecting them in the EUT port of the second LISN. By contrast, the attenuation introduced by the filters when connected at the same electrical port as the receiver are very high on some frequency channels. Therefore, the impact is considerably more noticeable when the filter is connected near the communications equipment, especially if it works as a receiver. It should be taken into account that the communication equipment deployed in the field performs both transmitting and receiving functions. Therefore, in practice, an EMC filter near a communication equipment might imply an additional problem for NB-PLC, especially when receiving frames from other equipment. Previous works had also shown that the channel characteristics are mainly dominated by appliances not very distant from the measurement location, and that channel characteristics are not necessarily symmetric [36] [37]. This is also observed in our case when connecting the EMC filter at A and C and obtaining different results. The asymmetry found in the characteristics of the transmission channel is precisely due to the couplers used for NB-PLC equipment [38].

It should also be noted that there are also some negative values that are due to the parallel and/or series resonances introduced by the EMC filters. These negative values do not represent an amplification of the signal. They reflect that, in some cases, there is a better situation of impedance matching when an EMC filter is connected with respect to the situation where no filter is connected to the setup.

Similar results are obtained when measuring the attenuation introduced by each filter when an external load is included, as shown in Figure 41.

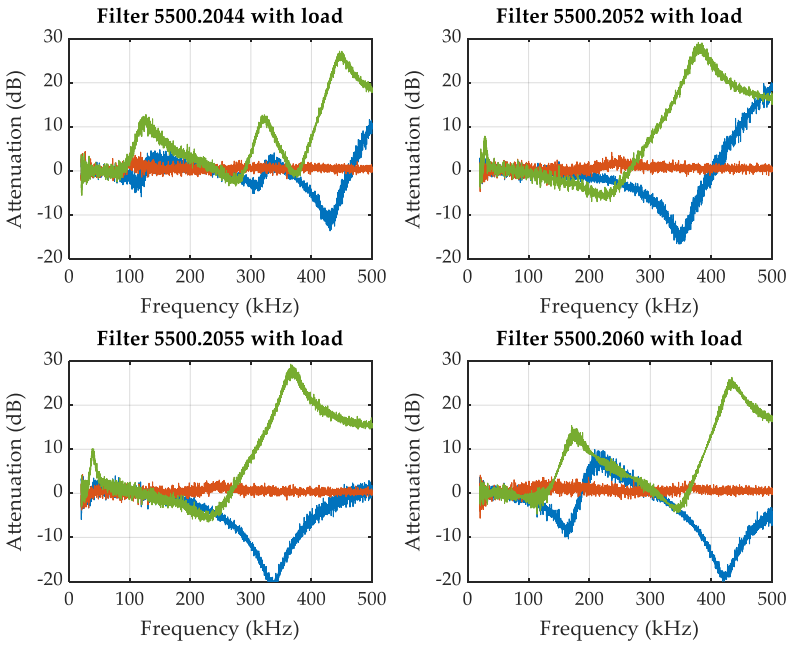

Figure 41. Attenuation due to the EMC filters under study, when a load is connected at ports L'-N'. Blue lines indicate that the filter is connected at point A, red lines indicate connection point B, and green lines indicate connection point C

In order to analyze the characteristics of attenuation in detail, Table 10 and Table 11 gather the mean value and the standard deviation of the attenuations measured when the EMC filters are connected at point C, for the different communication channels defined in PRIME [2], and for the open-circuit and loaded configurations respectively.

	Attenuation of 5500.2044 (dB)		Attenuation of 5500.2052 (dB)		Attenuation of 5500.2055 (dB)		Attenuation of 5500.2060 (dB)	
Channel	**Mean**	**Standard Deviation**	**Mean**	**Standard Deviation**	**Mean**	**Standard Deviation**	**Mean**	**Standard Deviation**
CH 1	-1.11	0.85	0.14	0.65	2.34	1.45	-0.78	1.03
CH 3	4.81	1.49	-3.30	0.85	-1.99	0.86	15.23	4.16
CH 4	0.77	1.23	-4.38	1.46	-4.49	0.84	6.66	1.55
CH 5	-0.24	3.65	6.05	3.13	5.62	3.48	2.23	1.47
CH 6	9.76	4.65	20.91	4.99	21.42	4.78	-2.92	1.10
CH 7	6.22	5.25	24.20	3.04	20.76	2.21	11.84	5.22
CH 8	23.04	2.33	17.35	0.92	15.76	0.72	23.57	2.06

Table 10. Mean and standard deviation of signal attenuation due to the EMC filters

	Attenuation of 5500.2044 + load (dB)		Attenuation of 5500.2052 + load (dB)		Attenuation of 5500.2055 + load (dB)		Attenuation of 5500.2060 + load (dB)	
Channel	**Mean**	**Standard Deviation**	**Mean**	**Standard Deviation**	**Mean**	**Standard Deviation**	**Mean**	**Standard Deviation**
CH 1	-0.08	0.51	0.23	0.55	2.30	1.56	-0.26	0.56
CH 3	4.93	1.30	-3.10	0.70	-2.13	0.73	11.10	1.88
CH 4	1.22	0.99	-4.88	0.87	-4.74	0.68	6.68	1.15
CH 5	0.41	2.99	4.11	2.90	4.39	3.25	2.38	1.20
CH 6	7.57	3.33	16.17	3.69	18.73	4.56	-2.19	1.03
CH 7	5.38	4.85	25.32	2.07	22.83	2.65	11.09	4.95
CH 8	23.25	2.31	18.73	1.00	17.00	0.79	22.51	1.91

Table 11. Mean and standard deviation of signal attenuation due to the EMC filters when connecting a load to L'-N'

As shown in the tables, the mean value of the attenuation can be even higher than 20 dB for some filters and frequency channels. This implies that NB-PLC can be greatly affected or even interrupted if the receiver is working near its sensitivity threshold and one of these components is connected nearby. Comparing the results of Table 10 and Table 11 with the measured impedance values of Table 8 and Table 9, it seems that low impedance values that are maintained along the communication channel, that is, with low standard deviation, and that show drastic variations in phase are more critical in terms of attenuation than abrupt drops on the impedance frequency response. More precisely, all the mean attenuation values higher than 15 dB are due to mean impedance values lower than 3 Ω and abrupt phase variations on the corresponding frequency channel. For example, when connecting filter 5500.2052 at point C in open-circuit configuration, in channel 7, the attenuation is very high, 24.20 dB. For this configuration, the mean value of the resulting impedance is 0.44 Ω and the standard deviation is 0.08 Ω. The phase changes drastically from capacitive to inductive.

Moreover, the standard deviation values of Table 10 and Table 11 indicate that there are important variations of the attenuation within certain communication channels, which might lead to degradations of the quality of NB-PLC. This aspect is analyzed in the following section.

5.3. FER-SNR curves

In the previous section, we proved that the introduction of the filter is only influential when connected near to the receiver. For that reason, FER-SNR curves will only be represented when the filter is connected at point C.

The analysis of the influence of the filters on PLC is carried out through the representation of FER-SNR curves. For each configuration, SNR is calculated as the mean value of the SNRs of the total number of received frames.

Initially, the idea was to obtain results for different modulations, DBPSK, DBPSK_C, DQPSK_C, R_DQPSK and R_DBPSK, in order to evaluate the influence of the EMC filters in modulations with and without error correction and repeating codes.

As an example, Figure 42 shows the SNR-FER curves obtained when no filter is connected and when the four EMC filters are connected near to the receiver for DBPSK modulation.

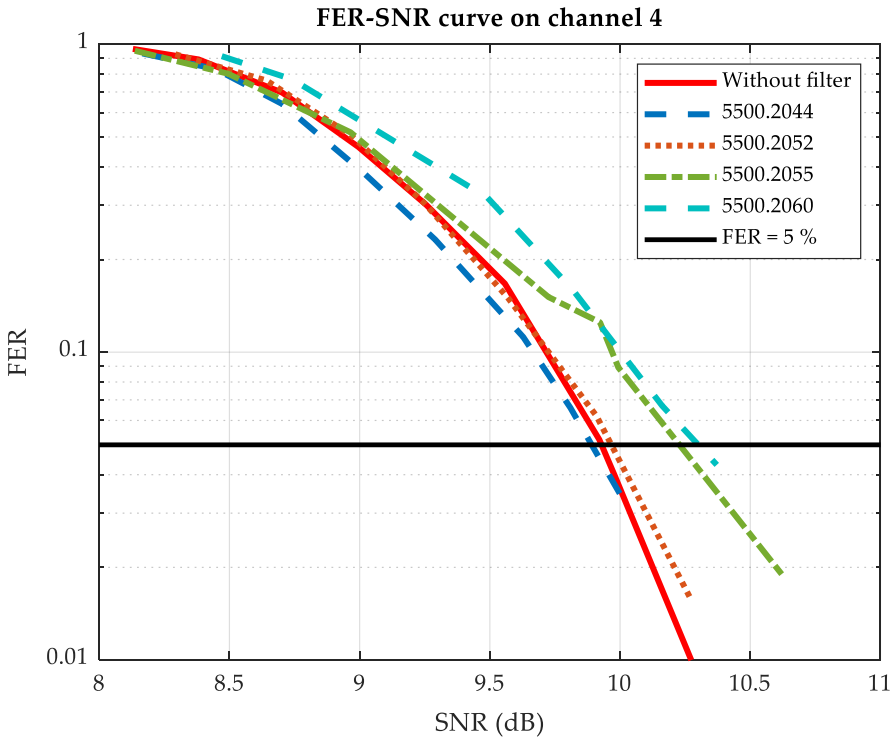

Figure 42. FER-SNR curve on channel 4 for DBPSK without filter and when filters are connected to point C

The SNRs required in each channel to obtain a FER = 5 % using DBPSK modulation, shown in Table 12 and Table 13, are similar to those simulated in [25] with a flat channel

and AWGN. It can be clearly observed that these thresholds are very similar in the absence of a filter and when each of the four EMC filters are connected, either in open-circuit configuration or when a load is included to the filters. The maximum difference is 0.6 dB, which corresponds to connecting the filter 5500.2055 in channel 3. These small differences are considered to be the result of the intrinsic limitations of the proposed methodology, which is based on laboratory trials with hardware equipment.

In [25], it is concluded that frequency – selective channels are very critical to modulations without FEC. However, in the scenario shown in Figure 42 where DBPSK modulation is used, the EMC filters do not introduce significant changes in the thresholds. This implies that in a better situation, that is, when using more robust modulations, the FER-SNR curves will not be affected.

	SNR (dB) for FER = 5 %				
Channel	**Without filter**	**5500.2044**	**5500.2052**	**5500.2055**	**5500.2060**
CH 1	11.0	10.9	10.9	10.6	10.9
CH 3	10.5	10.5	10.5	11.1	10.3
CH 4	9.9	9.9	10.0	10.3	10.3
CH 5	10.2	9.8	9.8	9.9	10.2
CH 6	10.5	10.5	10.7	10.3	10.8
CH 7	10.0	9.7	10.1	9.8	9.5
CH 8	11.0	11.4	11.1	10.5	10.4

Table 12. SNR required for FER = 5 % in each signal configuration when filters are not loaded

	SNR (dB) for FER = 5 %				
Channel	**Without filter**	**5500.2044 + load**	**5500.2052 + load**	**5500.2055 + load**	**5500.2060 + load**
CH 1	11.0	11.2	11.0	10.7	11.1
CH 3	10.5	10.8	10.7	10.7	10.7
CH 4	9.9	9.9	10.1	10.1	10.1
CH 5	10.2	9.9	9.9	9.8	10.1
CH 6	10.5	10.7	10.6	10.6	10.5
CH 7	10.0	9.9	10.1	10.0	10.1
CH 8	11.0	10.9	11.1	11.2	11.2

Table 13. SNR required for FER = 5 % in each signal configuration when filters are loaded

As a consequence, it can be concluded that the channel frequency responses due to the filters are not sufficiently selective to degrade NB-PLC in terms of the SNR thresholds. This implies that the estimation and equalization processes defined for PRIME v1.4 perform properly under these circumstances, not being affected by the channel characteristics caused by the introduction of the EMC filters.

5.4. Further analysis on attenuation

The results presented in the previous section show that, even though the introduction of the EMC filters does not modify the thresholds that define the quality of the communications, the attenuation suffered by the PLC signal when connecting the EMC filters near the receiver is very high on some frequency channels.

The schematics presented in Figure 24 show that the four EMC filters have capacitors in parallel to the L-N ports. However, if the filter presented a high-impedance inductive interface, it would decouple its capacitive load from the network, which could reduce the transmission losses. For that reason, we repeated the tests connecting the filters 5500.2052 and 5500.2055 reversed, that is, connecting the L'-N' ports to the setup, so that the first elements are inductive (L2 and L3). The impedances measured when connecting the two filters reversed are shown in Figure 43.

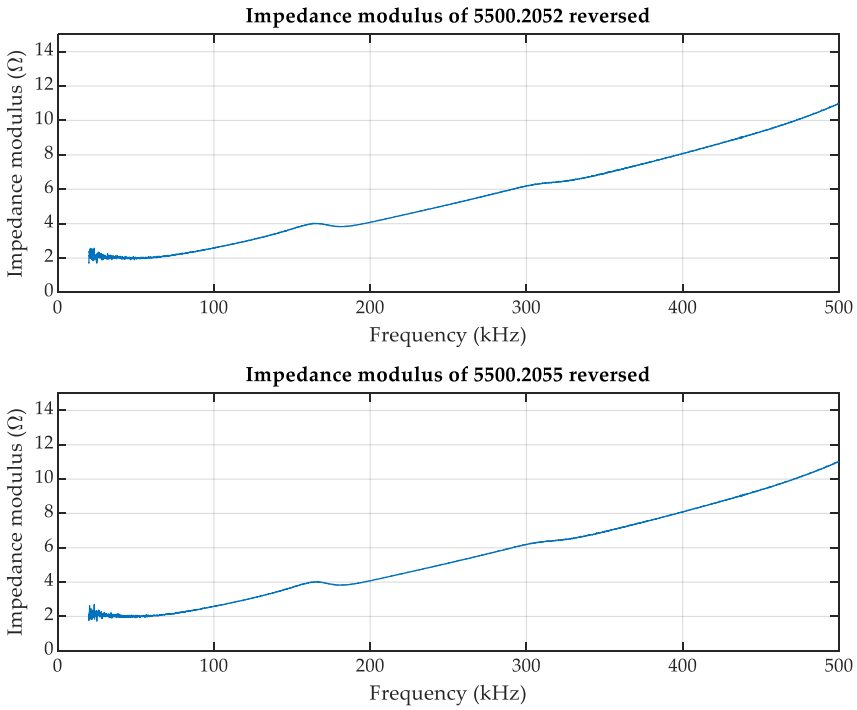

Figure 43. Impedance modulus of the filters 5500.2052 and 5500.2055

The results lead to conclude that, if the filters are connected reversed, the impedance measured corresponds to the impedance of the LISN without significant influence by the filter, as observed when comparing Figure 43 and Figure 12. Hence, in this situation, the PLC signal should not be attenuated by the introduction of the EMC filter. In order to analyze the attenuation in this case, each graph in Figure 44 shows the attenuation when the filters are connected to the setup through ports L-N (blue lines) and L'-N' (red lines). The column indicates the filter under study: the first column corresponds to 5500.2052 and the second column to 5500.2055. The row indicates the location of the EMC filter: A, B and C.

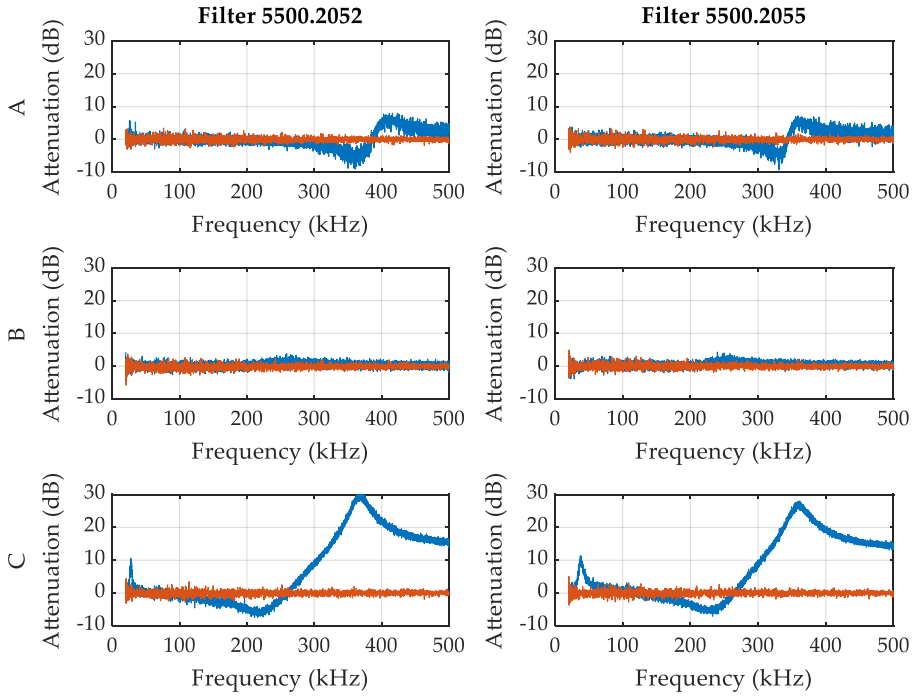

Figure 44. Attenuation of the EMC filters 5500.2052 and 5500.2055 when connected through ports L-N (blue lines) and L'-N' (red lines)

Figure 44 clearly shows how, regardless of their location, the attenuation introduced by the filters when connected to the setup through the L'-N' ports can be considered negligible. Thus, it is demonstrated that the attenuation introduced by the EMC filters is mainly due to the capacitive burden they present in the network interface.

6. Results – Time-variant loads

First, a selection of different household devices, which might potentially show short-term impedance variations, is performed. For that purpose, the impedance of the device connected to the setup is measured. Moreover, some metrics are selected to characterize short-term impedance variations.

Regarding the channel frequency response measurements, first, the channel frequency response when no device under test is connected is measured as a reference, covering the whole frequency range of interest. Then, with the objective of evaluating the influence of the location of the time-variant loads, the channel frequency response is measured when each load is connected in the EUT port of each of the three LISNs.

In regard to the potential effects of short-time variant impedances on NB-PLC systems, and starting from a reference in which no device under test is connected to the setup, the FER-SNR curves are represented for channels 1 and 3-8, as defined by PRIME v1.4 specification. Then, FER-SNR curves are obtained for the previously selected loads under test connected at points A, B and C.

Finally, five modulations from PRIME v1.4 specification are considered in order to analyze their robustness against channel variability: DBPSK, DBPSK_C, DQPSK_C, R_DBPSK and R_DQPSK.

6.1. Impedance variations due to time-variant loads

6.1.1. Definition of metrics to characterize short-time impedance variations

In order to characterize short-time impedance variations, three parameters are calculated for the different impedances measured [31]. The definition of these parameters is shown below.

$$k_1(f) = \frac{Z_{ON}(f)}{Z_{AV}(f)}$$

$$k_2 = \frac{T_{ON}}{T_{AV}}$$

$$k_3(f) = \frac{Z_{ON}(f)}{Z_{OFF}(f)}$$

$Z_{ON}(f)$ corresponds, for each frequency, to the impedance values for those time instants for which an ON state is assumed. $Z_{OFF}(f)$, on the contrary, are the values for the OFF state. $Z_{AV}(f)$ indicates the average impedance in T_{AV}, that is, in 20 ms of the fundamental period. T_{ON} is the time in which an ON state is considered.

If $k_1(f)$ is low, it indicates that $Z_{ON}(f)$ is significantly different from $Z_{AV}(f)$ and that the influence of the electronic device must be taken into account. k_2 quantifies the time in which the impedance shows the ON state, that is, a lower impedance, within the 20 ms of the fundamental period. $k_3(f)$ provides an overview of the level of impedance variation between the ON and OFF states. It is only useful if the impedance in the OFF state is different from infinite [31].

$k_1(f)$ and $k_3(f)$ are obtained as a function of frequency and averaged for each PRIME channel and for all frequencies, in order to obtain a value that characterizes each of the time-variant loads under study.

It should be mentioned that the calculation of the above mentioned parameters requires correctly determining the instants in which the impedance is in the ON state (diodes in conduction) and the OFF state (diodes in open circuit). In the next section, the procedure followed to define ON-OFF states is explained.

6.1.2. Definition of ON-OFF states

First, the minimum and maximum value of impedance for each frequency bin are calculated. With these values, a threshold is set in order to discern between the ON and OFF states, which is calculated as $\frac{\text{maximum}-\text{minimum}}{2}$. Then, each instantaneous impedance sample corresponding to that frequency bin is compared with the previously obtained threshold.

- If the impedance is greater than the difference between the maximum and the threshold, the OFF state is considered for that sample.
- If the impedance is lower than the sum of the minimum and the threshold, the ON state is considered for that sample.

Once the impedance samples have been correctly classified, for each time instant, the number of ON and OFF samples are counted, classifying each time instant into a state:

- If the number of samples in the ON state is greater than in the OFF state, the impedance frequency response for that time instant is considered ON.
- If the number of samples in the OFF state is greater than in the ON state, the impedance frequency response for that time instant is considered OFF.

T_{ON} is calculated multiplying the number of impedance frequency responses considered in the ON state by the interval between different time instants.

6.1.3. Analysis of impedance variations due to time-variant loads

As explained in Section 5.1, the connection of a load to the setup implies time-variability on the measured impedance. The following figures show the modulus and phase of the impedances of the equipment under test (LEDs, Nokia phone charger, safety razor, hair removal razor, hair clippers and alarm clock).

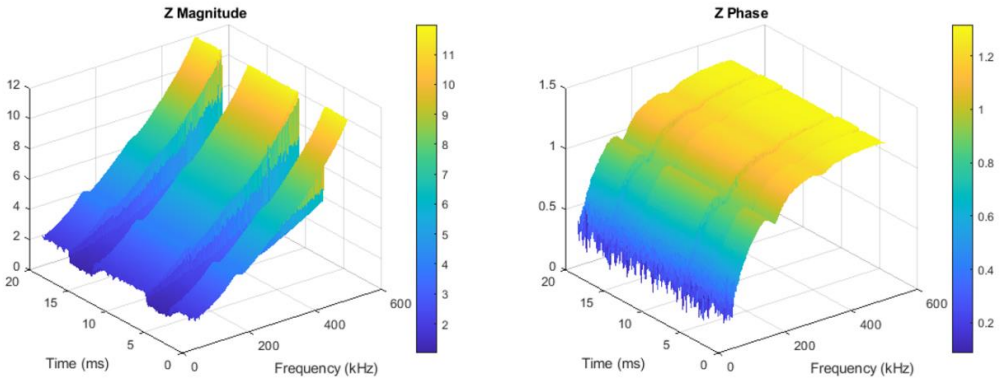

Figure 45. Modulus and phase of the impedance of the LEDs

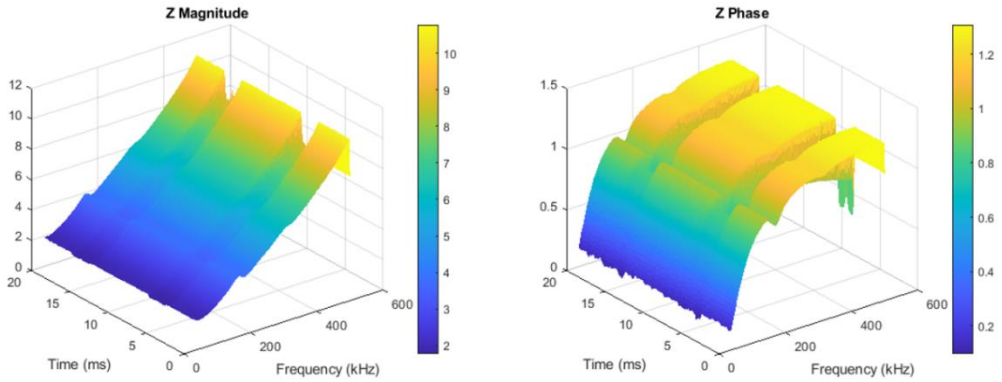

Figure 46. Modulus and phase of the impedance of the Nokia phone charger

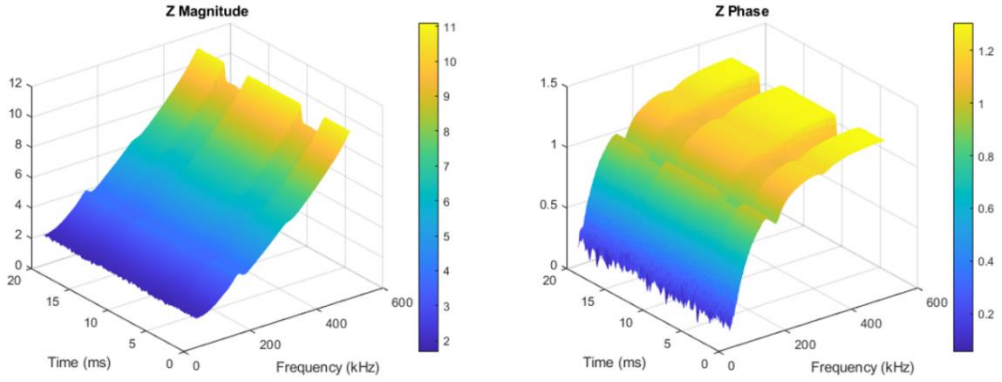

Figure 47. Modulus and phase of the impedance of the safety razor

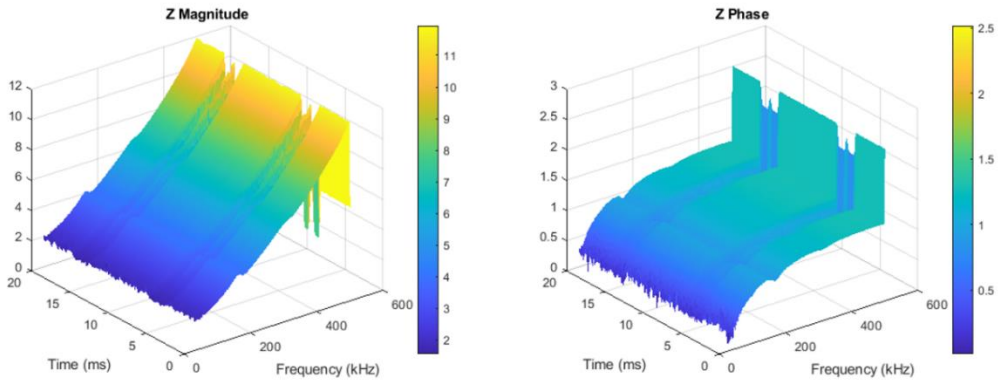

Figure 48. Modulus and phase of the impedance of the hair removal razor

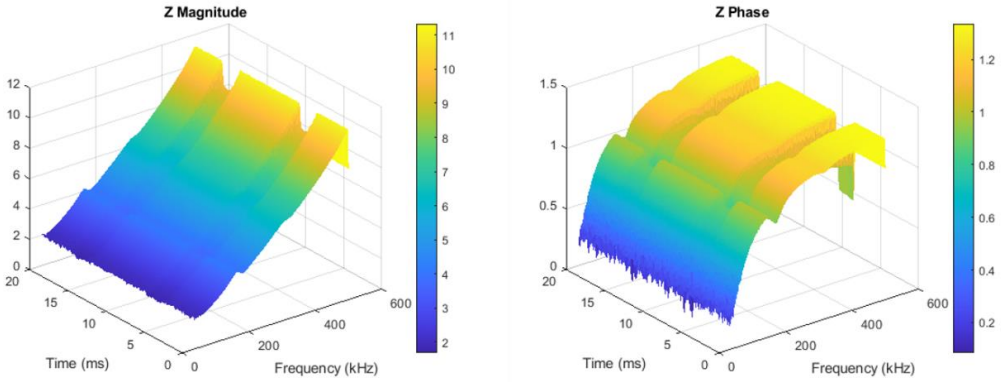

Figure 49. Modulus and phase of the impedance of the hair clippers

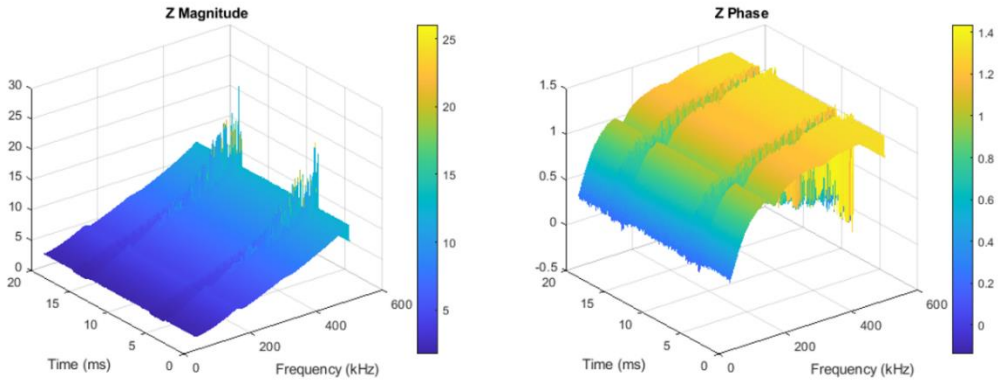

Figure 50. Modulus and phase of the impedance of the alarm clock

These figures clearly show that, as expected, two different states are present in the impedances measured. Low impedances correspond to the parallel of the impedance of the LISN and the impedance of the connected load, when the diode is in a conduction state (ON). Since the impedance of the load is much smaller than the impedance of the LISN, the parallel results in, approximately, the impedance of the load. High impedances,

in contrast, correspond to the impedance of the LISN, since the impedance of the load is not connected to the circuit whenthe diodes are in a non-conducting state (OFF).

In Annex III – Time-variant loads the mean and standard deviation of each impedance modulus for both ON and OFF states are detailed. It is important to mention that, for the ON state, that is, when the impedance of the load is connected to the network, the mean values obtained are similar to those presented for the EMC filters.

As explained before, in order to characterize the difference between the modulus of the impedance in the ON and OFF states, the k parameters are calculated. Table 14 shows the value of each parameter for the selected time-variant impedances, which will be analyzed in following sections. In Annex III – Time-variant loads the k_1 and k_3 parameters for each frequency channel are detailed.

Parameter	LEDs	Safety razor	Hair removal razor	Hair clippers	Nokia charger	Alarm clock
k_1	0.62	0.96	0.86	0.94	0.92	0.81
k_2	0.32	0.27	0.21	0.22	0.21	0.18
k_3	0.53	0.94	0.83	0.92	0.90	0.77

Table 14. Calculation of k parameters for the different time-variant loads under test

6.2. Attenuation due to time-variant impedance loads

In the same way as for the EMC filters, the attenuation introduced by the time-variant loads presented in the previous section is calculated as the difference of the channel frequency response when the load is connected at each of the three connection points of the setup (A, B, C) and in absence of it. The attenuations obtained for the different configurations, frequency and time dependent, are shown in the following figures.

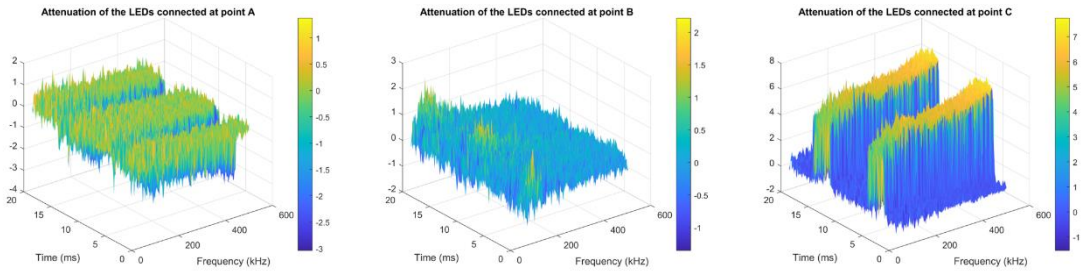

Figure 51. Attenuation of the LEDs connected at points A (left), B (center) and C (right)

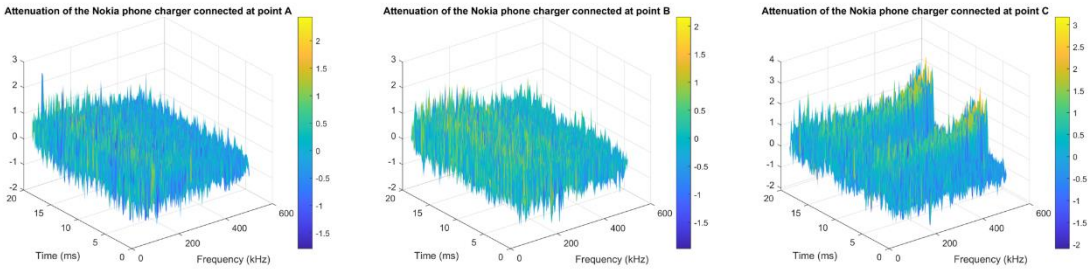

Figure 52. Attenuation of the Nokia phone charger connected at points A (left), B (center) and C (right)

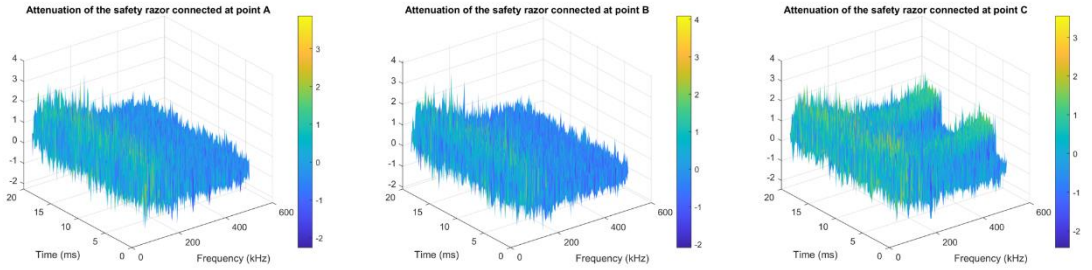

Figure 53. Attenuation of the safety razor connected at points A (left), B (center) and C (right)

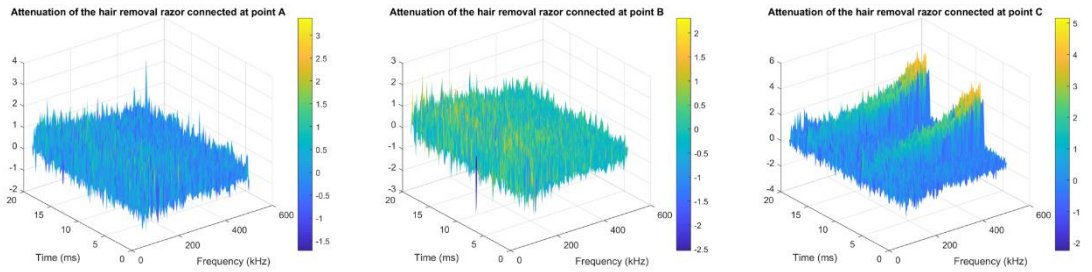

Figure 54. Attenuation of the hair removal razor connected at points A (left), B (center) and C (right)

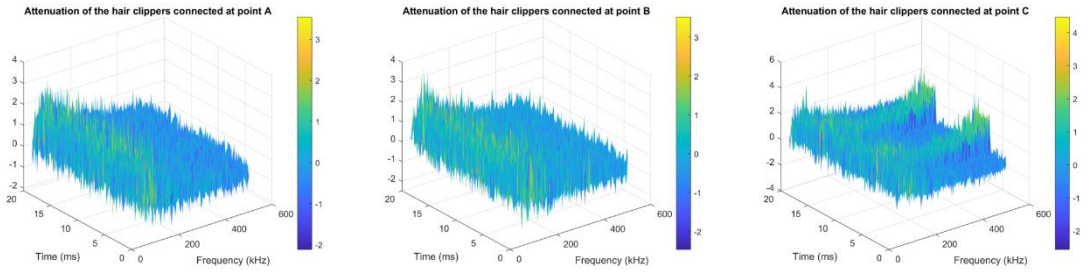

Figure 55. Attenuation of the hair clippers connected at points A (left), B (center) and C (right)

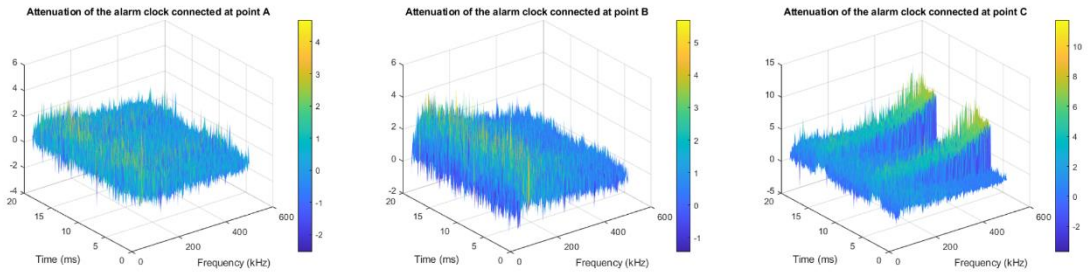

Figure 56. Attenuation of the alarm clock connected at points A (left), B (center) and C (right)

In order to study the attenuation introduced by each load, in Annex III – Time-variant loads the mean attenuation and standard deviation in each frequency channel for each configuration is shown. As example, the attenuation suffered by the PLC when connecting the LEDs at point C in the ON and OFF states is shown in Table 15 and Table 16.

ON state. Attenuation (dB)		
Channel	**Mean**	**Standard deviation**
CH 1	3.84	0.27
CH 3	4.40	0.38
CH 4	4.46	0.28
CH 5	4.63	0.31
CH 6	4.74	0.22
CH 7	4.89	0.31
CH 8	5.33	0.30

Table 15. Mean and standard deviation of the attenuation due to the LEDs connected at point C in the ON state

OFF state. Attenuation (dB)		
Channel	**Mean**	**Standard deviation**
CH 1	0.71	0.13
CH 3	0.83	0.23
CH 4	0.81	0.22
CH 5	0.89	0.22
CH 6	0.88	0.20
CH 7	0.97	0.15
CH 8	0.95	0.14

Table 16. Mean and standard deviation of the attenuation due to the LEDs connected at point C in the OFF state

As it can be seen, the highest attenuation, 5.33 dB, occurs in channel 8 when the LEDs are connected at point C, which is much lower than, for example, the attenuation obtained for the 5500.2052 filter in channel 7 (24.20 dB). For the filters, it was concluded that the low impedances values in module related to abrupt variations in phase were causing the highest attenuation values in the transmitted PLC signal. In Annex III – Time-variant loads, it is shown that the mean impedance modules within a frequency channel obtained for the loads under test are similar to those obtained for the EMC filters.

Therefore, it can be concluded that the phase is the main reason why these loads present low attenuations in the whole frequency band. Figure 57 shows the mean ON and OFF phase, considering the previously defined states.

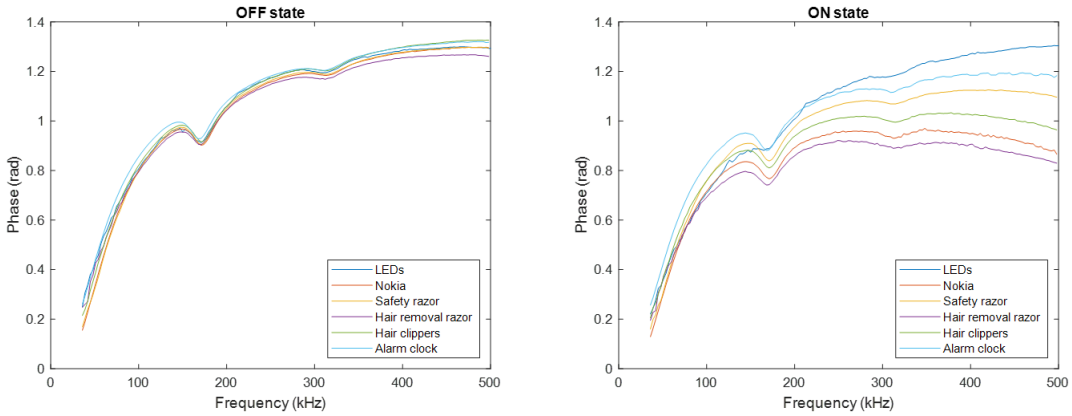

Figure 57. Phase of the loads under study for ON and OFF states

On the one hand, as expected, the phase presented by all the loads in the OFF state is practically identical, since it corresponds to the phase of the impedance of the LISN components. On the other hand, in the ON state, where the impedance of the load is connected to the circuit, the measured phase is very similar in the six analyzed cases. In contrast to the EMC filters, these loads do not present impedances with abrupt variations in phase in none of the two states. Therefore, it can be concluded that the attenuation suffered by the transmitted signal is high when a load with significant resonances in phase is connected near the communications equipment.

6.3. FER-SNR curves

6.3.1. Influence of time-variant loads on the quality of communications

Similarly to the results included in Section 5.3, the analysis of the potential quality degradation of the communications is carried out through the representation of the FER-SNR curves. In Annex III – Time-variant loads, the curves using a DBPSK modulation are shown, when connecting to the setup, as with the EMC filters near the receiver equipment, the different time-variant loads. Table 17 gathers the SNR required for FER = 5 % in these configurations.

SNR (dB) for FER = 5 %							
Channel	**Without load**	**LEDs**	**Safety razor**	**Hair removal razor**	**Hair clippers**	**Nokia charger**	**Alarm clock**
CH 1	11.0	13.1	11.1	11.2	11.3	11.2	10.8
CH 3	10.5	13.0	10.6	10.6	10.6	10.3	11.8
CH 4	9.9	12.6	10.0	10.4	10.0	10.1	12.1
CH 5	10.2	13.0	10.1	10.5	10.1	10.0	12.2
CH 6	10.5	12.8	10.5	10.9	10.7	10.6	12.6
CH 7	10.0	13.2	10.0	10.7	10.2	10.2	13.5
CH 8	11.0	13.9	11.0	11.4	11.0	10.9	13.3

Table 17. SNR required for FER = 5 % when different time-variant impedances are connected in Rx using a DBPSK modulation

As it can be seen, when the safety razor, the hair removal razor, the hair clippers and the charger of the Nokia are involved, the thresholds that set the quality of communications are practically not affected with respect to the situation where no load is connected . The maximum difference, 0.7 dB, occurs when connecting the hair removal razor on channel 7. These differences are similar to those presented with the EMC filters, so they can be considered negligible and caused by the limitations of the methodology used. By contrast, in the case of the LEDs and the alarm clock, the degradations increase up to 3.2 dB and 3.5 dB (in channel 7 in both cases), respectively.

These degradations may be due to two causes: abrupt variations on the channel frequency response or great changes in the impedance between ON and OFF states. The figures and tables shown in Annex III – Time-variant loads evidence that the attenuation introduced by the different loads can be considered flat in the whole frequency band (standard deviations of 0 dB in the seven frequency channels). In order to analyze the time-variations, k parameters will be taken into account. As mentioned above, low values of k_1 and k_3 indicate high variability, which can be critical for our communications. Table 14 gathers that these parameters take values away from the unit when the LEDs and the alarm clock are connected, being 0.62 and 0.53 and 0.81 and 0.77, respectively. However, k_1 and k_3 are very close to 1 for the safety razor, the hair removal razor, the hair clippers and the charger of the Nokia, that is, when the thresholds are similar to those obtained without load. Thus, it can be concluded that the short-time impedance variations between the ON and OFF states are those that degrade the SNR needed for reaching a FER of 5 %.

It is important to mention that the degradations in both cases, the LEDs and the alarm clock, are very similar, but that the k_3, 0.53 and 0.77, are considerably different. Figure 58 shows the k_3 parameter for each frequency channel with respect to the degradation of the thresholds that set the quality of the communications.

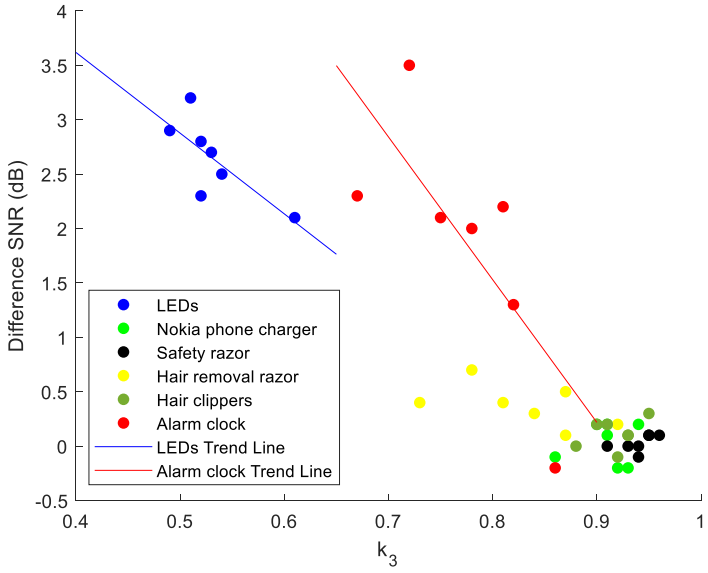

Figure 58. Representation of the k_3 parameter with respect to the difference of the SNR for each configuration

This figure leads to the conclusion that if the k_3 for each frequency channel is calculated, values higher than 0.73 do not imply variations in the SNR for a FER of 5 %, when the Nokia phone charger, the safety razor, the hair removal razor and the hair clippers are taken into account. If the LEDs are connected this parameter varies between 0.49 and 0.61, being the SNR degradations (2.1-3.2 dB) inversely proportional to the k_3. As explained before in a more general way, when the alarm clock is under study, the differences in SNR are similar to those obtained for the LEDs, but the k_3 differ from each other. In order to understand why different values of k_3 imply similar changes in SNR, the variations between the impedance frequency responses for the time instants in which the load is in the OFF state are analyzed in more detail for the alarm clock. Figure 50 shows how in the instants in which there is a change from OFF to ON a much higher impedance is measured for this load. Figure 59 shows the difference between the impedance frequency responses of two instants considered in the OFF state.

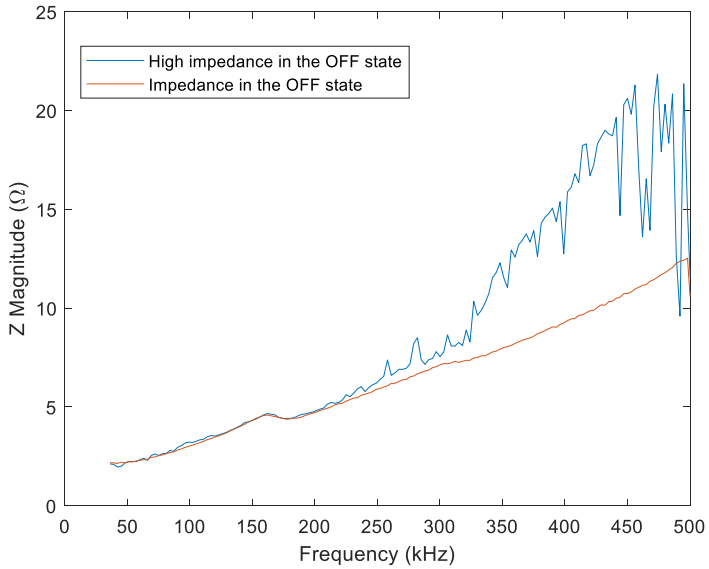

Figure 59. Difference between the impedance frequency responses of two instants considered in the OFF state

To make a comparison between the impedance frequency responses of the time instants considered in the OFF state, the standard deviation of these instants is calculated for each frequency channel and represented with respect to the degradation of the thresholds, as shown in Figure 60.

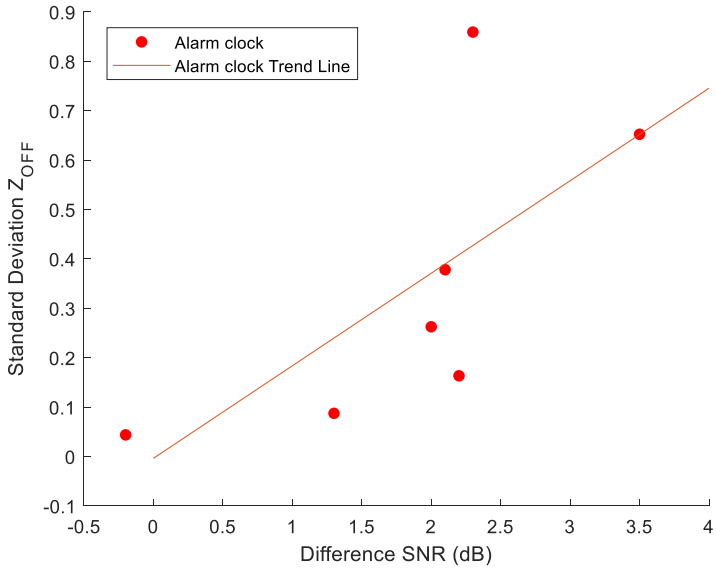

Figure 60. Representation of the difference of the SNR with respect to the standard deviation of the Z_{OFF} for the alarm clock

From Figure 60 it can be concluded that the obtained points follow the linear trend line represented. When the standard deviation between the frequency responses of the

considered OFF instants increases, an increase in the degradation of the thresholds is observed. This effect can be appreciated in the high frequency channels, where a high difference is observed between the SNR needed for reaching a FER of 5 % in the configuration when the load is connected and in absence of it.

Therefore, it is important not only to take into account the variations in impedance between the ON and OFF states, characterized by the k_3 parameter, but also to analyze the possible variations given within the same state.

6.3.2. Robustness of modulations against time-variant impedances

As it is explained in Section 6.3.1, the impedances of the LEDs and the alarm clock degrade NB-PLC, when connecting them near the receiver equipment using a DBPSK modulation. In order to study the robustness of the different modulations defined by PRIME against time-variant impedances, the FER-SNR curves are represented using DBPSK, DBPSK_C, DQPSK_C, R_DQPSK and R_DBPSK. Table 18 and Table 19 gather the SNR for a FER of 5 % connecting at point C both loads.

SNR (dB) for FER = 5 %										
Channel	DBPSK		DBPSK_C		DQPSK_C		R_DQPSK		R_DBPSK	
	Without load	LEDs	Without load	LEDs	Without load	LEDs	Without load	LEDs	Without load	LEDs
CH 1	11.0	13.1	5.6	6.1	8.3	10.7	6.2	6.3	3.7	3.8
CH 3	10.5	13.0	5.5	5.9	8.2	10.4	6.2	6.2	3.7	3.8
CH 4	9.9	12.6	5.5	5.9	8.0	10.5	6.0	6.2	3.7	3.7
CH 5	10.2	13.0	5.4	5.6	8.1	10.2	6.2	6.2	3.7	3.7
CH 6	10.5	12.8	5.5	5.6	8.4	11.2	6.2	6.2	3.7	3.7
CH 7	10.0	13.2	5.3	5.5	8.1	11.4	6.1	6.2	3.7	3.7
CH 8	11.0	13.9	5.4	5.6	8.0	11.8	6.1	6.2	3.7	3.7

Table 18. SNR required for FER = 5 % for the LEDs using different modulations

SNR (dB) for FER = 5 %										
Channel	DBPSK		DBPSK_C		DQPSK_C		R_DQPSK		R_DBPSK	
	Without load	Alarm clock	Without load	Alarm clock	Without load	Alarm clock	Without load	Alarm clock	Without load	Alarm clock
CH 1	11.0	10.8	5.6	5.6	8.3	8.4	6.2	6.2	3.7	3.7
CH 3	10.5	11.8	5.5	5.5	8.2	8.6	6.2	6.1	3.7	3.8
CH 4	9.9	12.1	5.5	5.8	8.0	8.6	6.0	6.1	3.7	3.7
CH 5	10.2	12.2	5.4	5.8	8.1	9.6	6.2	6.1	3.7	3.7
CH 6	10.5	12.6	5.5	6.1	8.4	10.9	6.2	6.2	3.7	3.7
CH 7	10.0	13.5	5.3	6.4	8.1	9.5	6.1	6.2	3.7	3.7
CH 8	11.0	13.3	5.4	7.0	8.0	13.6	6.1	6.2	3.7	3.8

Table 19. SNR required for FER = 5 % for the alarm clock for different modulations

The results lead to conclude that not very robust modulations, those with a larger number of symbols in the constellation and that do not include FEC or repetition codes,

suffer degradations in the thresholds that set the quality of communications if the LEDs or the alarm clock are connected to the setup.

If the case of the LEDs is analyzed, differences of 2-3 dB are observed in all PRIME frequency channels if DBPSK or DQPSK_C modulations are used. For the DBPSK_C, in contrast, these differences are considerably reduced, with the maximum difference occurring in channel 1 (0.5 dB). Finally, it is demonstrated that robust modulations, i.e., those that introduce repetition codes by four, are able to cope with these fast impedance variations within the fundamental frequency. For both modulations, the maximum difference is 0.1 dB, which can be due to the previously defined methodology.

When the alarm clock is connected to the setup, the degradation of the SNR for a FER of 5 % is 1.5-3 dB for channels 3-8, when using a DBPSK modulation. As the difference between the impedance in the ON and OFF states on channel one is negligible (mean impedance of 2.05 Ω and 2.38 Ω in ON and OFF states, respectively), the threshold in this frequency channel is not affected, despite the use of a modulation without robustness.

If the DQPSK_C is taken into account, the degradation of the SNR for a FER of 5 % is considerably increased in the frequency channels 5 to 8. As in the previous section, the k_3 parameter is represented with respect to the degradation of the thresholds for the LEDs and the alarm clock, as shown in Figure 61. Thus, it can be concluded, in the same way as using the DBPSK modulation, that different $k_3$for the LEDs and the alarm clock imply similar degradations in the thresholds, since there is a high variability in the impedance frequency responses in the OFF state. In Figure 62 the relation between the variation within the impedance frequency responses in the OFF state and the difference in the SNR is shown, which allows to conclude that are directly proportional.

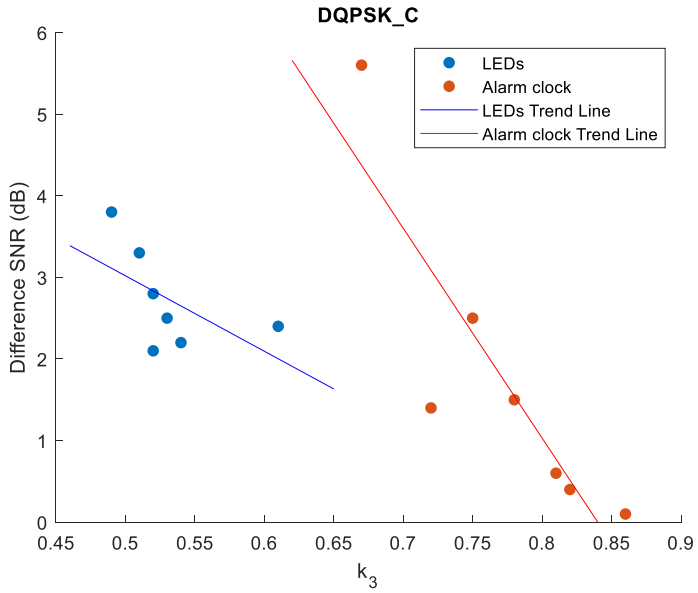

Figure 61. Representation of the k_3 parameter with respect to the difference of the SNR for the LEDs and the alarm clock using DQPSK_C

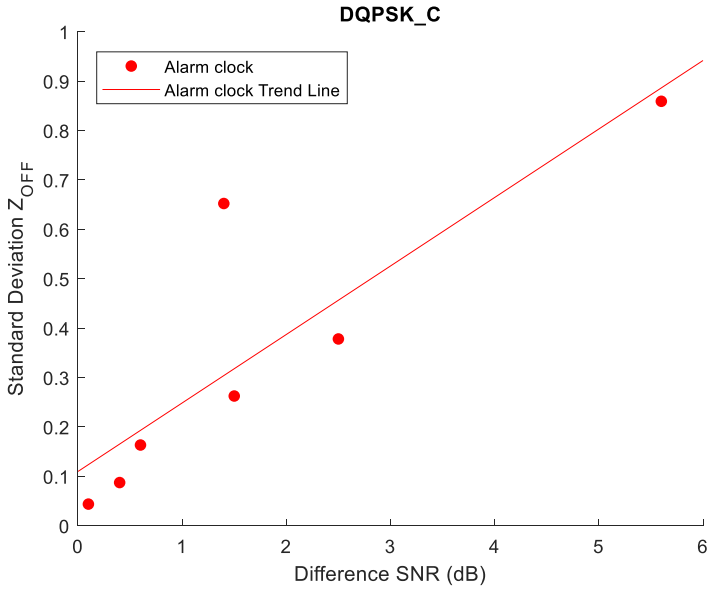

Figure 62. Representation of the difference of the SNR with respect to the standard deviation of the Z_OFF for the alarm clock using DQPSK_C

When DBPSK_C frame transmission is configured, as this a more robust modulation, a maximum difference of 0.5 dB is noted in channels 1-6. In channels 7 and 8, in contrast, 1.1 dB and 1.6 dB differences are measured, due to the variations between the impedances of the OFF state. Therefore, this modulation cannot cope with the variations given within the OFF state in the high frequency bands defined by PRIME. Figure 64 shows that the degradation in SNR and the deviation in impedance between different instants in the OFF state follow a linear relation, which correctly approximates the expected trend line.

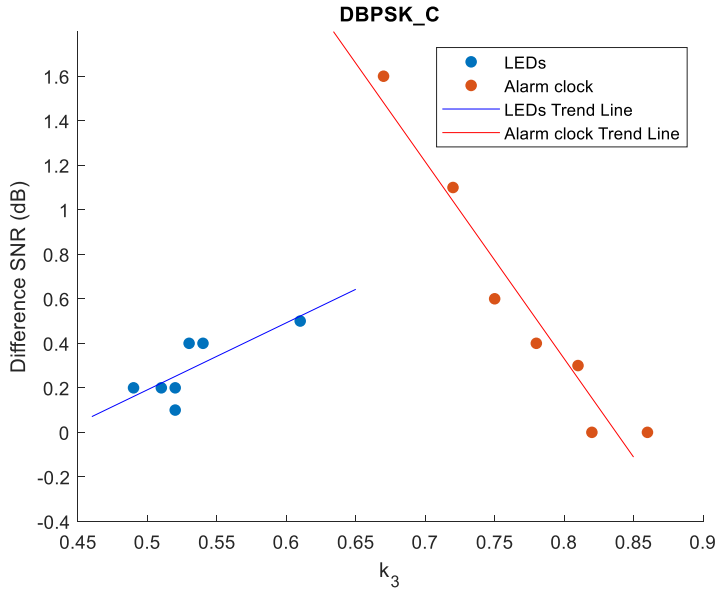

Figure 63. Representation of the k_3 parameter with respect to the difference of the SNR for the LEDs and the alarm clock using DBPSK_C

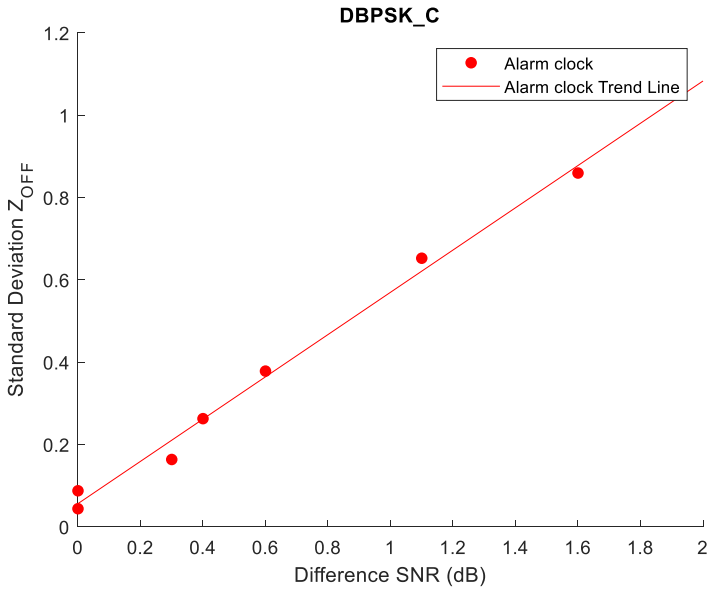

Figure 64. Representation of the difference of the SNR with respect to the standard deviation of the Z_{OFF} for the alarm clock using DBPSK_C

As it occurred when the LEDs were connected to the setup, the FER-SNR curves are not affected when connecting the alarm clock at point C if robust modulations are used. For both cases, R_DBPSK and R_DQPSK, the degradations are practically 0 dB.

Furthermore, it is worth mentioning that the minimum SNR required to achieve a FER = 5 % when no load is connected is lower for DBPSK_C compared to R_DQPSK. However, when connecting the LEDs and the alarm clock, it is shown how the R_DQPSK is able to cope with short-time impedance variations, while the FER-SNR curves if

DBPSK_C is used are shifted to the right. Therefore, it can be concluded that, although in an ideal situation where no time-variant impedance devices are connected using DBPSK_C modulation would require a lower SNR, R_DQPSK modulation, due to the repetition codes, is more suitable for a real situation where many equipment that can affect NB-PLC are connected.

6.3.3. Influence of the location of the time-variant loads

In order to analyze the influence of the location of the load, the LEDs and the alarm clock are connected at point A (Tx), point B (Channel) and point C (Rx) and the FER-SNR curves are represented. Table 20 and Table 21 gather the SNR for a FER of 5 % in each configuration.

SNR (dB) for FER = 5 %				
Channel	**Without load**	**LEDs in Tx**	**LEDs in Channel**	**LEDs in Rx**
CH 1	11.0	13.2	11.3	13.1
CH 3	10.5	13.2	10.5	13.0
CH 4	9.9	11.6	10.1	12.6
CH 5	10.2	10.2	10.1	13.0
CH 6	10.5	11.0	10.5	12.8
CH 7	10.0	10.6	9.9	13.2
CH 8	11.0	11.7	11.1	13.9

Table 20. SNRs required for FER = 5 % when connecting LEDs in different locations

SNR (dB) for FER = 5 %				
Channel	**Without load**	**Alarm clock in Tx**	**Alarm clock in Channel**	**Alarm clock in Rx**
CH 1	11.0	11.1	11.2	10.8
CH 3	10.5	12.1	10.6	11.8
CH 4	9.9	11.1	10.1	12.1
CH 5	10.2	10.6	10.1	12.2
CH 6	10.5	10.9	10.5	12.6
CH 7	10.0	10.5	10.0	13.5
CH 8	11.0	11.5	11.0	13.3

Table 21. SNRs required for FER = 5 % when connecting the alarm clock in different locations

On the one hand, the results lead to conclude that the communications are not affected when connecting the LEDs and the alarm clock at point B, since the SNR required to obtain a FER of 5% is identical to that obtained when no load is connected.

On the other hand, the degradation of the thresholds when connecting both loads at the transmitter, if transmitting on channels 3 and 4, is very similar to the degradation when they are connected at the receiver. However, at the higher frequencies, channels 5-8, the results obtained near to the transmitter equipment are identical to those obtained in the absence of load. Finally, it should be noted that when the alarm clock is connected to the setup at point A and a transmission on channel 1 is configured, due to

the small difference in impedance between the ON and OFF states, there is no difference in the FER-SNR curves represented.

7. Contributions and future research lines

This work analyzes the influence of impedance variations on NB-PLC according to PRIME standard. For that purpose, two types of loads are considered: static loads, that show frequency-dependent impedance variations but are constant over time; and dynamic loads, in which the impedance frequency response changes within the fundamental period of 50 Hz.

In order to achieve this objective, two different indicators were taken into account: the attenuation suffered by the PLC signal due to the connection of the load, and the SNR thresholds that set the quality of the communications.

On the one hand, four EMC filters were analyzed in an open-circuit and a loaded configuration. The results lead to the conclusion that the four filters under study do not introduce abrupt variations in the channel frequency response, so that the thresholds that set the quality of communications are not affected. However, they do present considerable signal attenuations, up to 25 dB, when they are connected near the receiver equipment. These attenuations could cause communications to fail if the noise level is high or if the received signal power is close to the sensitivity limit of the receiving equipment. These implies that the EMC filters used for power converters have an unintended side effect of attenuating communication signals that had not been analyzed before this work. These high attenuations are due to the capacitive interface of the filters with the grid. These results have been published in the scientific journal *MDPI Electronics* under the title *Characterization of the Potential Effects of EMC Filters for Power Converters on Narrowband Power Line Communications* [39].

On the other hand, a set of short-time variant impedances were considered. In contrast to the EMC filters, the attenuations measured are not very high regardless of the point of connection. In the case of the filters it was concluded that the considerable attenuations were due to the low impedance values in modulus that are maintained along the communication channel and due to important resonances in the impedance phase. Although the dynamic loads under study show similar values in the impedance modulus, they do not present abrupt changes in phase. This might be the main reason why only attenuations up to 4 dB were obtained in the presence of these type of loads. If the thresholds that set the quality of communications are analyzed, some degradations are observed. As the channel frequency responses because of the connection of the dynamic loads are flat for the whole frequency band 42-471 kHz, these degradations must be due to the difference between the impedance frequency responses in the ON and OFF states. The results lead to the conclusion that not only ON/OFF impedance variability, but also differences in the OFF impedance frequency responses can considerably affect NB-PLC.

It is worth mentioning that, in this work, only the attenuation and the degradation of the quality of the communications due to the impedance variations introduced by the loads under test have been taken into account. However, in a real situation, this equipment could also introduce Non-Intentional Emissions that can considerably degrade Narrowband Power Line Communications. Therefore, it could be interesting to study the impact of the impedance variations together with the NIEs introduced to the electrical grid, so that their effect on NB-PLC is completely characterized.

Finally, the study presented in this work only considers the influence of impedance variations in the frequency range 10-500 kHz. The possibility of using higher frequencies, up to 10 MHz, would allow a greater data transmission capacity. Consequently, it is necessary to characterize the electrical grid in terms of impedance, channel frequency response and NIEs, so that BB-PLC communication protocols can be developed considering the behavior of the grid in this frequency band.

8. References

[1] N. Uribe Pérez, '"Análisis de la capacidad de PRIME para gestión de red en entornos con generación distribuida y sistemas dealmacenamiento,", Mayo.

[2] PRIME Alliance, '"Specification for PoweRline Intelligent Metering Evolution v1.4,".

[3] A. Llano Palacios, '"Análisis del impacto de las perturbaciones de canal sobre las tecnologías PLC de banda estrecha,", Septiembre.

[4] G. Hallak and G. Bumiller, '"Time variant voltage and current modeling corresponding to access impedance measurements," *2018 IEEE International Symposium on Power Line Communications and its Applications (ISPLC)*, pp. 1-6.

[5] J. Anatory, N. Theethayi, R. Thottappillil, M.M. Kissaka and N.H. Mvungi, '"The Influence of Load Impedance, Line Length, and Branches on Underground Cable Power-Line Communications (PLC) Systems," *IEEE Transactions on Power Delivery*, vol. 23, no. 1, pp. 180-187.

[6] M. Antoniali and A.M. Tonello, '"Measurement and Characterization of Load Impedances in Home Power Line Grids," *IEEE Transactions on Instrumentation and Measurement*, vol. 63, no. 3, pp. 548-556.

[7] G. Hallak and G. Bumiller, '"Impedance measurement of electrical equipment loads on the power line network," *2017 IEEE International Symposium on Power Line Communications and its Applications (ISPLC)*, pp. 1-6.

[8] G. Hallak, G. Bumiller and C. Nieß, '"Accurate access impedance measurements on the power line with optimized calibration procedures," *2017 IEEE International Instrumentation and Measurement Technology Conference (I2MTC)*, pp. 1-6.

[9] F.J.C. Corripio, J.A.C. Arrabal, L.D. del Rio and J.T.E. Munoz, '"Analysis of the cyclic short-term variation of indoor power line channels," *IEEE Journal on Selected Areas in Communications*, vol. 24, no. 7, pp. 1327-1338.

[10] F.J. Canete, J.A. Cortes, L. Diez, J.T. Entrambasaguas and J.L. Carmona, '"Fundamentals of the cyclic short-time variation of indoor power-line channels," *International Symposium on Power Line Communications and Its Applications, 2005.*, pp. 157-161.

[11] I. Elfeki, S. Jacques, I. Aouichak, T. Doligez, Y. Raingeaud and J. Le Bunetel, '"Characterization of Narrowband Noise and Channel Capacity for Powerline Communication in France," *Energies*, vol. 11, no. 11.

[12] H. Gassara, F. Rouissi and A. Ghazel, '"Statistical Characterization of the Indoor Low-Voltage Narrowband Power Line Communication Channel," *IEEE Transactions on Electromagnetic Compatibility*, vol. 56, no. 1, pp. 123-131.

[13] M. Tlich, A. Zeddam, F. Moulin and F. Gauthier, '"Indoor Power-Line Communications Channel Characterization Up to 100 MHz—Part I: One-Parameter Deterministic Model," *IEEE Transactions on Power Delivery*, vol. 23, no. 3, pp. 1392-1401.

[14] M. Tlich, A. Zeddam, F. Moulin and F. Gauthier, '"Indoor Power-Line Communications Channel Characterization up to 100 MHz—Part II: Time-Frequency Analysis," *IEEE Transactions on Power Delivery*, vol. 23, no. 3, pp. 1402-1409.

[15] I. Fernández, A. Arrinda, I. Angulo, D. De La Vega, N. Uribe-Pérez and A. Llano, '"Field Trials for the Empirical Characterization of the Low Voltage Grid Access Impedance From 35 kHz to 500 kHz," *IEEE Access*, vol. 7, pp. 85786-85795.

[16] G. Chu, J. Li and W. Liu, '"Narrow band power line channel characteristics for low voltage access network in China," *2013 IEEE 17th International Symposium on Power Line Communications and Its Applications*, pp. 297-302.

[17] J. Popovic, J. Oliver, N. Cordero, T. Harder, J. Cobos, M. Hayes, C. O'Mathuna and E. Prem, '"Power Electronics Enabling Efficient Energy Usage: Energy Savings Potential and Technological Challenges," *IEEE Transactions on Power Electronics - IEEE TRANS POWER ELECT*, vol. 27, pp. 2338-2353.

[18] I. Fernandez, N. Uribe-Pérez, I. Eizmendi, I. Angulo, D. de la Vega, A. Arrinda and T. Arzuaga, '"Characterization of non-intentional emissions from distributed energy resources up to 500kHz: A case study in Spain," *International Journal of Electrical Power & Energy Systems*, vol. 105, pp. 549-563.

[19] Schaffner, '"Basics in EMC/EMI and Power Quality - Introduction, Annotations, Applications,".

[20] G. López, J.I. Moreno, E. Sánchez, C. Martínez and F. Martín, '"Noise Sources, Effects and Countermeasures in Narrowband Power-Line Communications Networks: A Practical Approach," *Energies*, vol. 10, no. 8.

[21] D. Roggo, '"Spectral Grid Impedance and Electromagnetic Interferences in the 150 kHz Frequency Range,", 2018, pp. 143-151.

[22] B. Rasool, A. Rasool and I. Khan, '"Impedance Characterization of Power Line Communication Networks," *Arabian Journal for Science and Engineering*, vol. 39, no. 8, pp. 6255-6267.

[23] J.A. Cortés, A. Sanz, P. Estopiñán and J.I. García, '"Analysis of narrowband power line communication channels for advanced metering infrastructure," *EURASIP Journal on Advances in Signal Processing*, vol. 2015, no. 1, pp. 27.

[24] M. Sigle, W. Liu and K.D. Karlsruhe, '"On the impedance of the low-voltage distribution grid at frequencies up to 500 kHz," *2012 IEEE International Symposium on Power Line Communications and Its Applications*, pp. 30-34.

[25] A. Llano, I. Angulo, P. Angueira, T. Arzuaga and D. De la Vega, '"Analysis of the Channel Influence to Power Line Communications Based on ITU-T G.9904 (PRIME)," *Energies*, vol. 9, no. 1.

[26] I. Fernández, I. Angulo, A. Arrinda, I. Arechalde, N. Uribe-Pérez and T. Arzuaga, '"Characterization of the frequency-dependent transmission losses of the grid up to 500 kHz,", 3-6 June 2019.

[27] I. Fernandez, M. Alberro, J. Montalban, A. Arrinda, I. Angulo and D. de la Vega, '"A new voltage probe with improved performance at the 10 kHz-500 kHz frequency range for field measurements in LV networks," *Measurement*, vol. 145, pp. 519-524.

[28] Comité International Spécial des Perturbations Radioélectriques, '"CISPR 16-1-1:2019,".

[29] IEC 60939-1:2010, '"Passive Filter Units for Electromagnetic Interference Suppression – Part 1: Generic Specification,".

[30] Schurter manufacturer, '"Schurter ,", vol. 2020, no. 16 December.

[31] D. Chakravorty, J. Meyer, P. Schegner, S. Yanchenko and M. Schocke, '"Impact of Modern Electronic Equipment on the Assessment of Network Harmonic Impedance," *IEEE Transactions on Smart Grid*, vol. 8, no. 1, pp. 382-390.

[32] Microchip, '"PL360G55CF-EK User Guide,".

[33] ETSI, '"Power Line Communications (PLT) Narrow Band Transceivers in the Range 9 kHz to 500 kHz Power Line Performance Test Method Guide,".

[34] L. Capponi, I. Fernandez, D. Roggo, A. Arrinda, I. Angulo and D. de la Vega, '"Comparison of measurement methods of grid impedance for Narrow Band-PLC up to 500 kHz," *2018 Ieee 9th International Workshop on Applied Measurements for Power Systems (Amps)*, pp. 82-87.

[35] I. Fernandez, D. de la Vega, D. Roggo, R. Stiegler, L. Capponi, I. Angulo, J. Meyer and A. Arrinda, '"Comparison of Measurement Methods of LV Grid Access Impedance in the Frequency Range Assigned to Nb-Plc Technologies," *Electronics*, vol. 8, no. 10, pp. 1155.

[36] Anonymous '"MIMO Power Line Communications: Narrow and Broadband Standards, EMC, and Advanced Processing,", 2014.

[37] L.d.R. Farias, L.F. Monteiro, M.O. Leme and S.L. Stevan Jr., '"Empirical Analysis of the Communication in Industrial Environment Based on G3-Power Line Communication and Influences from Electrical Grid," *Electronics*, vol. 7, no. 9, pp. 194.

[38] F. Passerini and A.M. Tonello, '"Secure PHY Layer Key Generation in the Asymmetric Power Line Communication Channel," *Electronics*, vol. 9, no. 4, pp. 605.

[39] J. González-Ramos, I. Angulo, I. Fernández, A. Arrinda and D. de la Vega, '"Characterization of the Potential Effects of EMC Filters for Power Converters on Narrowband Power Line Communications," *Electronics*, vol. 10, no. 2.

A. Annex I – Working team and task description

This annex gathers the working team and the description of the different tasks carried out during the project.

Jon González	Project developer
Igor Fernández	Co-director
Itziar Angulo	Co-director

Table 22. Working team of the master's thesis

P.T.1.	**Definition and validation of the methodology.**
T.1.1.	• **Definition of the measurement setup.** The measurement setup is defined. • Human resources: Jon González, Igor Fernández, Itziar Angulo. • Technical resources: LISNs, attenuators, Microchip PL360G55CF-EK, signal generator.
T.1.2.	• **Validation of the attenuation measurement system.** In order to measure the attenuation, some trials are carried out using the channel frequency response measurement system designed in TSR and the RSSI parameter given by the Microchip PL360G55CF-EK. • Human resources: Jon González. • Technical resources: LISNs, attenuators, Microchip PL360G55CF-EK, signal generator, channel frequency response measurement system.
T.1.3.	• **Validation of the attenuators.** The attenuators are validated, in order to know the potential degradation they can introduce in the channel frequency response. • Human resources: Jon González. • Technical resources: LISNs, attenuators, Microchip PL360G55CF-EK, signal generator, channel frequency response measurement system.
T.1.4.	• **Measure of the impedances and channel frequency response of the setup and representation of the FER-SNR curves when no load is connected.** In order to characterize the setup, the impedances and the channel frequency response is measured, together with the FER-SNR

	curves when no external load is connected on the eight frequency channels defined in PRIME v.1.4. • Human resources: Jon González. • Technical resources: LISNs, attenuators, Microchip PL360G55CF-EK, signal generator, impedance measurement system, channel frequency response measurement system.

Table 23. First work package: Definition and validation of the methodology

P.T.2.	**Analysis of the influence of EMC filters on NB – PLC.**
T.2.1.	• **Evaluation of the state of the art.** Analysis of the state of art on the influence of EMC filters on NB – PLC. • Human resources: Jon González. • Technical resources: computer.
T.2.2.	• **Offline impedance measurement of the EMC filters in an open-circuit configuration.** The offline impedances of the four EMC filters in an open-circuit configuration are measured using the impedance measurement system. • Human resources: Jon González. • Technical resources: computer, EMC filters, impedance measurement system, signal generator.
T.2.3.	• **Impedance measurement of the EMC filters in an open-circuit configuration when connected to the setup.** The impedances of the four EMC filters in an open-circuit configuration connected to the setup are measured by means of the impedance measurement system. • Human resources: Jon González. • Technical resources: computer, EMC filters, impedance measurement system, LISNs, attenuators, Microchip PL360G55CF-EK, signal generator.
T.2.4.	• **Measurement of the attenuation of the EMC filters in an open-circuit configuration when connected to the setup.** The attenuation introduced by the four EMC filters in an open-circuit configuration connected to the setup is measured by means of the channel frequency response measurement system. • Human resources: Jon González. • Technical resources: computer, EMC filters, channel frequency response measurement system, LISNs, attenuators, Microchip PL360G55CF-EK, signal generator.

T.2.5.	• **Representation of the FER-SNR curves when connecting the four EMC filters in an open-circuit configuration.** The FER-SNR curves when connecting the four EMC filters in an open-circuit configuration in the EUT port of the third LISN (C) using a DBPSK modulation on the eight channels defined in PRIME v1.4. • Human resources: Jon González. • Technical resources: computer, EMC filters, LISNs, attenuators, Microchip PL360G55CF-EK, signal generator.
T.2.6.	• **Impedance measurement of the EMC filters loaded when connected to the setup.** The impedances of the four EMC filters loaded connected to the setup are measured by means of the impedance measurement system. • Human resources: Jon González. • Technical resources: computer, EMC filters, impedance measurement system, LISNs, attenuators, Microchip PL360G55CF-EK, signal generator, 50 Ω, 560 nF capacitor.
T.2.7.	• **Measurement of the attenuation of the EMC filters loaded when connected to the setup.** The attenuation introduced by the four EMC filters loaded connected to the setup is measured by means of the channel frequency response measurement system. • Human resources: Jon González. • Technical resources: computer, EMC filters, channel frequency response measurement system, LISNs, attenuators, Microchip PL360G55CF-EK, signal generator, 50 Ω, 560 nF capacitor.
T.2.8.	• **Representation of the FER-SNR curves when connecting the four EMC filters loaded.** The FER-SNR curves when connecting the four EMC filters loaded in the EUT port of the third LISN (C) using a DBPSK modulation on the eight channels defined in PRIME v1.4 are represented. • Human resources: Jon González. • Technical resources: computer, EMC filters, LISNs, attenuators, Microchip PL360G55CF-EK, signal generator, 50 Ω, 560 nF capacitor.
T.2.9.	• **Measurement of the attenuation of the EMC filters reversed when connected to the setup.** The attenuation introduced by the four EMC filters connected to the setup reversed is measured by means of the channel frequency response measurement system.

	• Human resources: Jon González. • Technical resources: computer, EMC filters, channel frequency response measurement system, LISNs, attenuators, Microchip PL360G55CF-EK, signal generator.
T.2.10.	• **Analysis of the results related to EMC filters.** The results related to EMC filters are analyzed and conclusions are obtained. • Human resources: Jon González, Igor Fernández, Itziar Angulo. • Technical resources: computer.
H.2.	**Completion of the analysis of the influence of EMC filters on NB – PLC.**

Table 24. Second work package: Analysis of the influence of EMC filters on NB – PLC

P.T.3.	**Analysis of the influence of time-variant impedances on NB – PLC.**
T.3.1.	• **Evaluation of the state of the art.** The state of art on the influence of time-variant impedances on NB – PLC is analyzed. • Human resources: Jon González. • Technical resources: computer.
T.3.2.	• **Selection of devices with time-variant impedance within the fundamental frequency cycle (impedance measurements).** Different loads are connected to the setup and their impedances are calculated, so that devices that present time-variant impedance within the fundamental frequency cycle are found. • Human resources: Jon González. • Technical resources: computer, different loads under test, channel frequency response measurement system, LISNs, attenuators, Microchip PL360G55CF-EK, signal generator.
T.3.3.	• **Measurement of the NIEs introduced by the loads that introduce time-variant impedances.** The NIEs introduced by the selected loads are measured in the setup by means of the NIE measurement system. • Human resources: Jon González. • Technical resources: computer, time-variant impedances, NIE measurement system, LISNs, attenuators, Microchip PL360G55CF-EK, signal generator.

T.3.4.	• **Measurement of the attenuation suffered by the NB – PLC signal due to the time-variant impedances.** The attenuation introduced by the loads selected, when connected to the setup, is measured by means of the channel frequency response measurement system. • Human resources: Jon González. • Technical resources: computer, time-variant impedances, channel frequency response measurement system, LISNs, attenuators, Microchip PL360G55CF-EK, signal generator.
T.3.5.	• **Representation of the FER-SNR curves when connecting the selected time-variant impedances.** The FER-SNR curves when connecting the selected loads at A, B and C for different modulations on the eight channels defined in PRIME v1.4 are represented. • Human resources: Jon González. • Technical resources: computer, time-variant impedances, LISNs, attenuators, Microchip PL360G55CF-EK, signal generator.
T.3.6.	• **Selection and calculation of metrics to characterize short-term impedance variations.** In order to characterize short-term impedance variations, some metrics are selected and calculated for the developed measurements. • Human resources: Jon González. • Technical resources: computer.
T.3.7.	• **Analysis of the results related to time-variant impedances.** The results related to short-term impedance variations are analyzed and conclusions are obtained. • Human resources: Jon González, Igor Fernández, Itziar Angulo. • Technical resources: computer.
H.3.	• **Completion of the analysis of the influence of time-variant impedances on NB – PLC.**

Table 25. Third work package: Analysis of the influence of the time-variant impedances on NB – PLC

P.T.4.	**Project management and documentation.**
T.4.1.	• **Meetings with the project directors.** Meetings are held to discuss the progress of the project and to analyze the results obtained.

	• Human resources: Jon González, Igor Fernández, Itziar Angulo. • Technical resources: computer.
T.4.2.	• **Writing and supervision of the project.** Documentation of the partial results of the project and final draft. • Human resources: Jon González, Igor Fernández, Itziar Angulo. • Technical resources: computer.

Table 26. Fourth work package: Project management and documentation

B. Annex II – EMC filters

B.1. EMC filters not loaded. FER-SNR curves

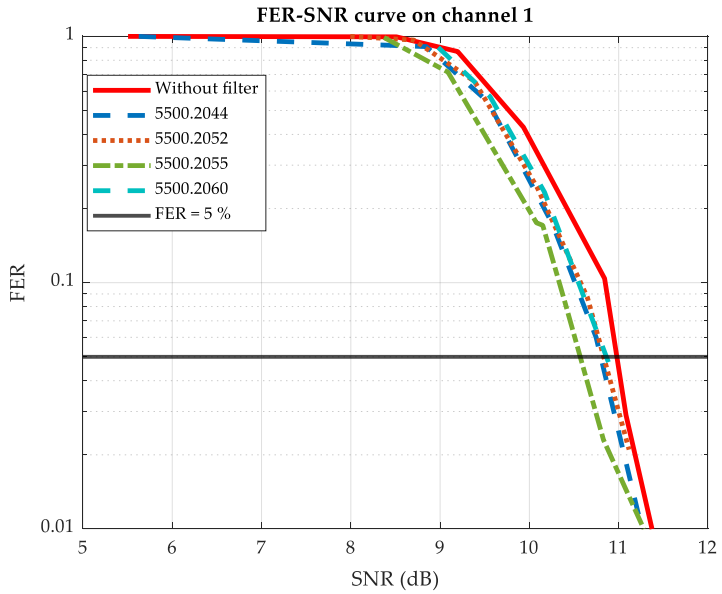

Figure 65. FER-SNR curve on channel 1 for DBPSK without filter and when filters not loaded are connected to point C

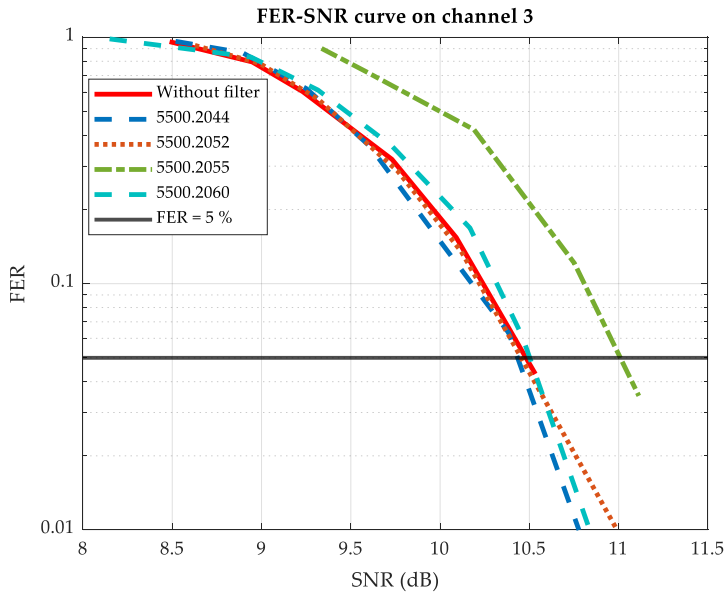

Figure 66. FER-SNR curve on channel 3 for DBPSK without filter and when filters not loaded are connected to point C

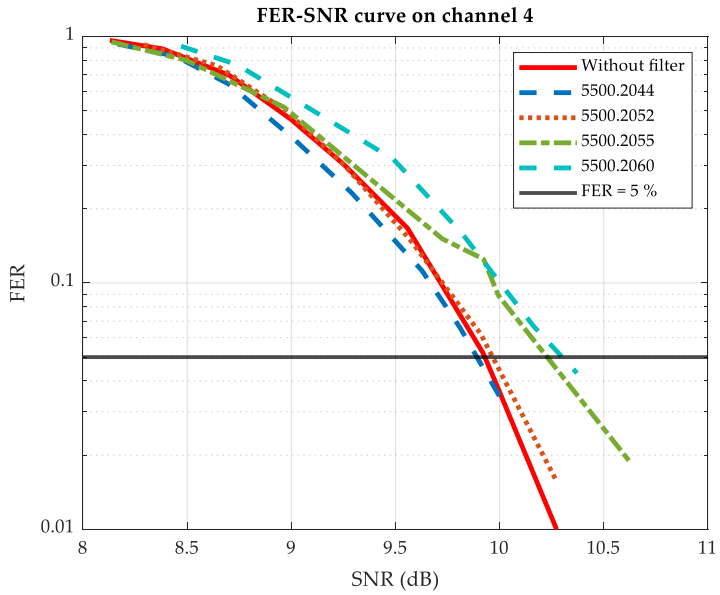

Figure 67. FER-SNR curve on channel 4 for DBPSK without filter and when filters not loaded are connected to point C

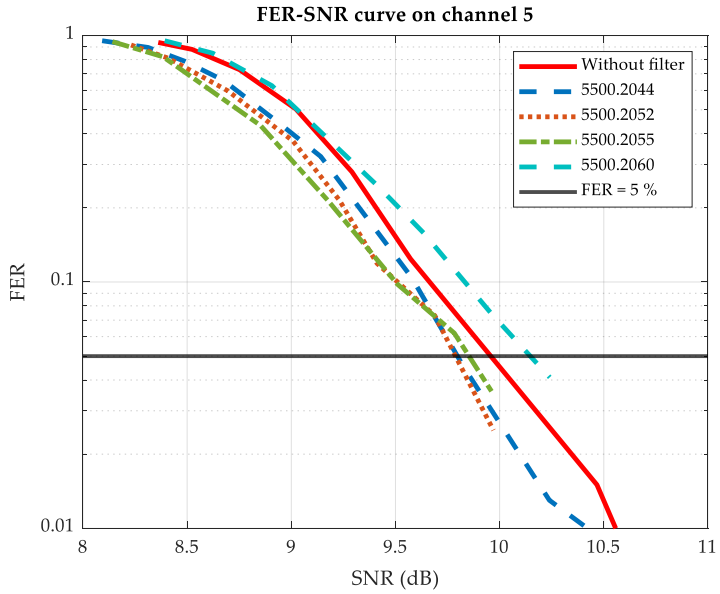

Figure 68. FER-SNR curve on channel 5 for DBPSK without filter and when filters not loaded are connected to point C

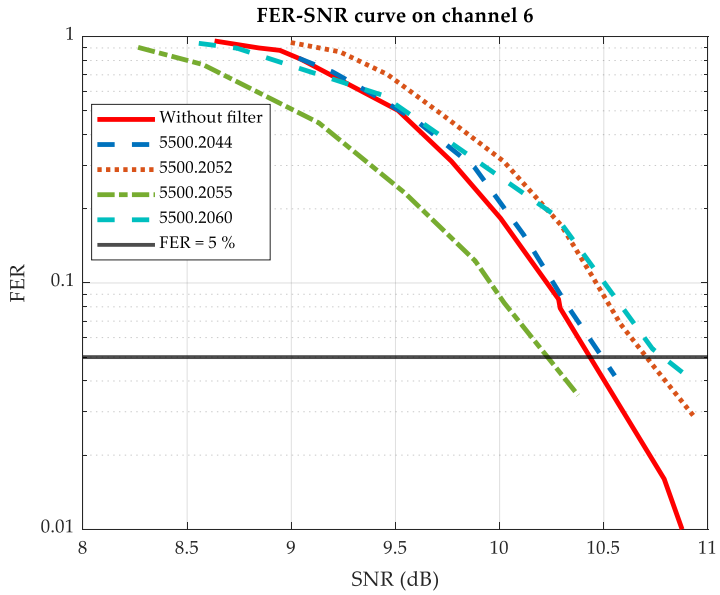

Figure 69. FER-SNR curve on channel 6 for DBPSK without filter and when filters not loaded are connected to point C

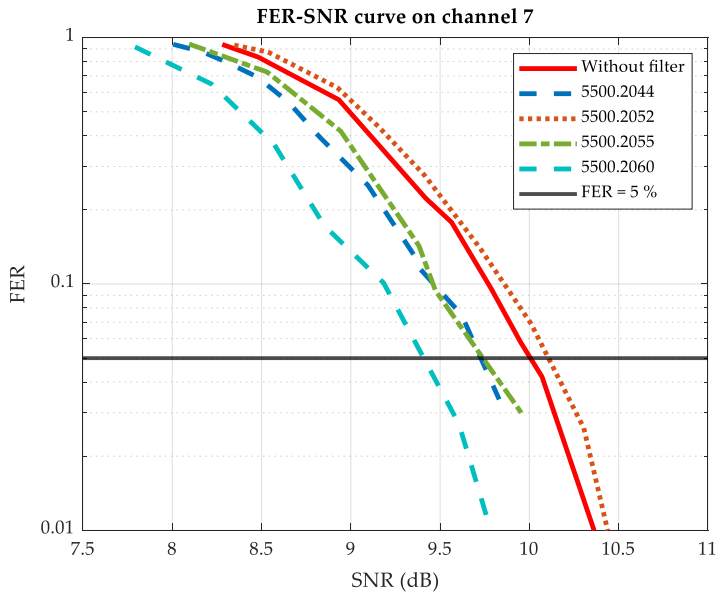

Figure 70. FER-SNR curve on channel 7 for DBPSK without filter and when filters not loaded are connected to point C

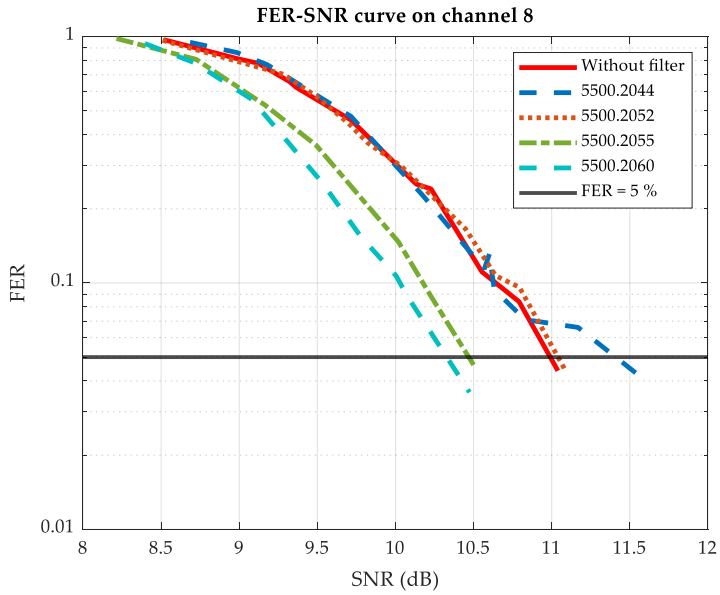

Figure 71. FER-SNR curve on channel 8 for DBPSK without filter and when filters not loaded are connected to point C

C. Annex III – Time-variant loads

C.1. Measured impedances

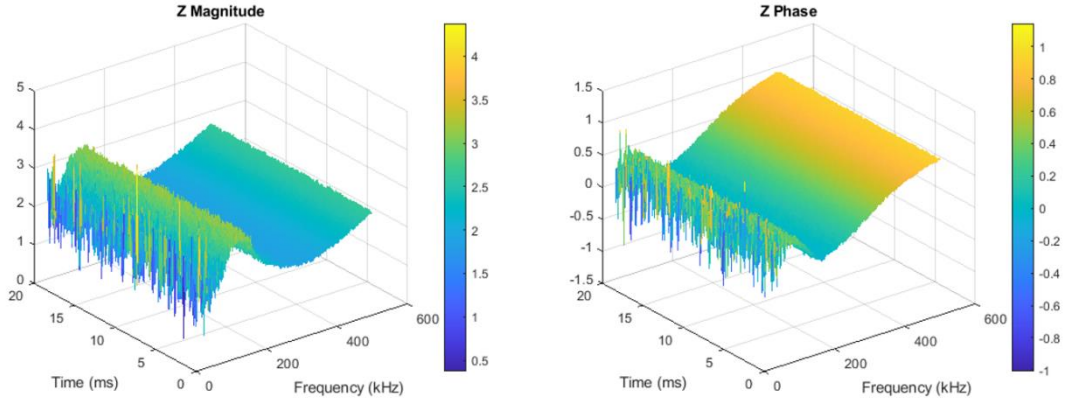

Figure 72. Modulus and phase of the impedance of a blender

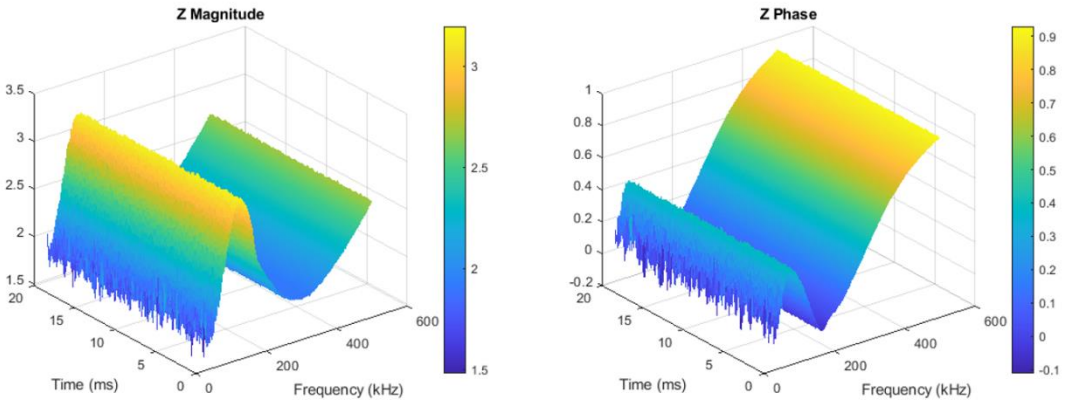

Figure 73. Modulus and phase of the impedance of a blender with rotation speed 2

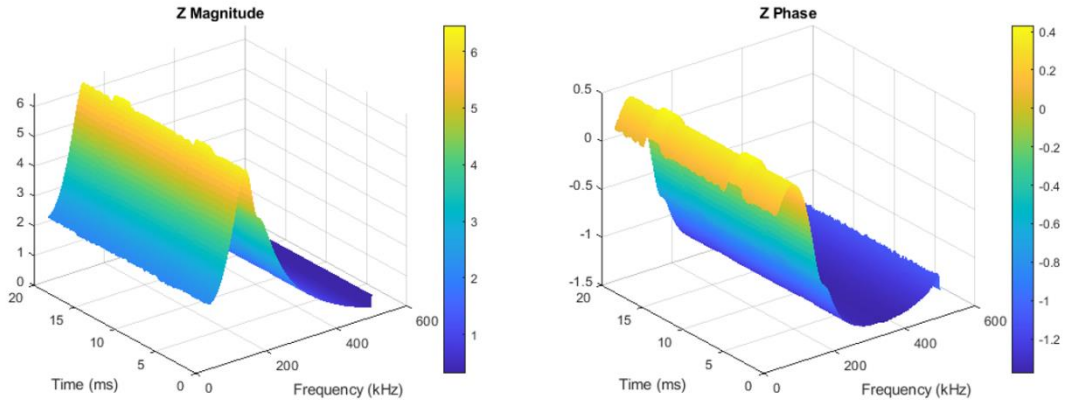

Figure 74. Modulus and phase of the impedance of a wireless charger when a phone is connected

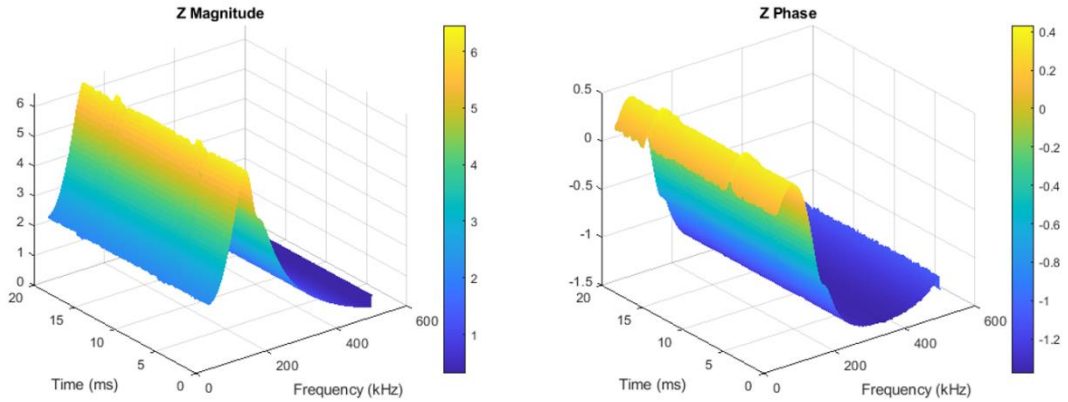

Figure 75. Modulus and phase of the impedance of a wireless charger when no phone is connected

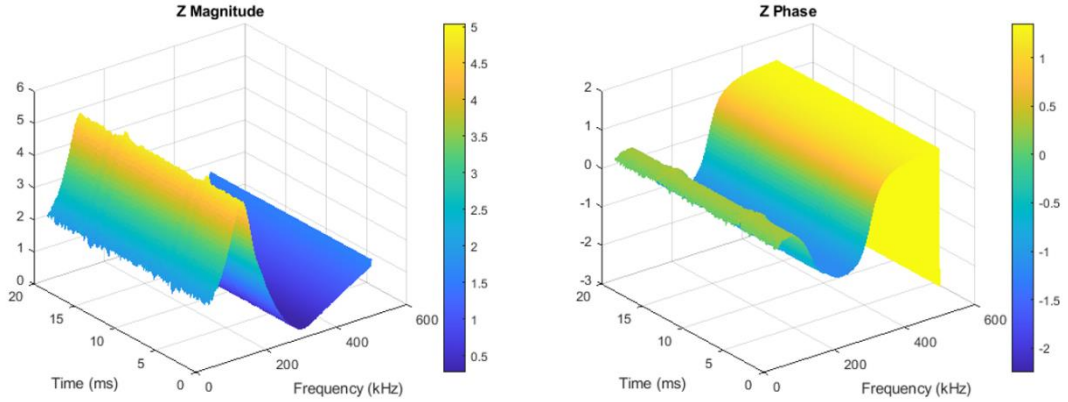

Figure 76. Modulus and phase of the impedance of a computer charger

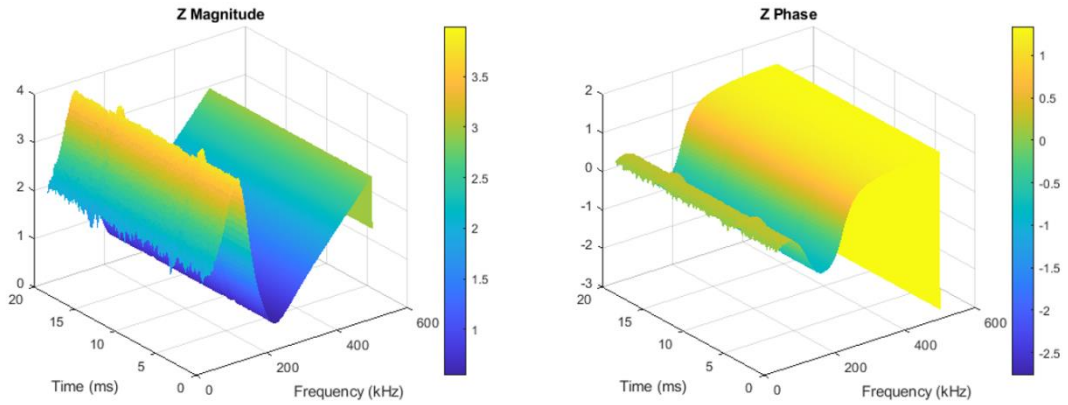

Figure 77. Modulus and phase of the impedance of a second computer charger

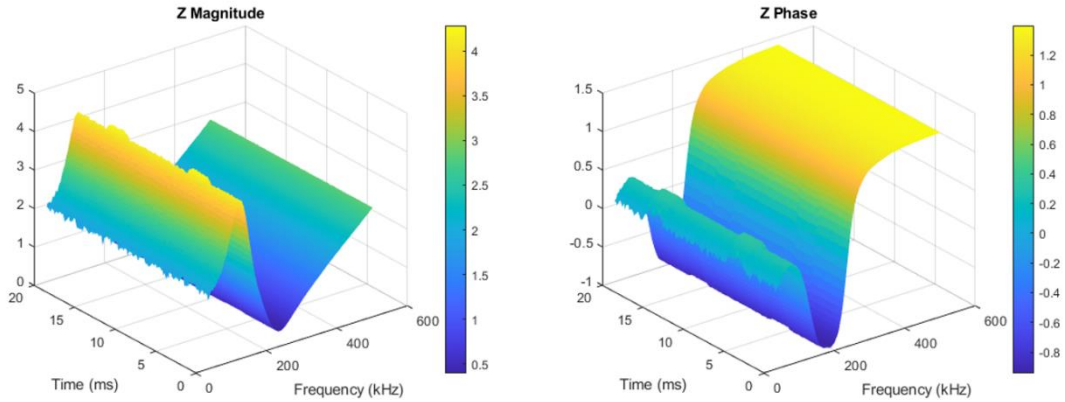

Figure 78. Modulus and phase of the impedance of a third computer charger

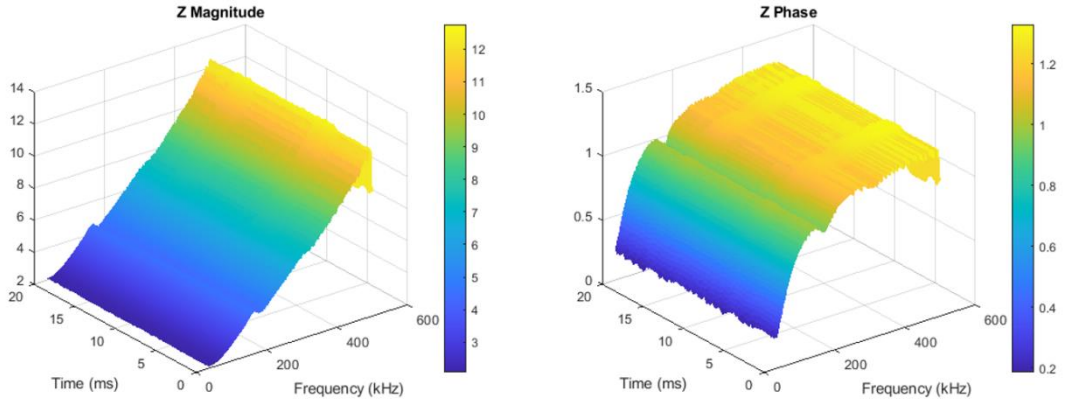

Figure 79. Modulus and phase of the impedance of a toothbrush charger

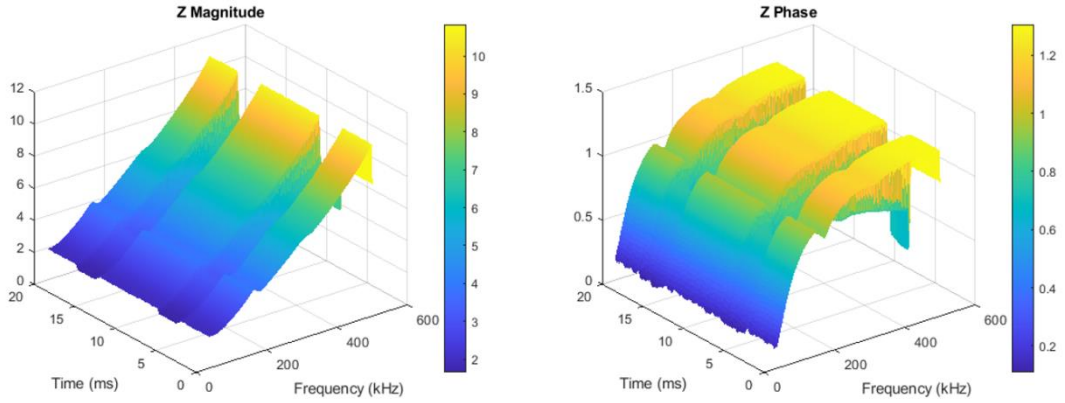

Figure 80. Modulus and phase of the impedance of a Huawei phone charger when the phone is connected

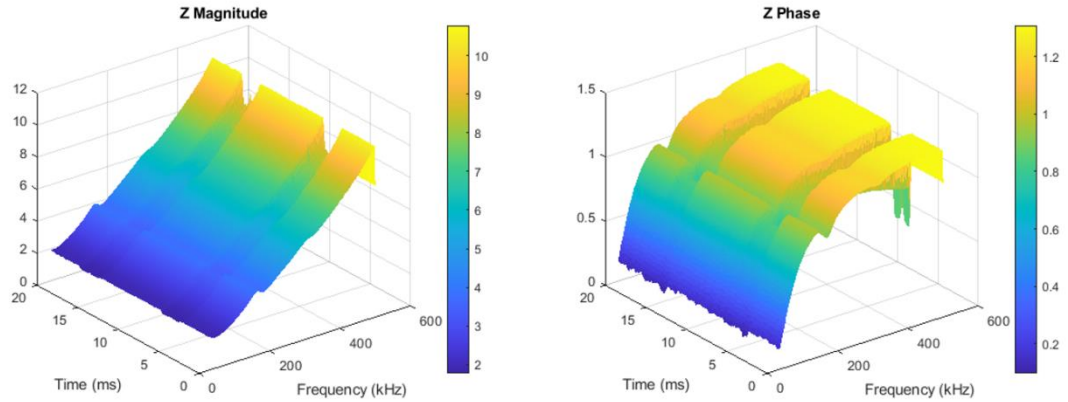

Figure 81. Modulus and phase of the impedance of a Nokia phone charger when the phone is connected

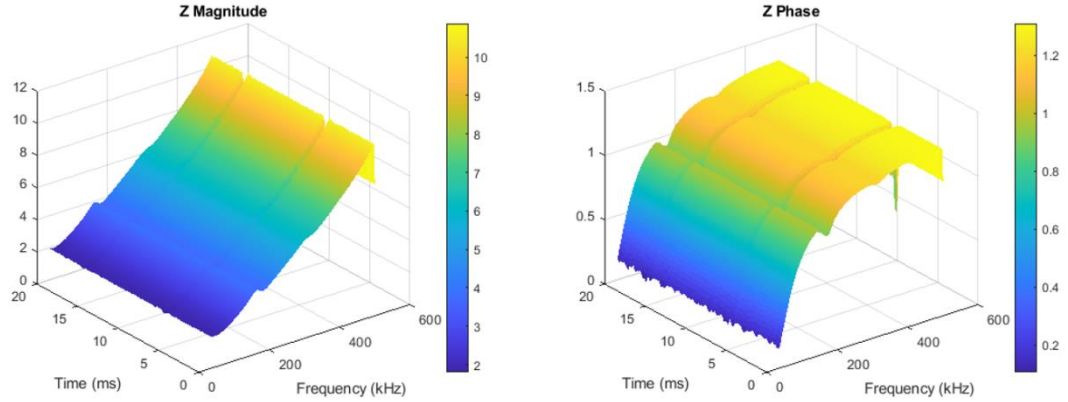

Figure 82. Modulus and phase of the impedance of a Nokia phone charger when no phone is connected

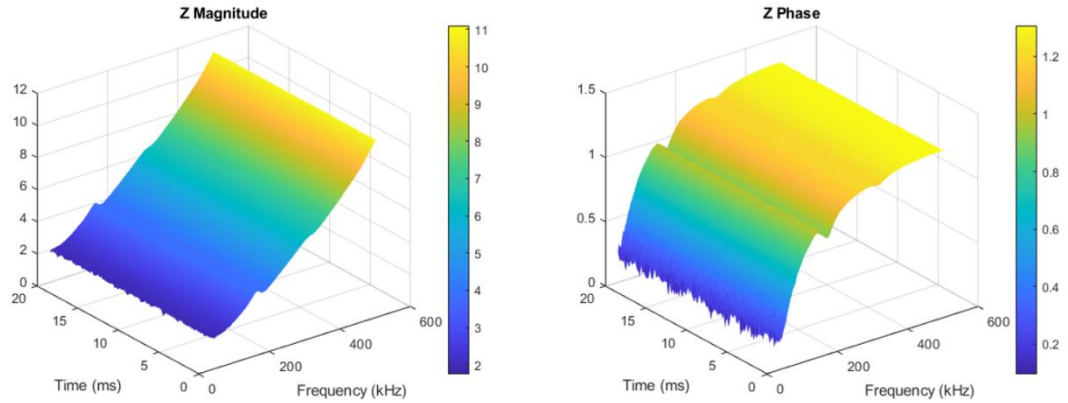

Figure 83. Modulus and phase of the impedance of a nail clipper set at high speed

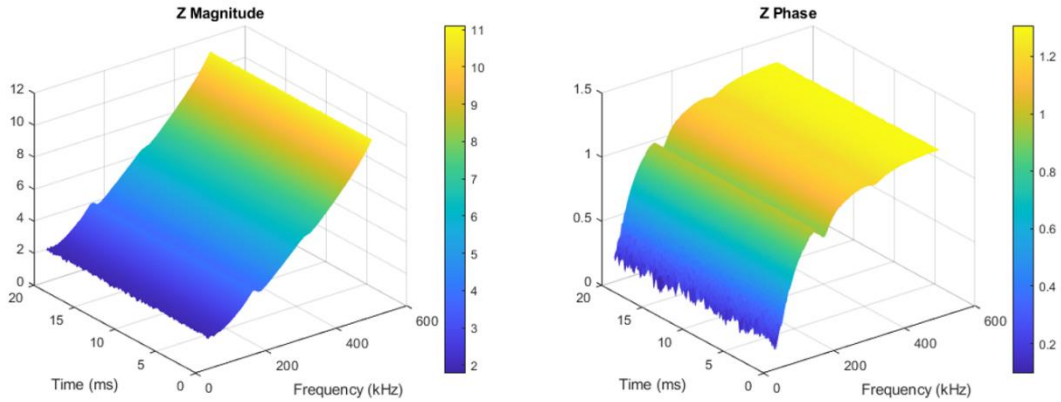

Figure 84. Modulus and phase of the impedance of a nail clipper set at low speed

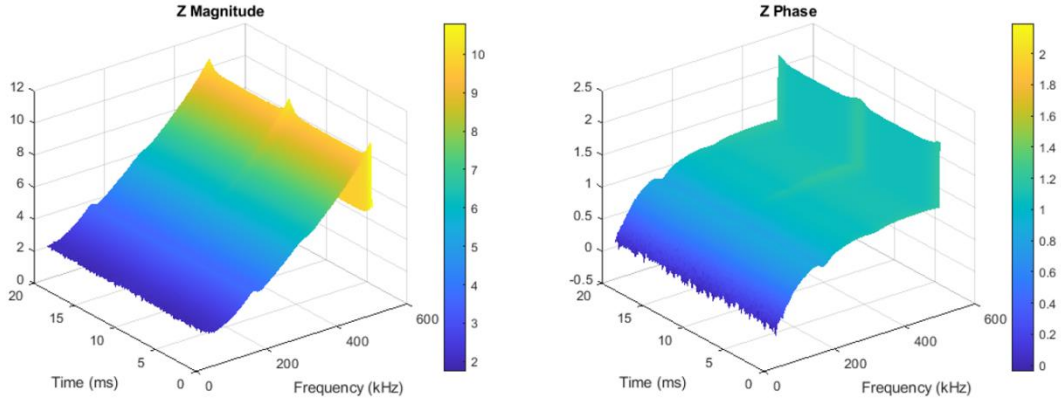

Figure 85. Modulus and phase of the impedance of a stove

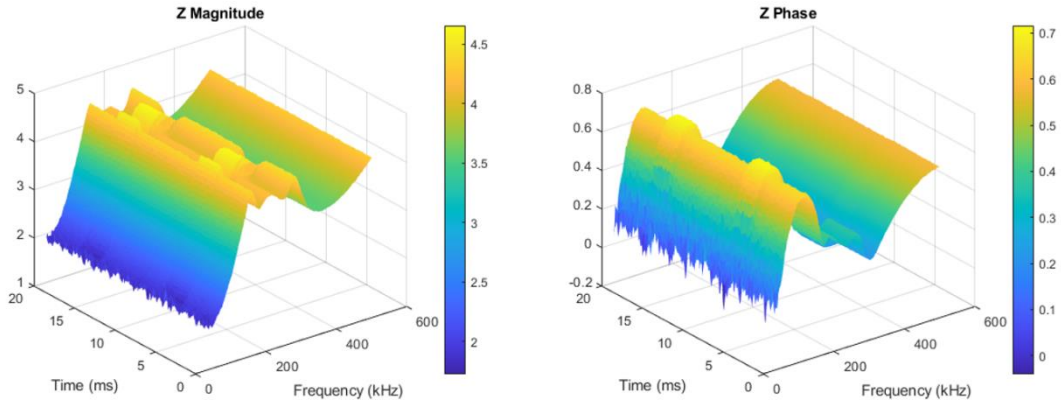

Figure 86. Modulus and phase of the impedance of a signal generator

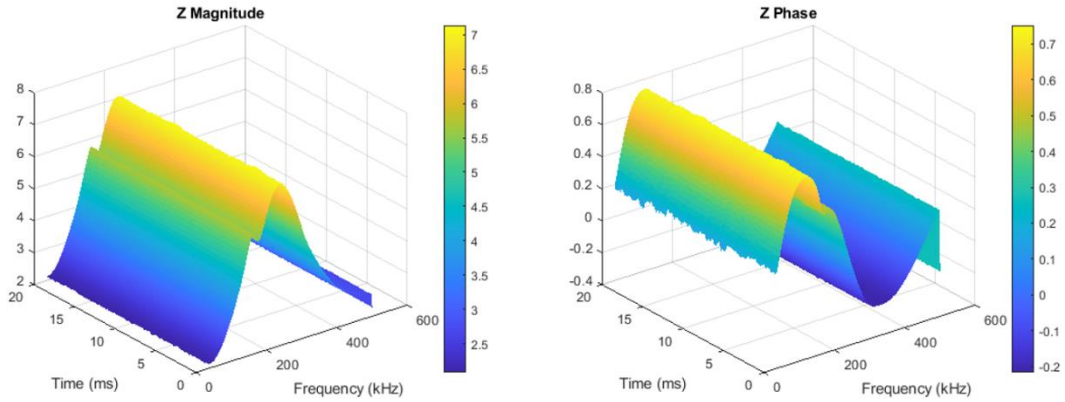

Figure 87. Modulus and phase of the impedance of a LED

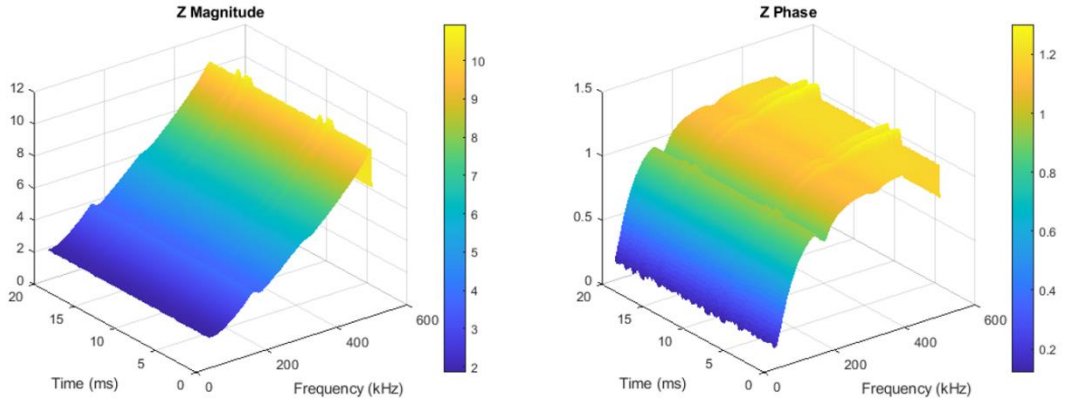

Figure 88. Modulus and phase of the impedance of an electric blanket

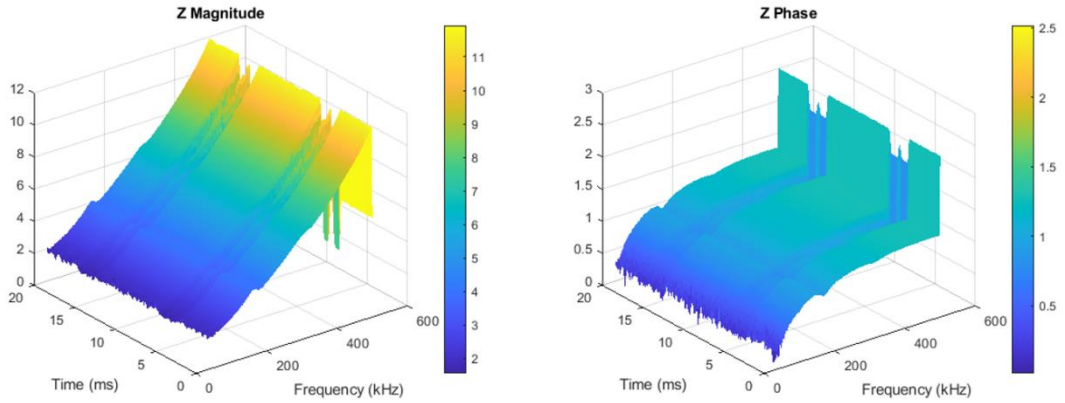

Figure 89. Modulus and phase of the impedance of a hair removal razor set at speed 2

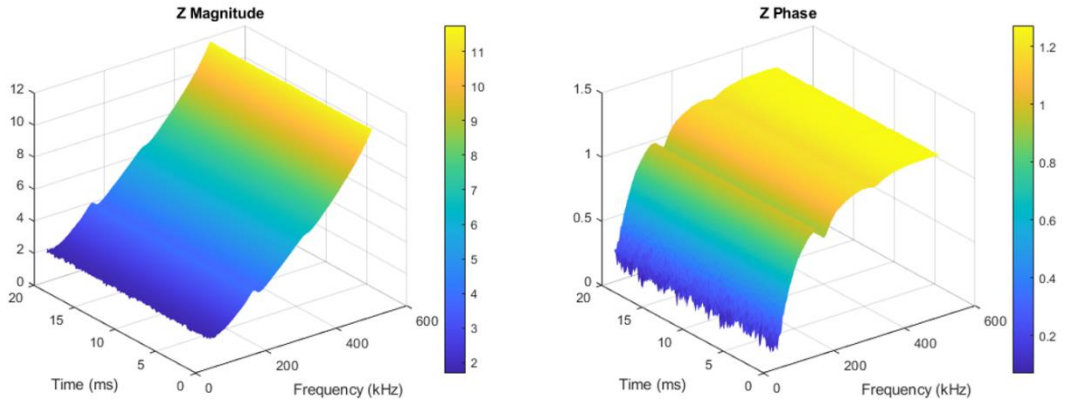

Figure 90. Modulus and phase of the impedance of a kill-bugs

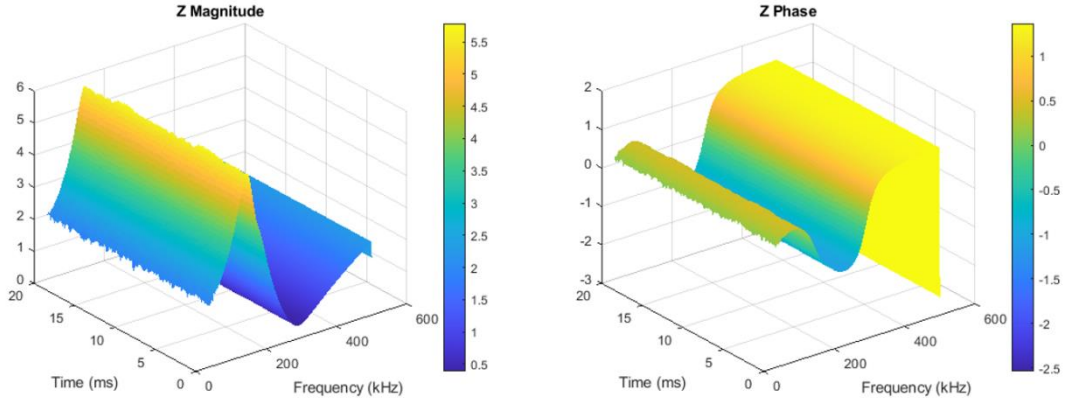

Figure 91. Modulus and phase of the impedance of a monitor

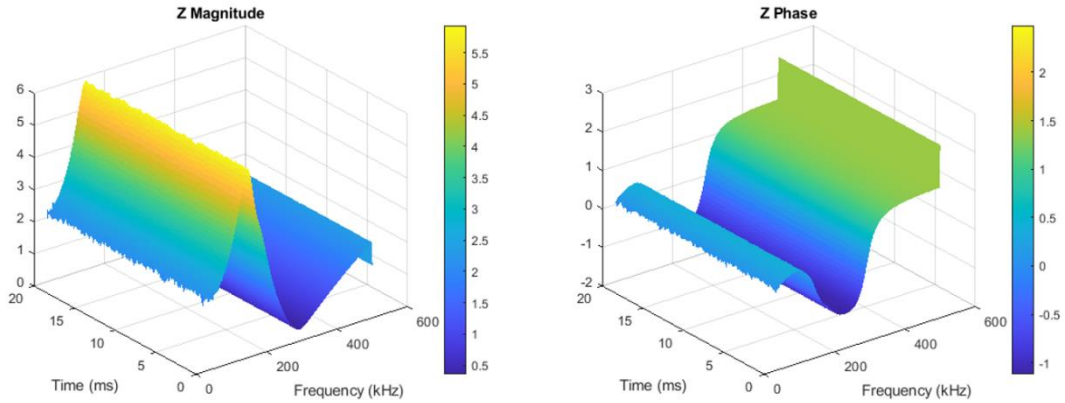

Figure 92. Modulus and phase of the impedance of a second monitor

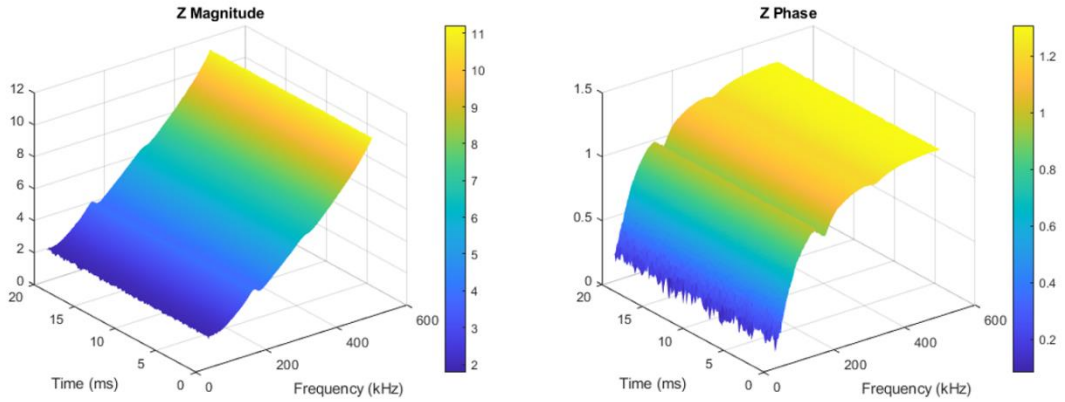

Figure 93. Modulus and phase of the impedance of an iron

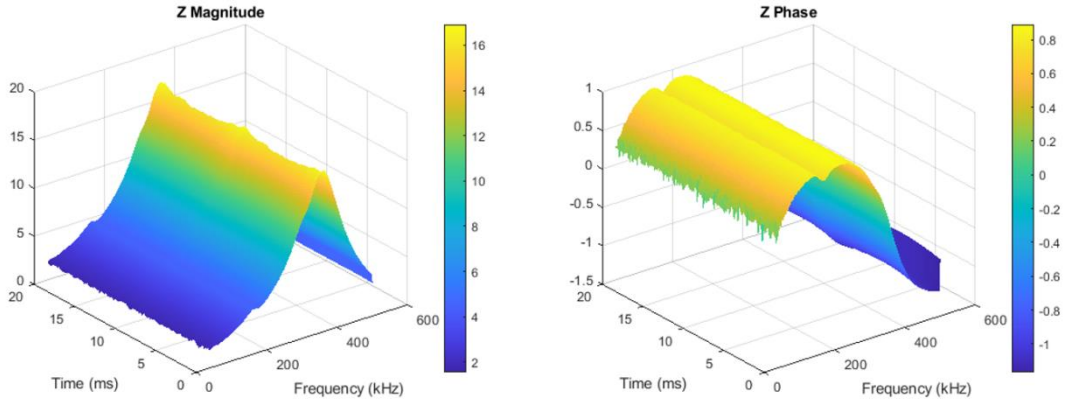

Figure 94. Modulus and phase of the impedance of a hair dryer set at speed 1

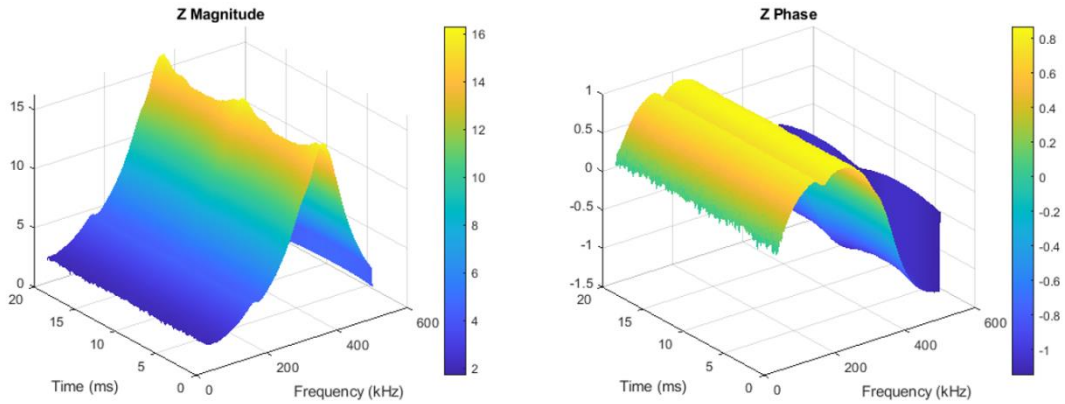

Figure 95. Modulus and phase of the impedance of a hair dryer set at speed 2

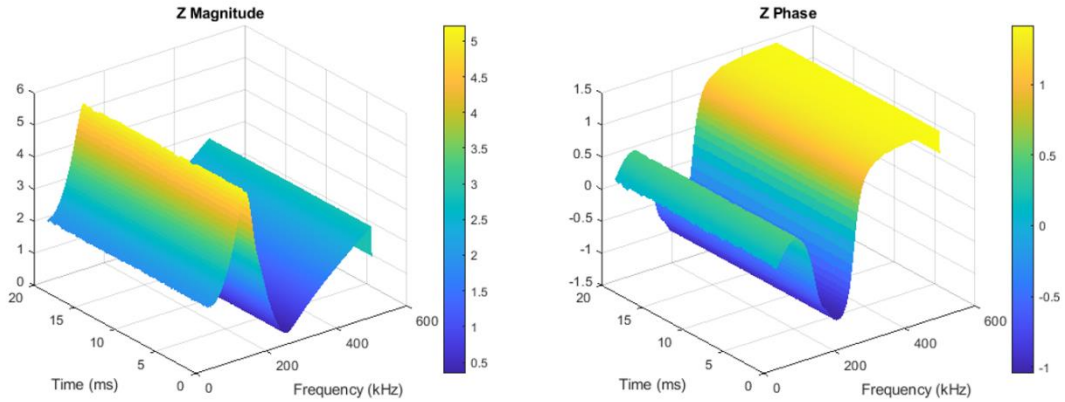

Figure 96. Modulus and phase of the impedance of a saw

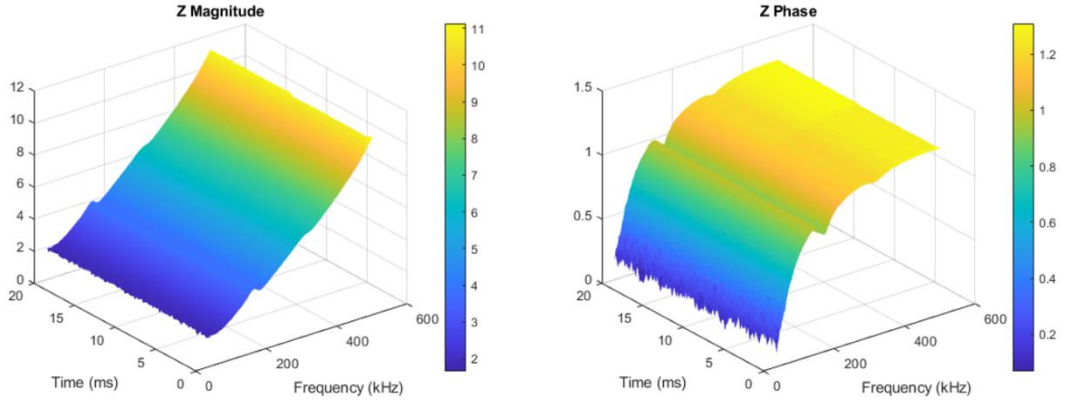

Figure 97. Modulus and phase of the impedance of a soldering iron

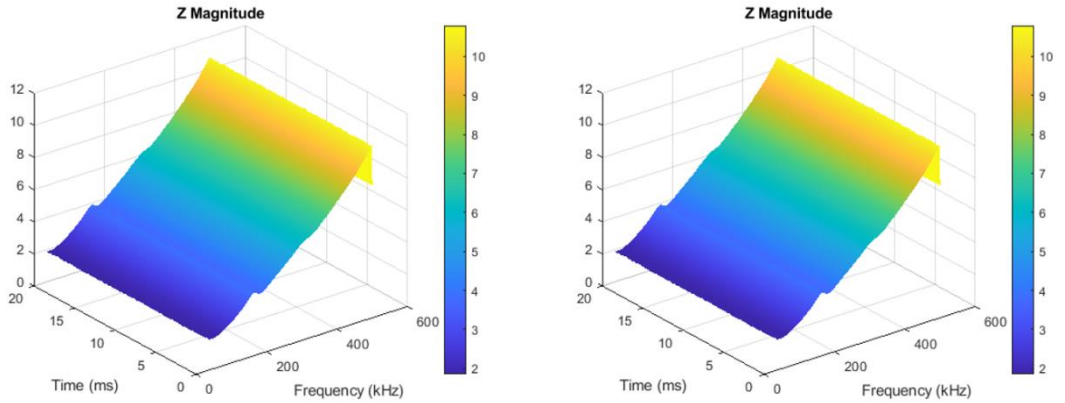

Figure 98. Modulus and phase of the impedance of a drill

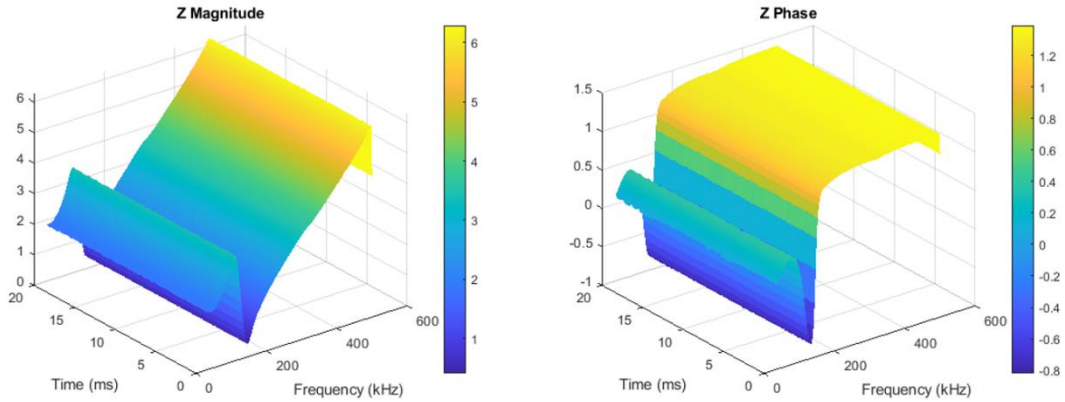

Figure 99. Modulus and phase of the impedance of an analog TV powered ON

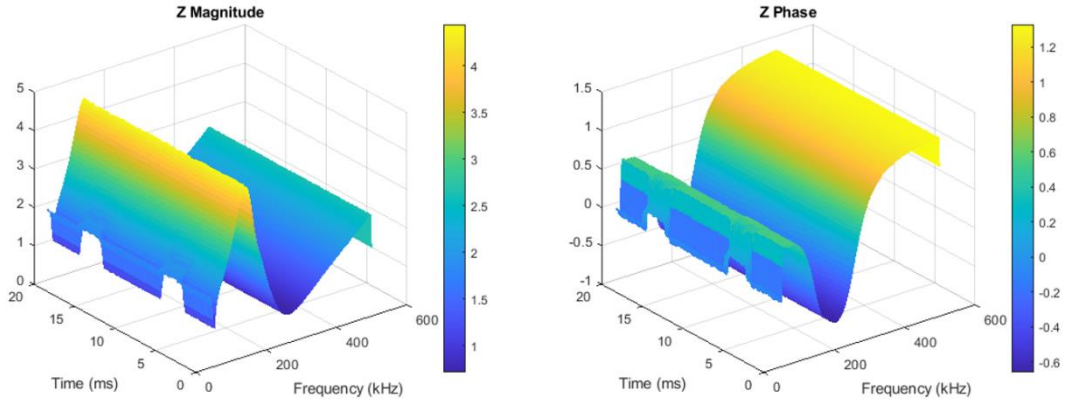

Figure 100. Modulus and phase of the impedance of a digital TV connecting an antenna

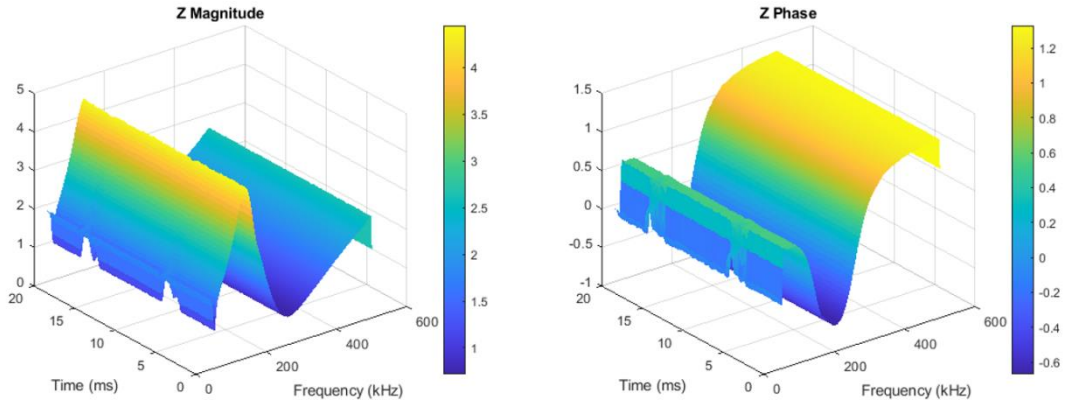

Figure 101. Modulus and phase of the impedance of a digital TV powered OFF

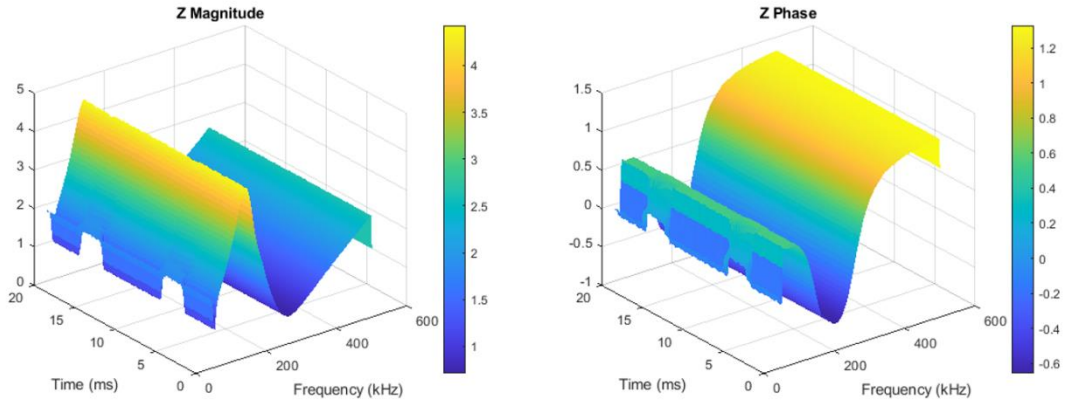

Figure 102. Modulus and phase of the impedance of a digital TV powered ON

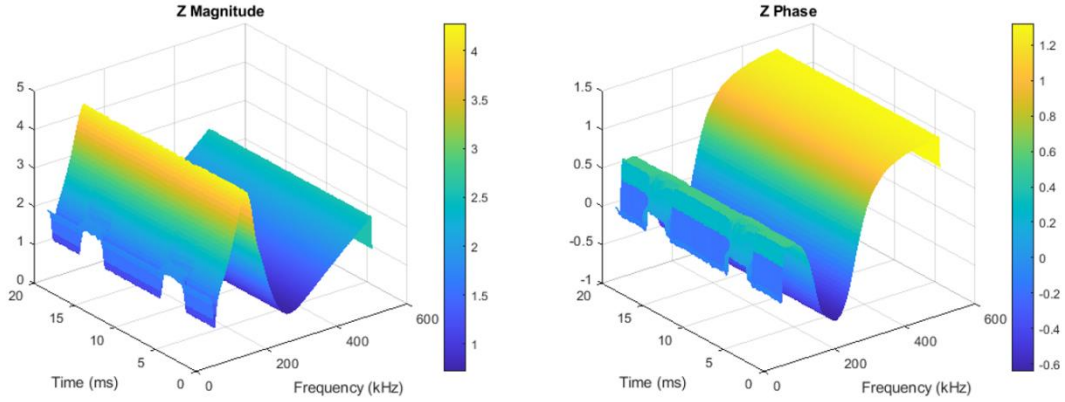

Figure 103. Modulus and phase of the impedance of a digital TV connecting a HDMI

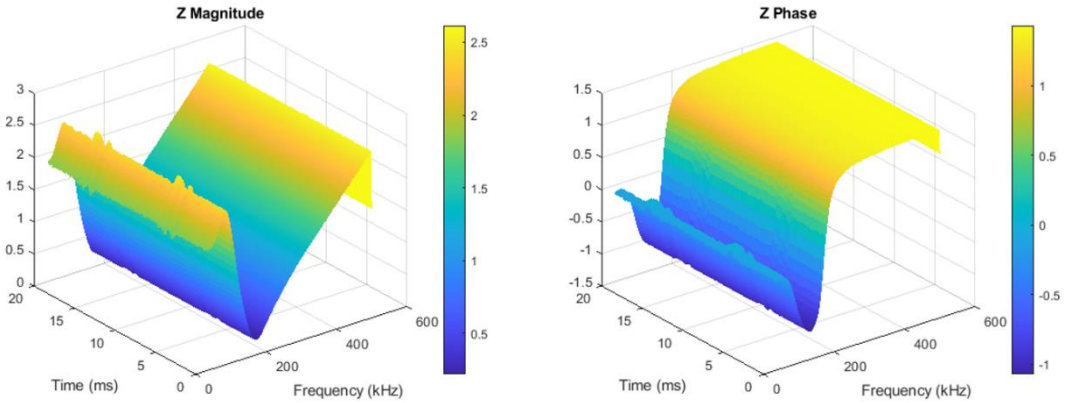

Figure 104. Modulus and phase of the impedance of a computer powered OFF

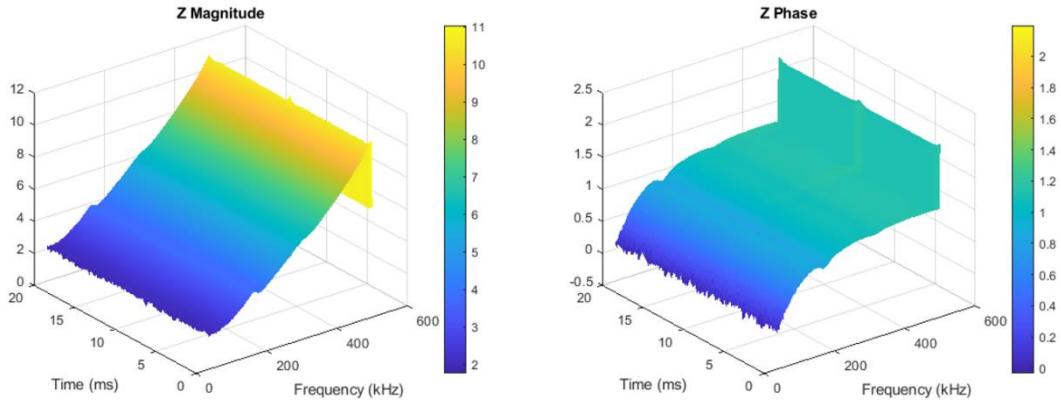

Figure 105. Modulus and phase of the impedance of a toaster

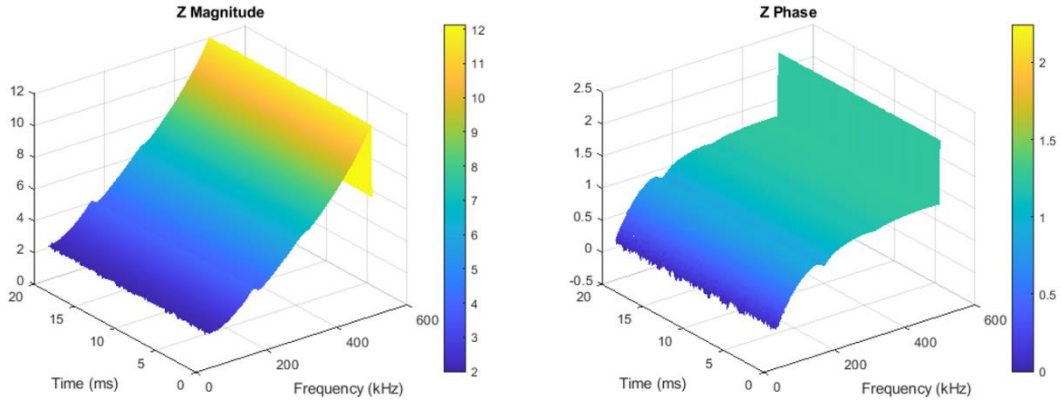

Figure 106. Modulus and phase of the impedance of a fan with motion deactivated

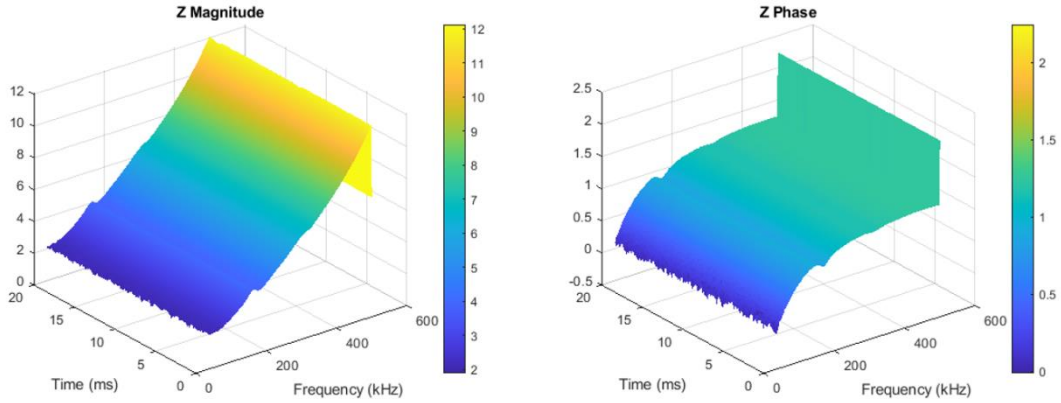

Figure 107. Modulus and phase of the impedance of a fan with motion activated

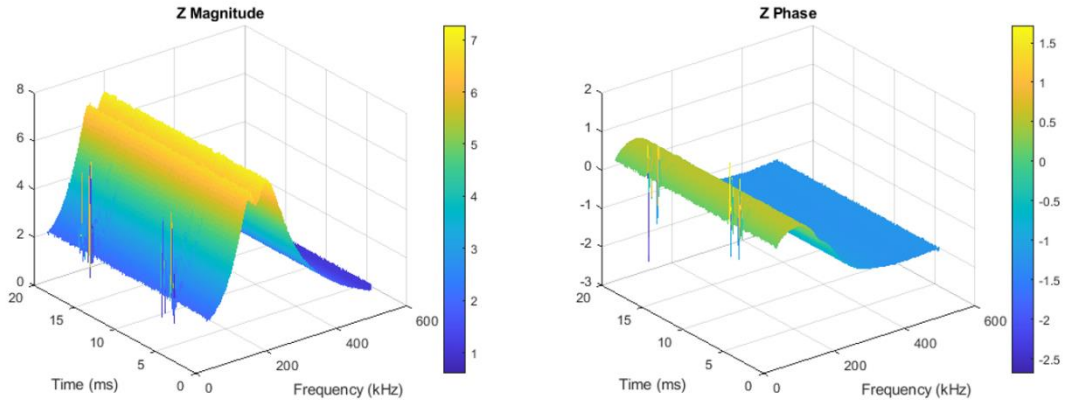

Figure 108. Modulus and phase of the impedance of a halogen lamp connected to a dimmer

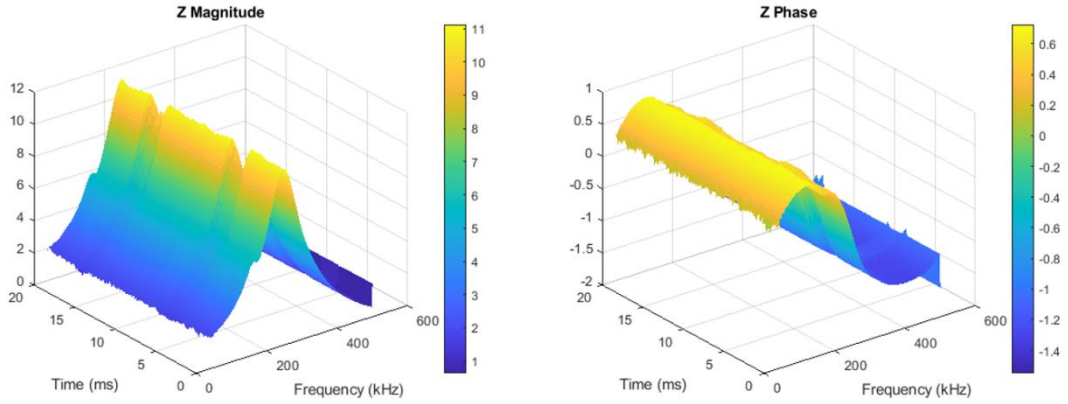

Figure 109. Modulus and phase of the impedance of a microwave oven

C.2. Mean and standard deviation of measured time-variant impedances

ON state. Impedance (Ω)		
Channel	**Mean**	**Standard deviation**
CH 1	1.33	0.08
CH 3	2.14	0.06
CH 4	2.55	0.14
CH 5	3.10	0.15
CH 6	3.62	0.15
CH 7	4.25	0.17
CH 8	4.90	0.18

Table 27. Mean and standard deviation of the impedance of the LEDs in the ON state

OFF state. Impedance (Ω)		
Channel	**Mean**	**Standard deviation**
CH 1	2.19	0.18
CH 3	3.99	0.08
CH 4	4.80	0.30
CH 5	6.01	0.33
CH 6	7.01	0.32
CH 7	8.40	0.39
CH 8	9.98	0.46

Table 28. Mean and standard deviation of the impedance of the LEDs in the OFF state

ON state. Impedance (Ω)		
Channel	**Mean**	**Standard deviation**
CH 1	1.94	0.13
CH 3	3.52	0.07
CH 4	4.21	0.25
CH 5	5.16	0.24
CH 6	5.91	0.24
CH 7	6.85	0.26
CH 8	7.88	0.27

Table 29. Mean and standard deviation of the impedance of the Nokia phone charger in the ON state

OFF state. Impedance (Ω)		
Channel	**Mean**	**Standard deviation**
CH 1	2.06	0.14
CH 3	3.84	0.07
CH 4	4.59	0.28
CH 5	5.70	0.30
CH 6	6.59	0.27
CH 7	7.78	0.33
CH 8	9.13	0.39

Table 30. Mean and standard deviation of the impedance of the Nokia phone charger in the OFF state

ON state. Impedance (Ω)		
Channel	**Mean**	**Standard deviation**
CH 1	2.02	0.12
CH 3	3.69	0.07
CH 4	4.43	0.27
CH 5	5.47	0.27
CH 6	6.29	0.25
CH 7	7.37	0.30
CH 8	8.53	0.32

Table 31. Mean and standard deviation of the impedance of the safety razor in the ON state

OFF state. Impedance (Ω)		
Channel	**Mean**	**Standard deviation**
CH 1	2.10	0.13
CH 3	3.90	0.08
CH 4	4.67	0.30
CH 5	5.82	0.31
CH 6	6.74	0.27
CH 7	7.96	0.34
CH 8	9.33	0.39

Table 32. Mean and standard deviation of the impedance of the safety razor in the OFF state

ON state. Impedance (Ω)		
Channel	**Mean**	**Standard deviation**
CH 1	2.02	0.16
CH 3	3.49	0.08
CH 4	4.24	0.24
CH 5	5.10	0.21
CH 6	5.72	0.21
CH 7	6.54	0.19
CH 8	7.26	0.19

Table 33. Mean and standard deviation of the impedance of the hair removal razor in the ON state

OFF state. Impedance (Ω)		
Channel	**Mean**	**Standard deviation**
CH 1	2.21	0.18
CH 3	4.03	0.08
CH 4	4.87	0.31
CH 5	6.08	0.32
CH 6	7.08	0.32
CH 7	8.44	0.38
CH 8	10.00	0.45

Table 34. Mean and standard deviation of the impedance of the hair removal razor in the OFF state

ON state. Impedance (Ω)		
Channel	**Mean**	**Standard deviation**
CH 1	2.07	0.15
CH 3	3.79	0.07
CH 4	4.53	0.27
CH 5	5.56	0.26
CH 6	6.35	0.25
CH 7	7.40	0.28
CH 8	8.48	0.30

Table 35. Mean and standard deviation of the impedance of the hair clippers in the ON state

OFF state. Impedance (Ω)		
Channel	**Mean**	**Standard deviation**
CH 1	2.18	0.16
CH 3	4.07	0.08
CH 4	4.84	0.30
CH 5	6.02	0.32
CH 6	6.95	0.28
CH 7	8.20	0.35
CH 8	9.61	0.41

Table 36. Mean and standard deviation of the impedance of the hair clippers in the OFF state

OFF state. Impedance (Ω)		
Channel	**Mean**	**Standard deviation**
CH 1	2.05	0.17
CH 3	3.69	0.08
CH 4	4.39	0.23
CH 5	5.21	0.20
CH 6	5.79	0.20
CH 7	6.52	0.18
CH 8	7.15	0.17

Table 37. Mean and standard deviation of the impedance of the alarm clock in the ON state

OFF state. Impedance (Ω)		
Channel	**Mean**	**Standard deviation**
CH 1	2.38	0.20
CH 3	4.50	0.09
CH 4	5.41	0.33
CH 5	6.72	0.35
CH 6	7.75	0.32
CH 7	9.16	0.39
CH 8	10.74	0.45

Table 38. Mean and standard deviation of the impedance of the alarm clock in the ON state

C.3. Calculation of k_1 and k_3 on the different frequency channels

Load	k_1	k_3
CH 1	0.69	0.61
CH 3	0.63	0.54
CH 4	0.62	0.53
CH 5	0.61	0.52
CH 6	0.61	0.52
CH 7	0.60	0.51
CH 8	0.59	0.49

Table 39. k_1 and k_3 parameters on the different frequency channels for the LEDs

Load	k_1	k_3
CH 1	0.95	0.94
CH 3	0.93	0.93
CH 4	0.93	0.91
CH 5	0.92	0.92
CH 6	0.92	0.91
CH 7	0.90	0.90
CH 8	0.89	0.86

Table 40. k_1 and k_3 parameters on the different frequency channels for the Nokia phone charger

Load	k_1	k_3
CH 1	0.97	0.96
CH 3	0.96	0.95
CH 4	0.96	0.95
CH 5	0.96	0.94
CH 6	0.95	0.93
CH 7	0.94	0.93
CH 8	0.94	0.91

Table 41. k_1 and k_3 parameters on the different frequency channels for the safety razor

Load	k_1	k_3
CH 1	0.93	0.92
CH 3	0.89	0.87
CH 4	0.89	0.87
CH 5	0.87	0.84
CH 6	0.84	0.81
CH 7	0.91	0.78
CH 8	0.77	0.73

Table 42. k_1 and k_3 parameters on the different frequency channels for the hair removal razor

Load	$\mathbf{k_1}$	$\mathbf{k_3}$
CH 1	0.96	0.95
CH 3	0.95	0.93
CH 4	0.95	0.93
CH 5	0.94	0.92
CH 6	0.93	0.91
CH 7	0.92	0.90
CH 8	0.90	0.88

Table 43. k_1 and k_3 parameters on the different frequency channels for the hair clippers

Load	$\mathbf{k_1}$	$\mathbf{k_3}$
CH 1	0.88	0.86
CH 3	0.85	0.82
CH 4	0.84	0.81
CH 5	0.81	0.78
CH 6	0.78	0.75
CH 7	0.75	0.72
CH 8	0.71	0.67

Table 44. k_1 and k_3 parameters on the different frequency channels for the alarm clock

C.4. Mean and standard deviation of the attenuation due to time-variant impedances

C.4.1. LEDs

ON state. Attenuation (dB)		
Channel	**Mean**	**Standard deviation**
CH 1	-0.17	0.10
CH 3	-1.15	0.17
CH 4	-1.04	0.14
CH 5	-1.12	0.11
CH 6	-1.22	0.10
CH 7	-1.31	0.12
CH 8	-1.36	0.10

Table 45. Mean and standard deviation of the attenuation due to the LEDs connected at point A in the ON state

OFF state. Attenuation (dB)		
Channel	**Mean**	**Standard deviation**
CH 1	-0.02	0.04
CH 3	-0.16	0.08
CH 4	-0.14	0.06
CH 5	-0.16	0.05
CH 6	-0.15	0.04
CH 7	-0.17	0.06
CH 8	-0.21	0.05

Table 46. Mean and standard deviation of the attenuation due to the LEDs connected at point A in the OFF state

ON state. Attenuation (dB)		
Channel	**Mean**	**Standard deviation**
CH 1	0.13	0.10
CH 3	0.06	0.09
CH 4	0.09	0.06
CH 5	0.07	0.05
CH 6	0.07	0.04
CH 7	0.07	0.04
CH 8	0.08	0.04

Table 47. Mean and standard deviation of the attenuation due to the LEDs connected at point B in the ON state

OFF state. Attenuation (dB)		
Channel	**Mean**	**Standard deviation**
CH 1	0.28	0.19
CH 3	0.19	0.06
CH 4	0.15	0.03
CH 5	0.09	0.04
CH 6	0.08	0.03
CH 7	0.05	0.04
CH 8	0.04	0.05

Table 48. Mean and standard deviation of the attenuation due to the LEDs connected at point B in the OFF state

ON state. Attenuation (dB)		
Channel	**Mean**	**Standard deviation**
CH 1	3.84	0.27
CH 3	4.40	0.38
CH 4	4.46	0.28
CH 5	4.63	0.31
CH 6	4.74	0.22
CH 7	4.89	0.31
CH 8	5.33	0.30

Table 49. Mean and standard deviation of the attenuation due to the LEDs connected at point C in the ON state

OFF state. Attenuation (dB)		
Channel	**Mean**	**Standard deviation**
CH 1	0.71	0.13
CH 3	0.83	0.23
CH 4	0.81	0.22
CH 5	0.89	0.22
CH 6	0.88	0.20
CH 7	0.97	0.15
CH 8	0.95	0.14

Table 50. Mean and standard deviation of the attenuation due to the LEDs connected at point C in the OFF state

C.4.2. Nokia phone charger

ON state. Attenuation (dB)		
Channel	**Mean**	**Standard deviation**
CH 1	0.20	0.15
CH 3	-0.03	0.14
CH 4	-0.05	0.18
CH 5	-0.01	0.14
CH 6	-0.13	0.09
CH 7	-0.14	0.16
CH 8	-0.16	0.08

Table 51. Mean and standard deviation of the attenuation due to the Nokia phone charger connected at point A in the ON state

OFF state. Attenuation (dB)		
Channel	**Mean**	**Standard deviation**
CH 1	0.16	0.11
CH 3	0.01	0.08
CH 4	-0.04	0.12
CH 5	-0.03	0.10
CH 6	-0.14	0.06
CH 7	-0.14	0.06
CH 8	-0.19	0.07

Table 52. Mean and standard deviation of the attenuation due to the Nokia phone charger connected at point A in the OFF state

ON state. Attenuation (dB)		
Channel	**Mean**	**Standard deviation**
CH 1	0.23	0.16
CH 3	0.10	0.15
CH 4	0.11	0.22
CH 5	0.07	0.11
CH 6	-0.06	0.12
CH 7	-0.09	0.09
CH 8	-0.08	0.11

Table 53. Mean and standard deviation of the attenuation due to the Nokia phone charger connected at point B in the ON state

OFF state. Attenuation (dB)		
Channel	**Mean**	**Standard deviation**
CH 1	0.16	0.08
CH 3	0.01	0.07
CH 4	0.02	0.15
CH 5	-0.01	0.10
CH 6	-0.11	0.05
CH 7	-0.13	0.05
CH 8	-0.14	0.06

Table 54. Mean and standard deviation of the attenuation due to the Nokia phone charger connected at point B in the OFF state

ON state. Attenuation (dB)		
Channel	**Mean**	**Standard deviation**
CH 1	0.50	0.14
CH 3	0.38	0.15
CH 4	0.28	0.18
CH 5	0.44	0.11
CH 6	0.56	0.17
CH 7	0.65	0.18
CH 8	0.72	0.18

Table 55. Mean and standard deviation of the attenuation due to the Nokia phone charger connected at point C in the ON state

OFF state. Attenuation (dB)		
Channel	**Mean**	**Standard deviation**
CH 1	0.20	0.08
CH 3	0.03	0.07
CH 4	0.03	0.13
CH 5	0.03	0.10
CH 6	-0.04	0.07
CH 7	-0.03	0.06
CH 8	-0.02	0.07

Table 56. Mean and standard deviation of the attenuation due to the Nokia phone charger connected at point C in the OFF state

C.4.3. Safety razor

ON state. Attenuation (dB)		
Channel	**Mean**	**Standard deviation**
CH 1	0.71	0.13
CH 3	-0.03	0.27
CH 4	0.00	0.08
CH 5	-0.09	0.09
CH 6	-0.18	0.06
CH 7	-0.22	0.05
CH 8	-0.25	0.05

Table 57. Mean and standard deviation of the attenuation due to the safety razor connected at point A in the ON state

OFF state. Attenuation (dB)		
Channel	**Mean**	**Standard deviation**
CH 1	0.70	0.13
CH 3	-0.03	0.23
CH 4	0.02	0.04
CH 5	-0.12	0.05
CH 6	-0.18	0.04
CH 7	-0.21	0.04
CH 8	-0.26	0.03

Table 58. Mean and standard deviation of the attenuation due to the safety razor connected at point A in the OFF state

ON state. Attenuation (dB)		
Channel	**Mean**	**Standard deviation**
CH 1	0.72	0.15
CH 3	-0.04	0.26
CH 4	0.00	0.06
CH 5	-0.08	0.07
CH 6	-0.15	0.06
CH 7	-0.19	0.05
CH 8	-0.23	0.04

Table 59. Mean and standard deviation of the attenuation due to the safety razor connected at point B in the ON state

OFF state. Attenuation (dB)		
Channel	**Mean**	**Standard deviation**
CH 1	0.67	0.14
CH 3	-0.05	0.21
CH 4	-0.03	0.04
CH 5	-0.12	0.05
CH 6	-0.19	0.05
CH 7	-0.24	0.04
CH 8	-0.26	0.04

Table 60. Mean and standard deviation of the attenuation due to the safety razor connected at point B in the OFF state

ON state. Attenuation (dB)		
Channel	**Mean**	**Standard deviation**
CH 1	0.89	0.17
CH 3	0.21	0.27
CH 4	0.27	0.11
CH 5	0.28	0.12
CH 6	0.26	0.11
CH 7	0.30	0.10
CH 8	0.46	0.17

Table 61. Mean and standard deviation of the attenuation due to the safety razor connected at point C in the ON state

OFF state. Attenuation (dB)		
Channel	**Mean**	**Standard deviation**
CH 1	0.71	0.11
CH 3	0.02	0.24
CH 4	0.03	0.05
CH 5	-0.07	0.07
CH 6	-0.11	0.04
CH 7	-0.12	0.05
CH 8	-0.13	0.08

Table 62. Mean and standard deviation of the attenuation due to the safety razor connected at point C in the OFF state

C.4.4. Hair removal razor

ON state. Attenuation (dB)		
Channel	**Mean**	**Standard deviation**
CH 1	0.24	0.16
CH 3	0.10	0.13
CH 4	0.03	0.21
CH 5	-0.00	0.17
CH 6	-0.00	0.13
CH 7	-0.02	0.17
CH 8	-0.08	0.14

Table 63. Mean and standard deviation of the attenuation due to the hair removal razor connected at point A in the ON state

OFF state. Attenuation (dB)		
Channel	**Mean**	**Standard deviation**
CH 1	0.26	0.11
CH 3	0.05	0.08
CH 4	0.03	0.10
CH 5	0.01	0.08
CH 6	-0.07	0.06
CH 7	-0.11	0.05
CH 8	-0.08	0.06

Table 64. Mean and standard deviation of the attenuation due to the hair removal razor connected at point A in the OFF state

ON state. Attenuation (dB)		
Channel	**Mean**	**Standard deviation**
CH 1	0.25	0.12
CH 3	0.05	0.12
CH 4	0.09	0.16
CH 5	0.11	0.16
CH 6	-0.01	0.14
CH 7	-0.06	0.09
CH 8	-0.04	0.11

Table 65. Mean and standard deviation of the attenuation due to the hair removal razor connected at point B in the ON state

OFF state. Attenuation (dB)		
Channel	**Mean**	**Standard deviation**
CH 1	0.15	0.09
CH 3	0.00	0.07
CH 4	-0.01	0.14
CH 5	0.00	0.11
CH 6	-0.10	0.05
CH 7	-0.14	0.06
CH 8	-0.14	0.06

Table 66. Mean and standard deviation of the attenuation due to the hair removal razor connected at point B in the OFF state

ON state. Attenuation (dB)		
Channel	**Mean**	**Standard deviation**
CH 1	0.66	0.19
CH 3	0.79	0.18
CH 4	0.72	0.24
CH 5	1.05	0.18
CH 6	1.24	0.24
CH 7	1.39	0.26
CH 8	1.77	0.15

Table 67. Mean and standard deviation of the attenuation due to the hair removal razor connected at point C in the ON state

OFF state. Attenuation (dB)		
Channel	**Mean**	**Standard deviation**
CH 1	0.17	0.11
CH 3	0.07	0.07
CH 4	0.09	0.18
CH 5	0.12	0.08
CH 6	0.09	0.08
CH 7	0.10	0.08
CH 8	0.15	0.07

Table 68. Mean and standard deviation of the attenuation due to the hair removal razor connected at point C in the OFF state

C.4.5. Hair clippers

ON state. Attenuation (dB)		
Channel	**Mean**	**Standard deviation**
CH 1	0.80	0.19
CH 3	0.01	0.25
CH 4	0.06	0.07
CH 5	-0.05	0.06
CH 6	-0.14	0.08
CH 7	-0.17	0.05
CH 8	-0.19	0.08

Table 69. Mean and standard deviation of the attenuation due to the hair clippers razor connected at point A in the ON state

OFF state. Attenuation (dB)		
Channel	**Mean**	**Standard deviation**
CH 1	0.80	0.13
CH 3	0.04	0.25
CH 4	0.07	0.04
CH 5	-0.06	0.06
CH 6	-0.13	0.03
CH 7	-0.19	0.04
CH 8	-0.21	0.04

Table 70. Mean and standard deviation of the attenuation due to the hair clippers razor connected at point A in the OFF state

ON state. Attenuation (dB)		
Channel	**Mean**	**Standard deviation**
CH 1	0.74	0.18
CH 3	0.09	0.30
CH 4	0.09	0.10
CH 5	0.00	0.08
CH 6	-0.09	0.05
CH 7	-0.12	0.05
CH 8	-0.19	0.07

Table 71. Mean and standard deviation of the attenuation due to the hair clippers razor connected at point B in the ON state

OFF state. Attenuation (dB)		
Channel	**Mean**	**Standard deviation**
CH 1	0.72	0.13
CH 3	0.02	0.23
CH 4	0.06	0.05
CH 5	-0.07	0.04
CH 6	-0.14	0.03
CH 7	-0.20	0.02
CH 8	-0.22	0.03

Table 72. Mean and standard deviation of the attenuation due to the hair clippers razor connected at point B in the OFF state

ON state. Attenuation (dB)		
Channel	**Mean**	**Standard deviation**
CH 1	1.03	0.17
CH 3	0.38	0.22
CH 4	0.45	0.20
CH 5	0.45	0.15
CH 6	0.43	0.17
CH 7	0.51	0.21
CH 8	0.61	0.24

Table 73. Mean and standard deviation of the attenuation due to the hair clippers connected at point C in the ON state

OFF state. Attenuation (dB)		
Channel	**Mean**	**Standard deviation**
CH 1	0.86	0.15
CH 3	0.15	0.26
CH 4	0.16	0.04
CH 5	0.06	0.05
CH 6	0.02	0.06
CH 7	0.01	0.05
CH 8	0.08	0.07

Table 74. Mean and standard deviation of the attenuation due to the hair clippers connected at point C in the OFF state

C.4.6. Alarm clock

ON state. Attenuation (dB)		
Channel	**Mean**	**Standard deviation**
CH 1	0.66	0.21
CH 3	0.09	0.23
CH 4	0.25	0.16
CH 5	0.16	0.13
CH 6	0.10	0.07
CH 7	0.09	0.08
CH 8	0.07	0.08

Table 75. Mean and standard deviation of the attenuation due to the alarm clock razor connected at point A in the ON state

OFF state. Attenuation (dB)		
Channel	**Mean**	**Standard deviation**
CH 1	0.64	0.14
CH 3	0.09	0.20
CH 4	0.18	0.11
CH 5	0.13	0.05
CH 6	0.06	0.04
CH 7	0.06	0.03
CH 8	0.06	0.04

Table 76. Mean and standard deviation of the attenuation due to the alarm clock razor connected at point A in the OFF state

ON state. Attenuation (dB)		
Channel	**Mean**	**Standard deviation**
CH 1	1.67	0.48
CH 3	1.21	0.21
CH 4	1.25	0.16
CH 5	1.00	0.11
CH 6	0.81	0.08
CH 7	0.71	0.07
CH 8	0.65	0.10

Table 77. Mean and standard deviation of the attenuation due to the alarm clock razor connected at point B in the ON state

OFF state. Attenuation (dB)		
Channel	**Mean**	**Standard deviation**
CH 1	1.59	0.41
CH 3	1.07	0.16
CH 4	1.07	0.12
CH 5	0.81	0.08
CH 6	0.66	0.06
CH 7	0.55	0.04
CH 8	0.49	0.03

Table 78. Mean and standard deviation of the attenuation due to the alarm clock razor connected at point B in the OFF state

ON state. Attenuation (dB)		
Channel	**Mean**	**Standard deviation**
CH 1	2.65	0.41
CH 3	2.84	0.38
CH 4	2.75	0.21
CH 5	3.18	0.35
CH 6	3.38	0.33
CH 7	3.97	0.33
CH 8	4.73	0.39

Table 79. Mean and standard deviation of the attenuation due to the alarm clock connected at point C in the ON state

OFF state. Attenuation (dB)		
Channel	**Mean**	**Standard deviation**
CH 1	1.84	0.41
CH 3	1.45	0.15
CH 4	1.43	0.14
CH 5	1.24	0.12
CH 6	1.19	0.12
CH 7	1.23	0.09
CH 8	1.42	0.12

Table 80. Mean and standard deviation of the attenuation due to the alarm clock connected at point C in the OFF state

C.5. Analysis of the influence of time-variant impedances connected in Rx. FER-SNR curves

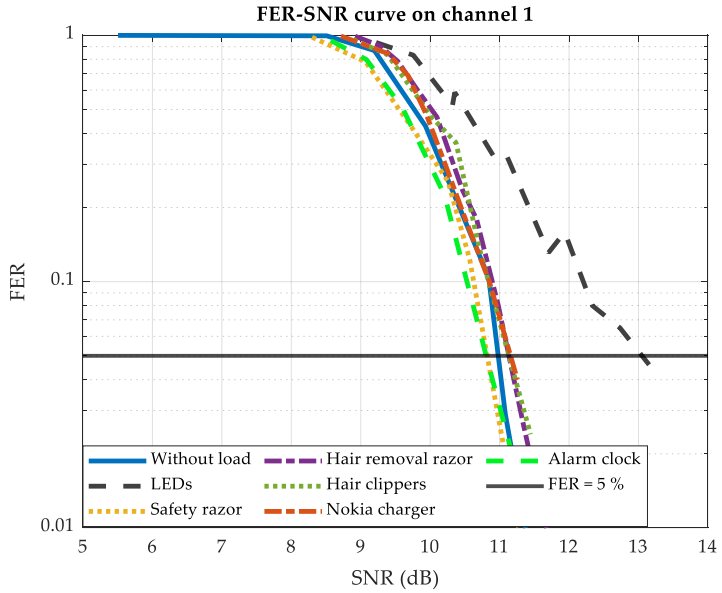

Figure 110. FER-SNR curve on channel 1 for DBPSK without load and when the time-variant loads are connected to point C

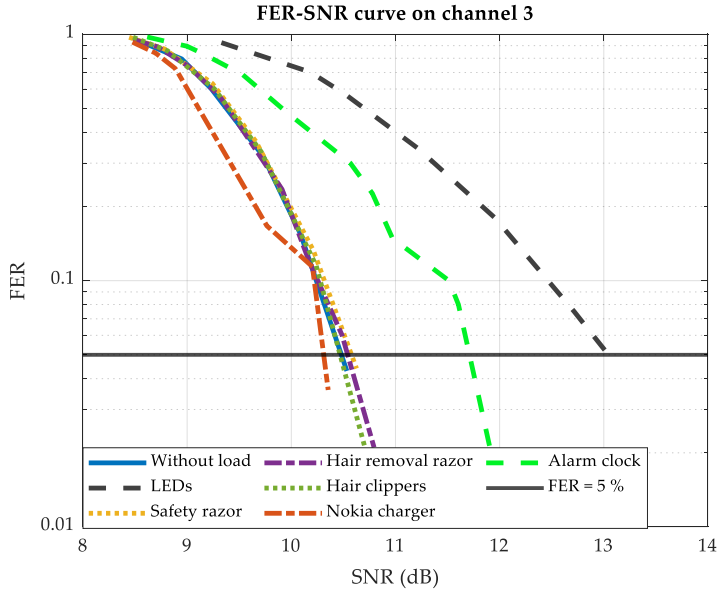

Figure 111. FER-SNR curve on channel 3 for DBPSK without load and when the time-variant loads are connected to point C

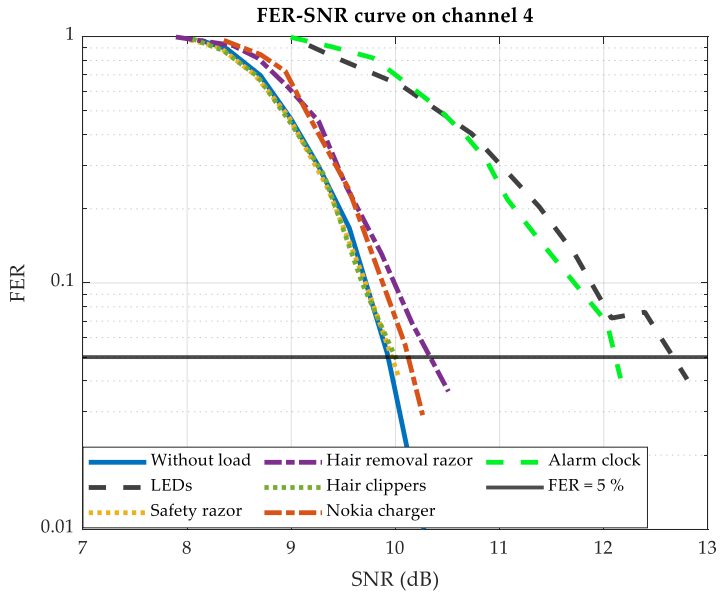

Figure 112. FER-SNR curve on channel 4 for DBPSK without load and when the time-variant loads are connected to point C

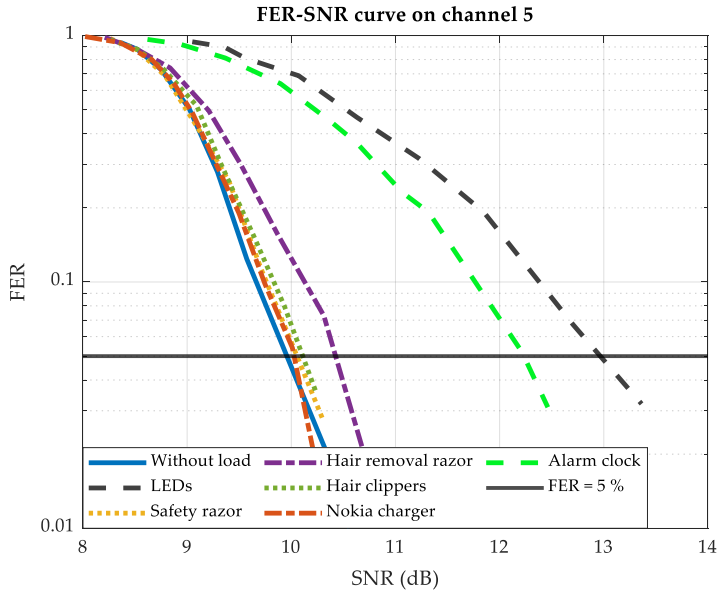

Figure 113. FER-SNR curve on channel 5 for DBPSK without load and when the time-variant loads are connected to point C

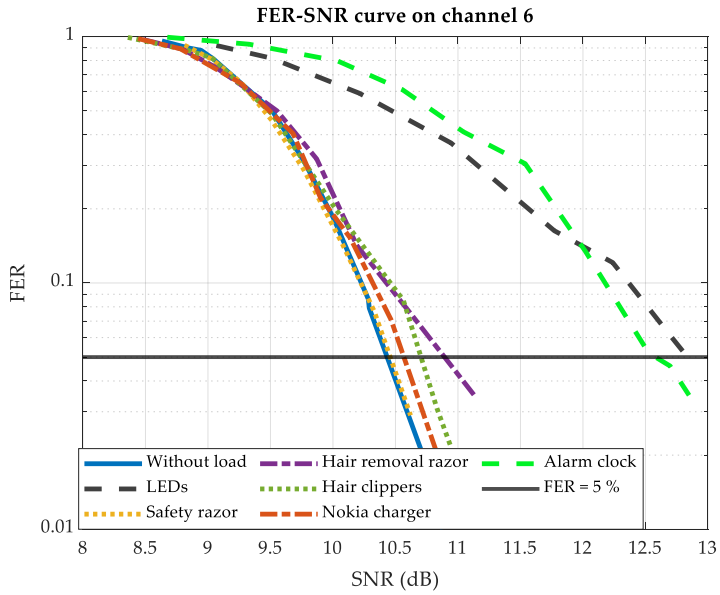

Figure 114. FER-SNR curve on channel 6 for DBPSK without load and when the time-variant loads are connected to point C

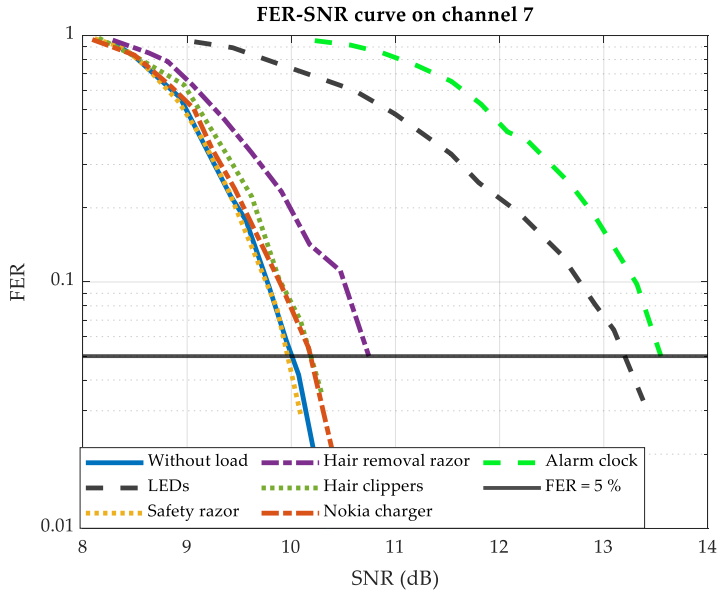

Figure 115. FER-SNR curve on channel 7 for DBPSK without load and when the time-variant loads are connected to point C

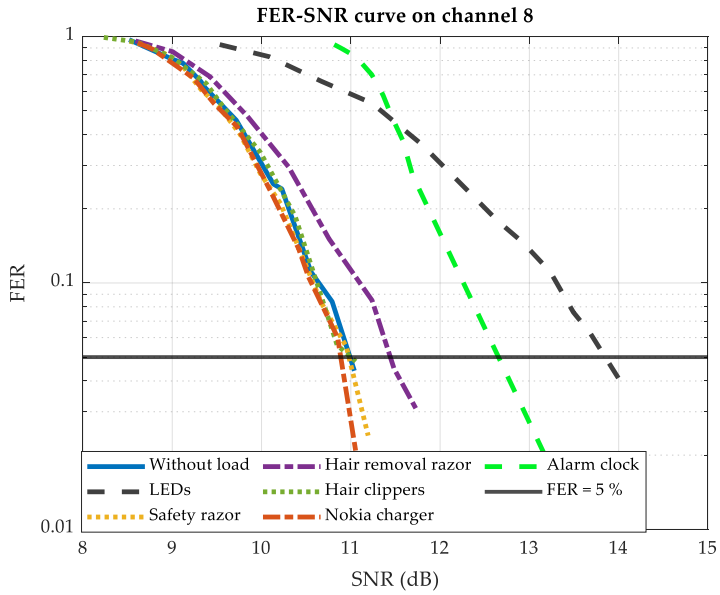

Figure 116. FER-SNR curve on channel 8 for DBPSK without load and when the time-variant loads are connected to point C

C.6. Analysis of the influence of the robustness of modulations against time-variant loads. FER-SNR curves

C.6.1. LEDs

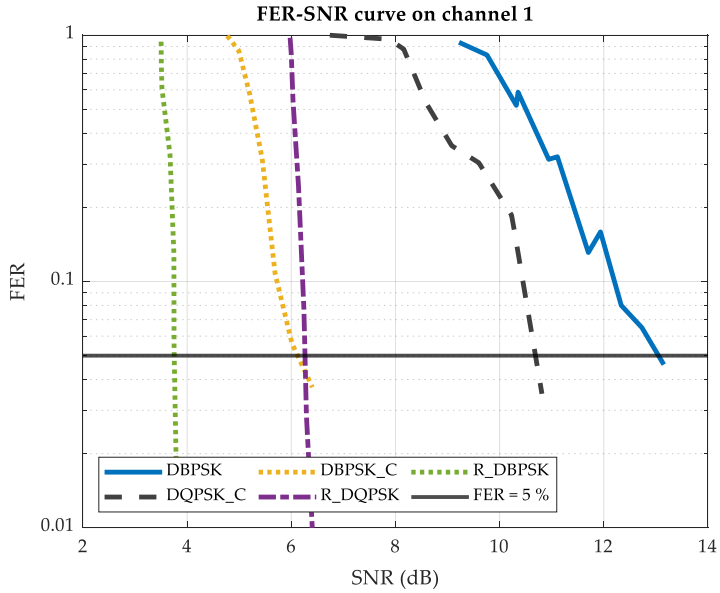

Figure 117. FER-SNR curve on channel 1 for different modulations when the LEDs connected to point C

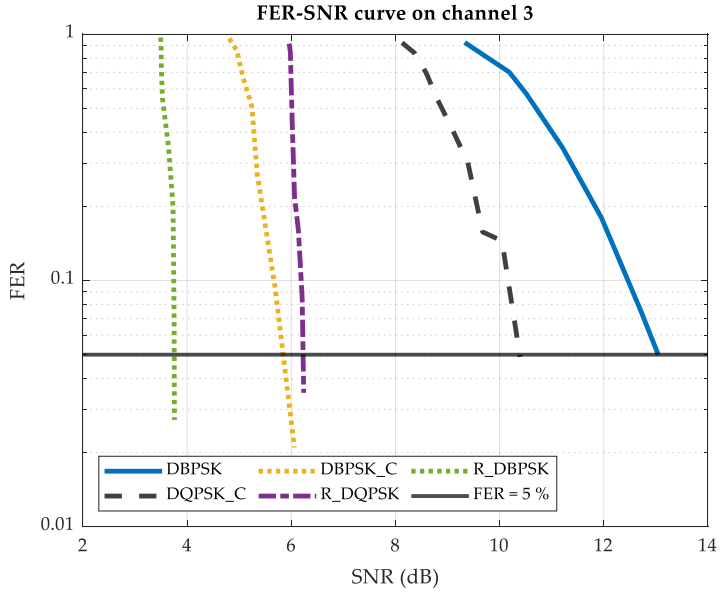

Figure 118. FER-SNR curve on channel 3 for different modulations when the LEDs connected to point C

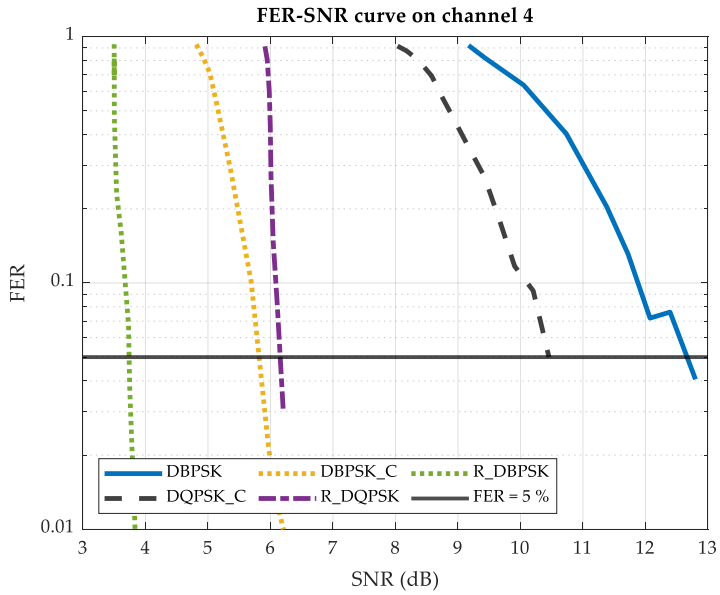

Figure 119. FER-SNR curve on channel 4 for different modulations when the LEDs connected to point C

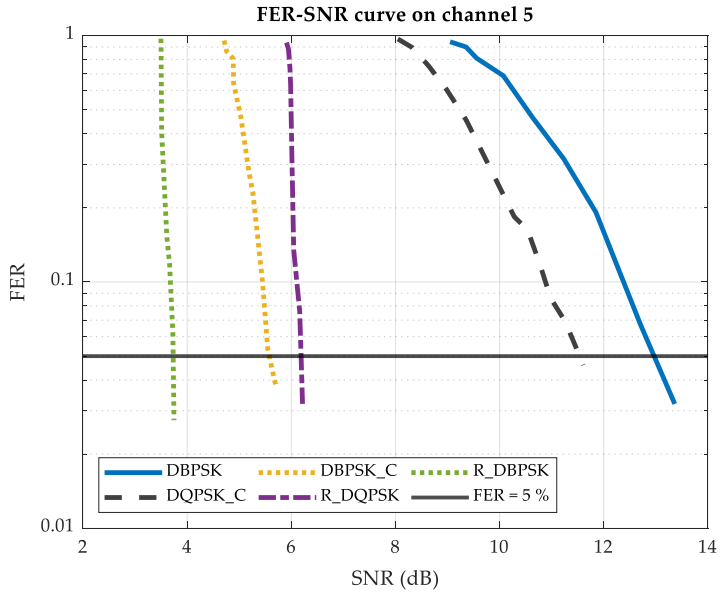

Figure 120. FER-SNR curve on channel 5 for different modulations when the LEDs connected to point C

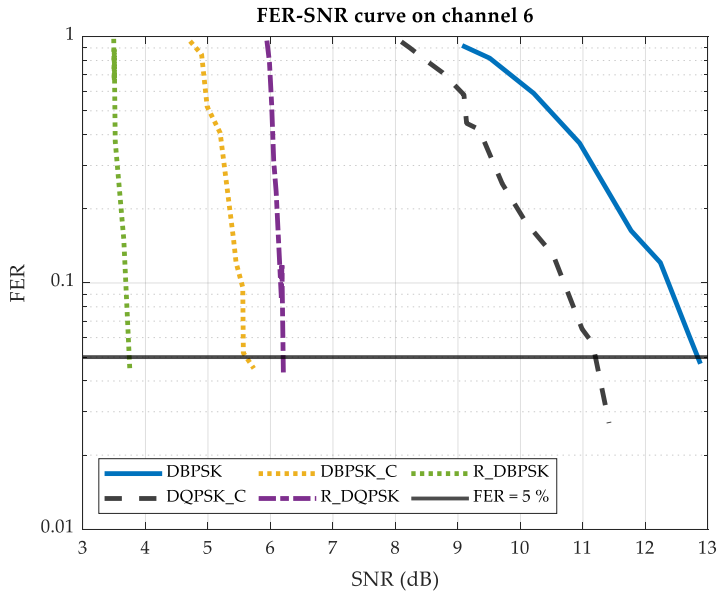

Figure 121. FER-SNR curve on channel 6 for different modulations when the LEDs connected to point C

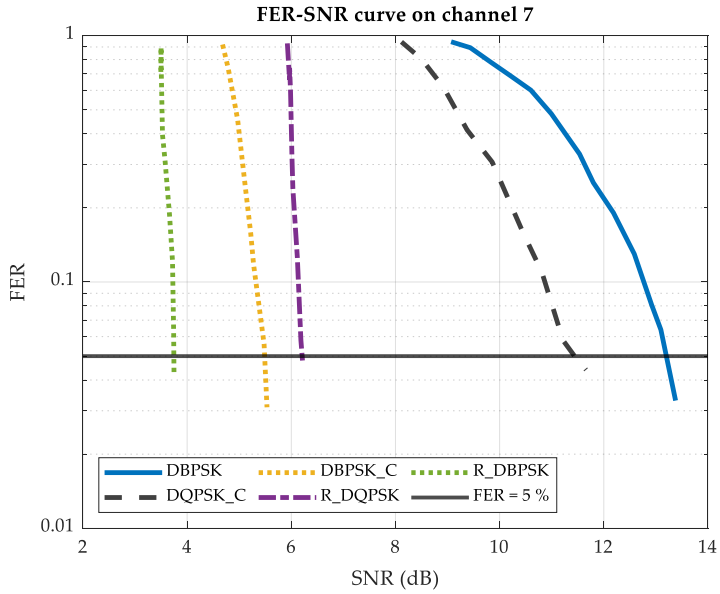

Figure 122. FER-SNR curve on channel 7 for different modulations when the LEDs connected to point C

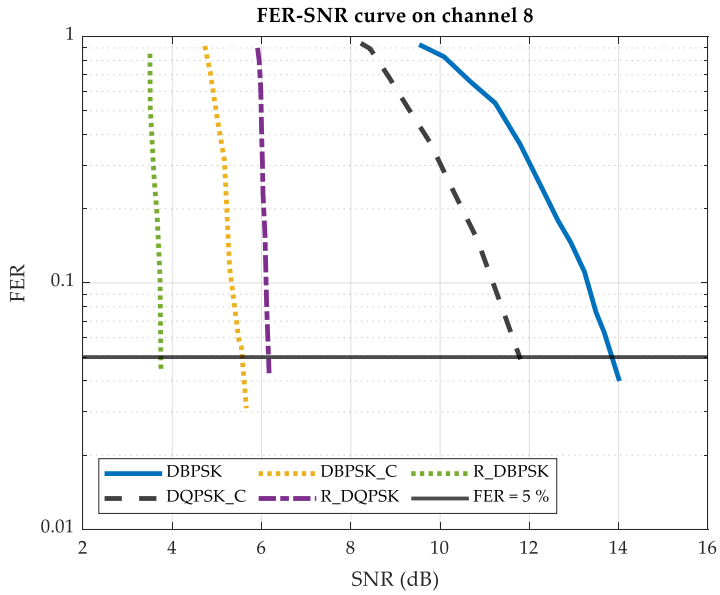

Figure 123. FER-SNR curve on channel 8 for different modulations when the LEDs connected to point C

C.6.2. Alarm clock

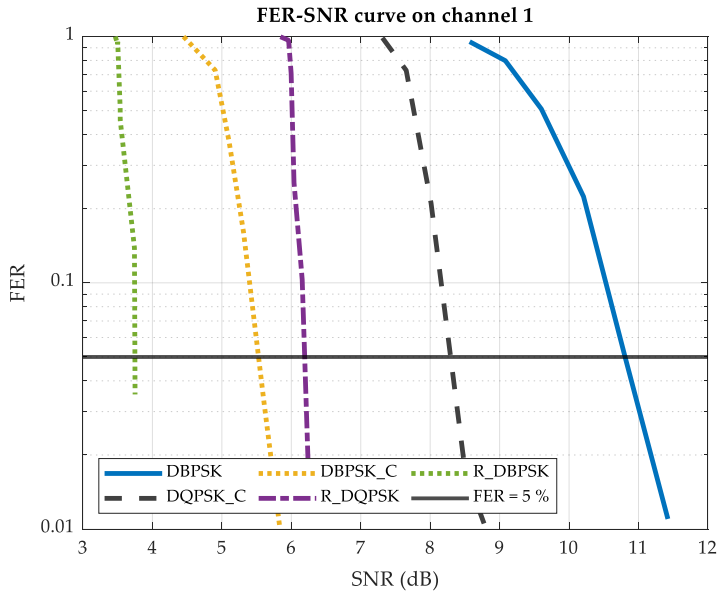

Figure 124. FER-SNR curve on channel 1 for different modulations when the alarm clock connected to point C

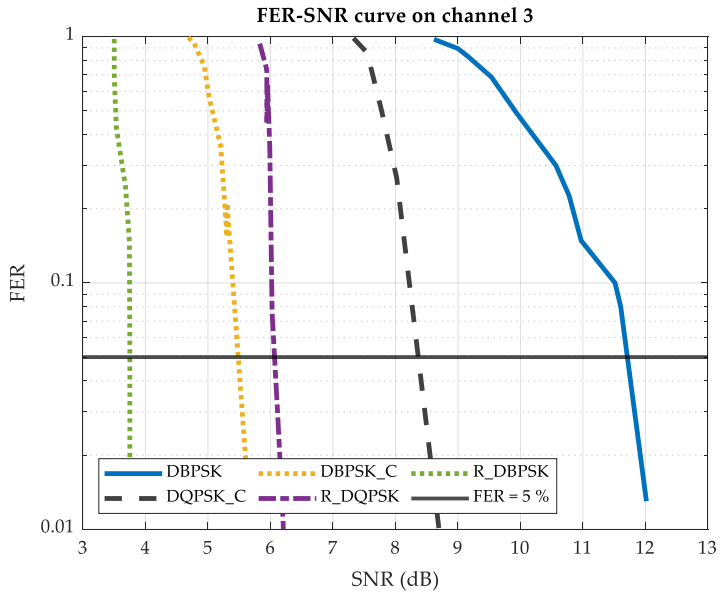

Figure 125. FER-SNR curve on channel 3 for different modulations when the alarm clock connected to point C

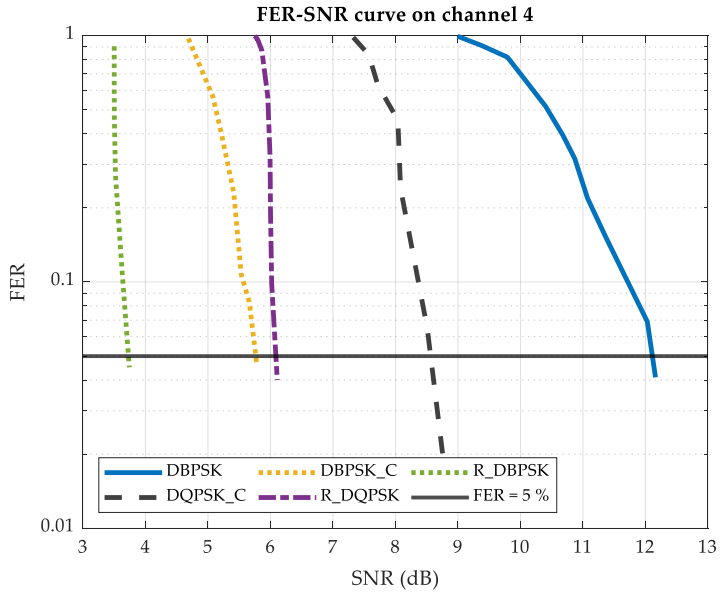

Figure 126. FER-SNR curve on channel 4 for different modulations when the alarm clock connected to point C

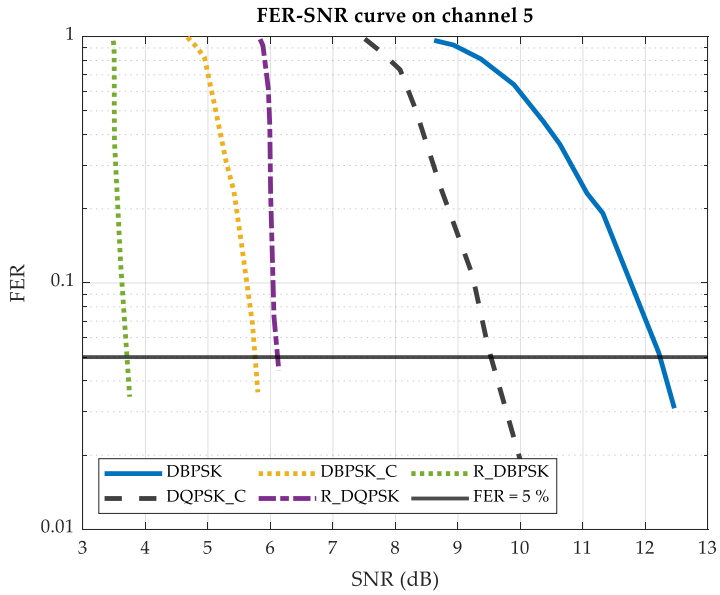

Figure 127. FER-SNR curve on channel 5 for different modulations when the alarm clock connected to point C

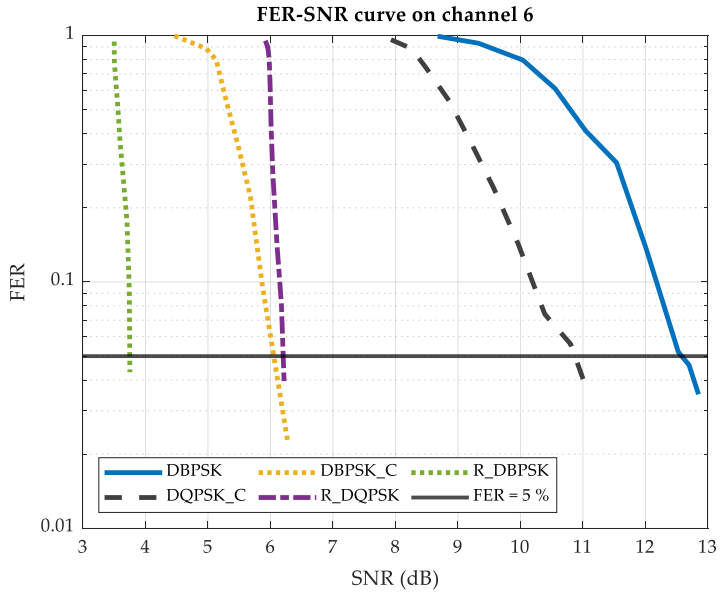

Figure 128. FER-SNR curve on channel 6 for different modulations when the alarm clock connected to point C

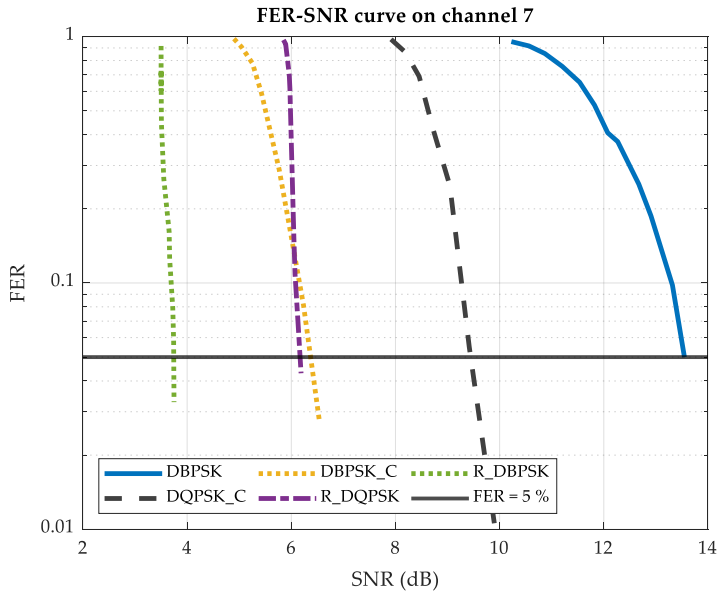

Figure 129. FER-SNR curve on channel 7 for different modulations when the alarm clock connected to point C

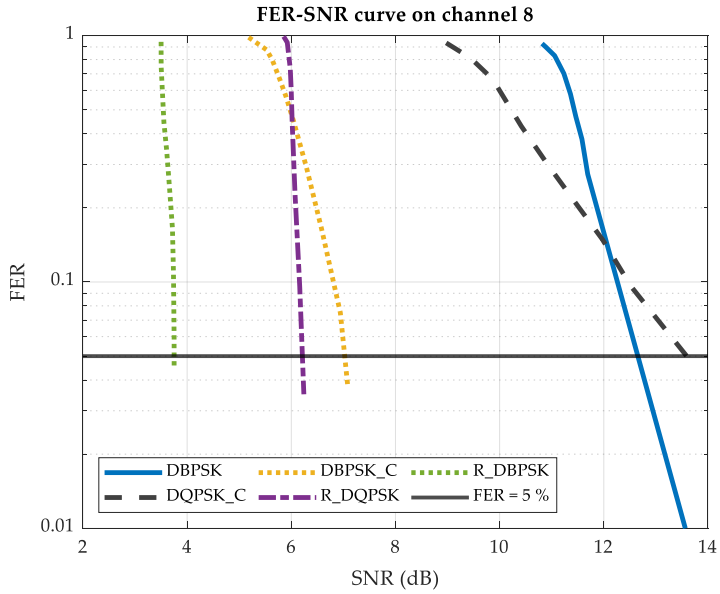

Figure 130. FER-SNR curve on channel 8 for different modulations when the alarm clock connected to point C

C.7. Analysis of the influence of the location of the time-variant load. FER-SNR curves

C.7.1. LEDs

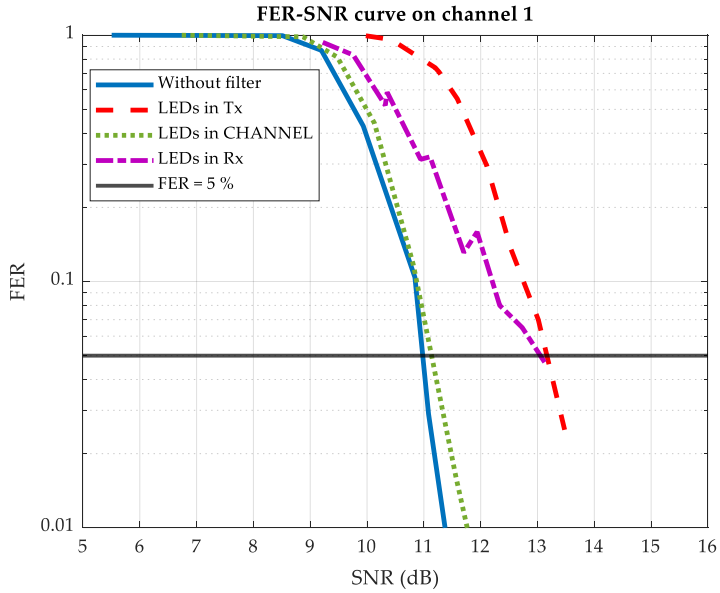

Figure 131. FER-SNR curve on channel 1 for DBPSK without filter and when the LEDs are connected in Tx, the Channel and Rx

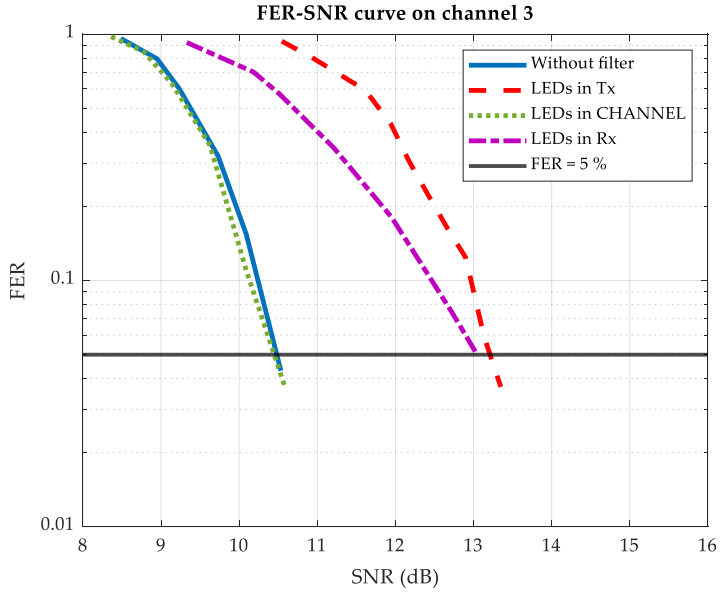

Figure 132. FER-SNR curve on channel 3 for DBPSK without filter and when the LEDs are connected in Tx, the Channel and Rx

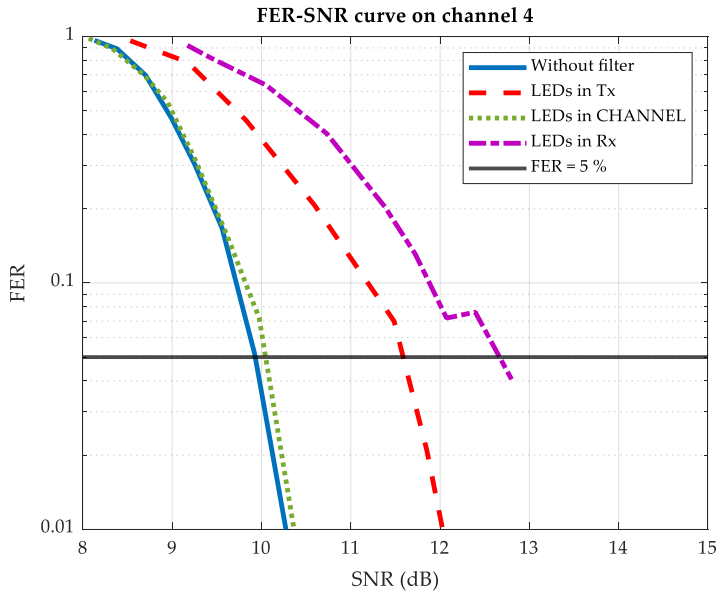

Figure 133. FER-SNR curve on channel 4 for DBPSK without filter and when the LEDs are connected in Tx, the Channel and Rx

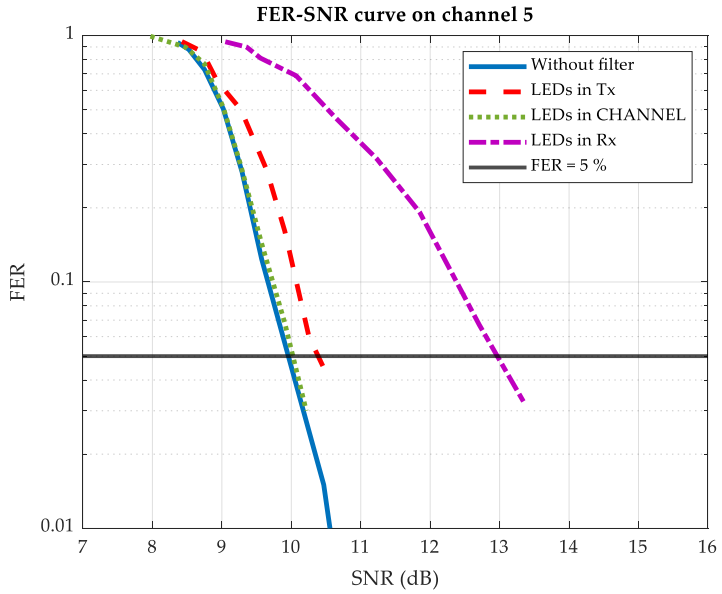

Figure 134. FER-SNR curve on channel 5 for DBPSK without filter and when the LEDs are connected in Tx, the Channel and Rx

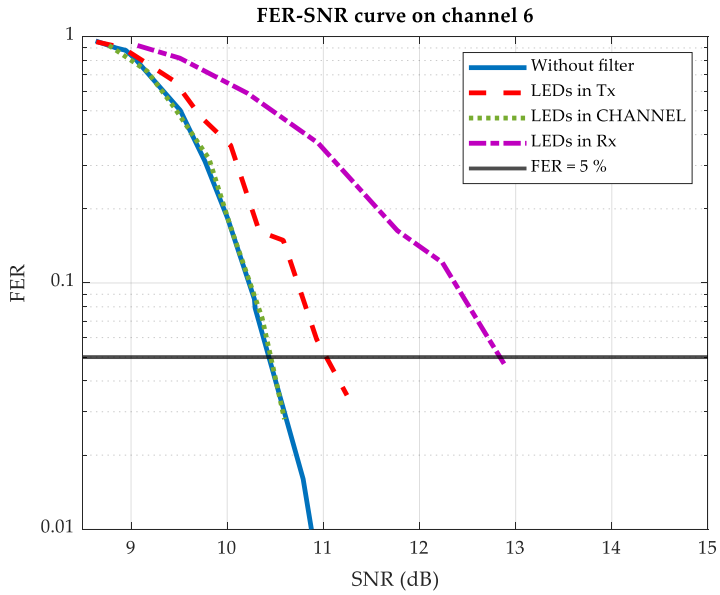

Figure 135. FER-SNR curve on channel 6 for DBPSK without filter and when the LEDs are connected in Tx, the Channel and Rx

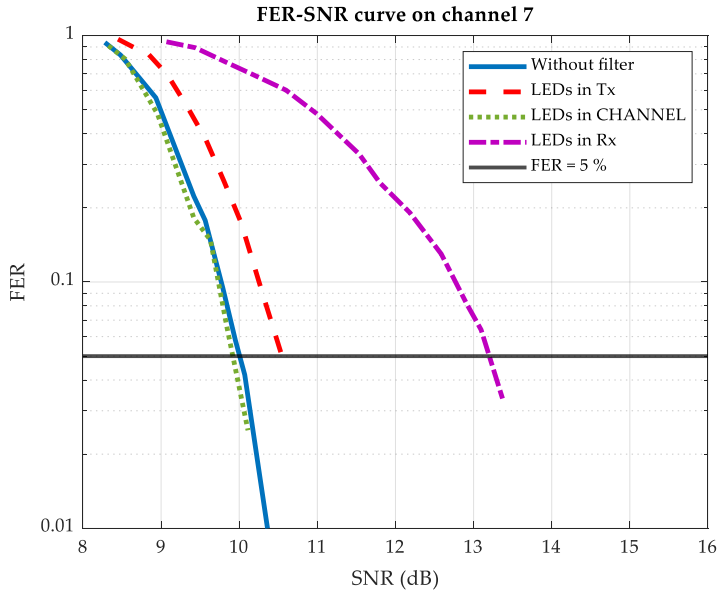

Figure 136. FER-SNR curve on channel 7 for DBPSK without filter and when the LEDs are connected in Tx, the Channel and Rx

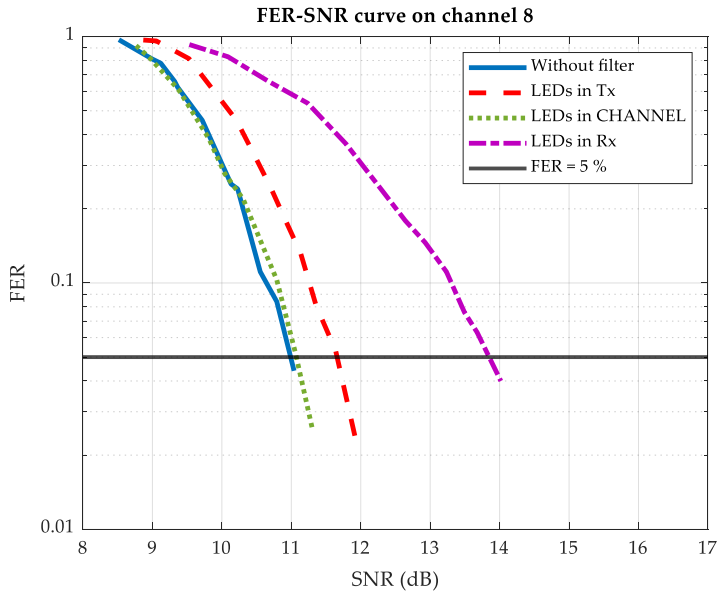

Figure 137. FER-SNR curve on channel 8 for DBPSK without filter and when the LEDs are connected in Tx, the Channel and Rx

C.7.2. Alarm clock

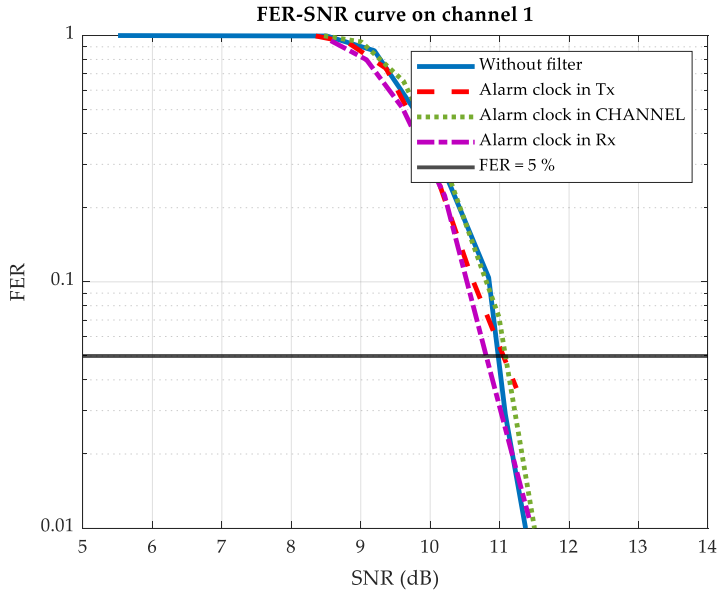

Figure 138. FER-SNR curve on channel 1 for DBPSK without filter and when the alarm clock is connected in Tx, the Channel and Rx

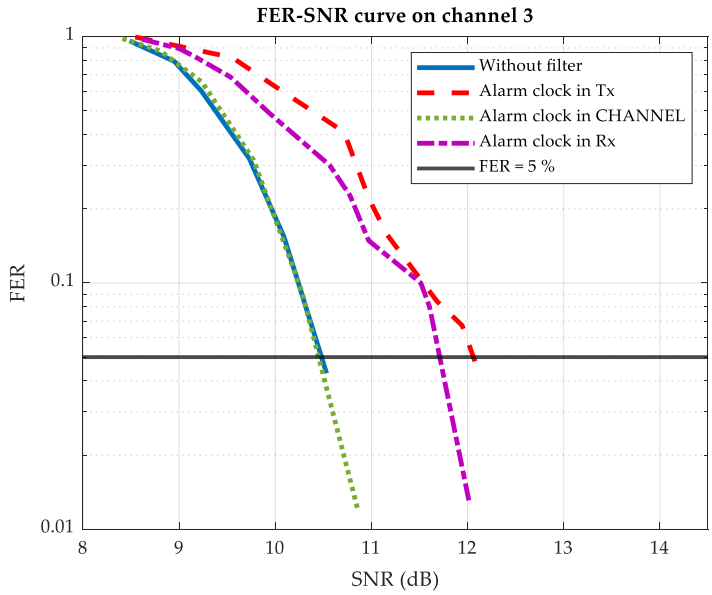

Figure 139. FER-SNR curve on channel 3 for DBPSK without filter and when the alarm clock is connected in Tx, the Channel and Rx

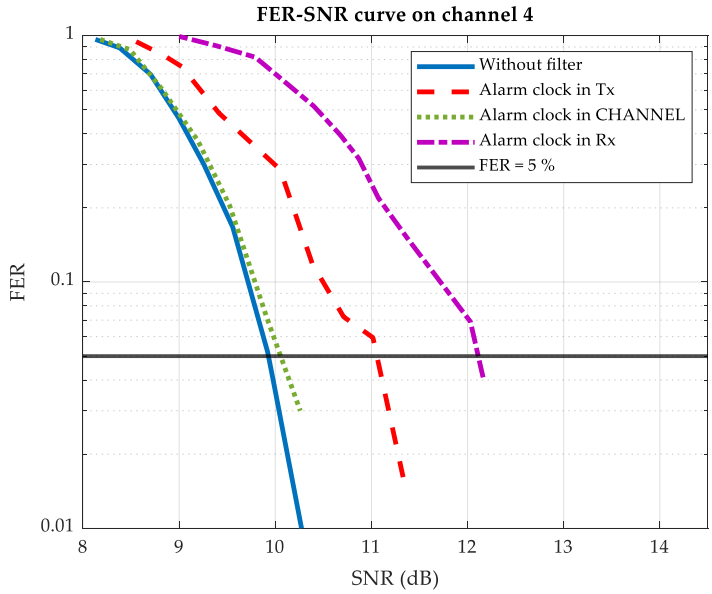

Figure 140. FER-SNR curve on channel 4 for DBPSK without filter and when the alarm clock is connected in Tx, the Channel and Rx

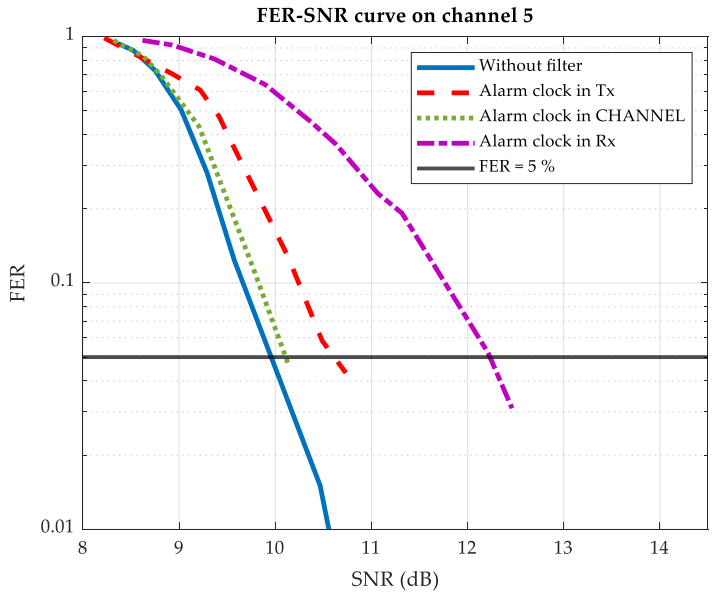

Figure 141. FER-SNR curve on channel 5 for DBPSK without filter and when the alarm clock is connected in Tx, the Channel and Rx

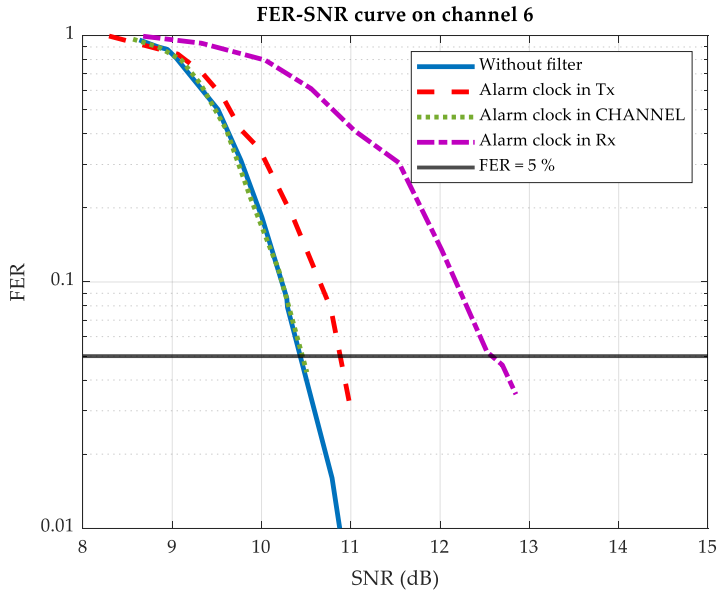

Figure 142. FER-SNR curve on channel 6 for DBPSK without filter and when the alarm clock is connected in Tx, the Channel and Rx

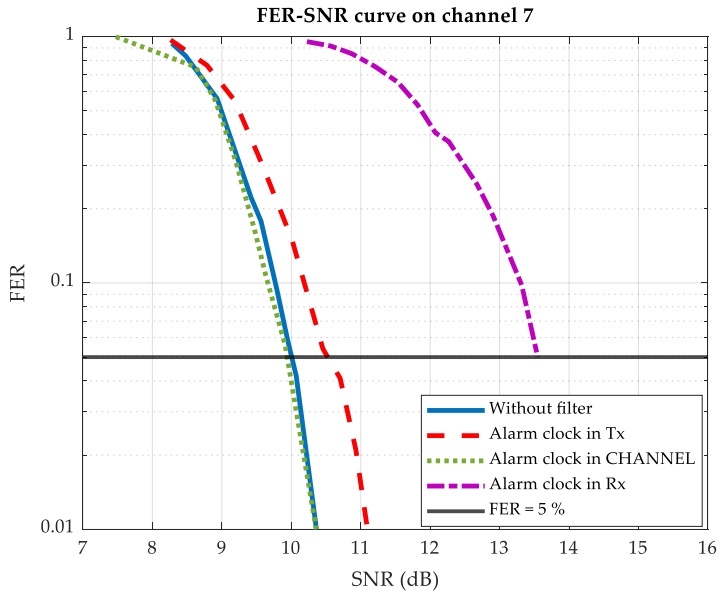

Figure 143. FER-SNR curve on channel 7 for DBPSK without filter and when the alarm clock is connected in Tx, the Channel and Rx

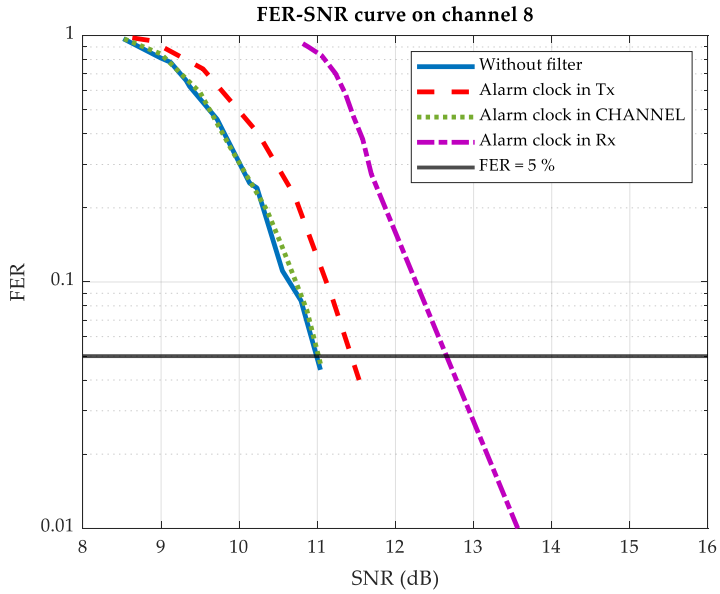

Figure 144. FER-SNR curve on channel 8 for DBPSK without filter and when the alarm clock is connected in Tx, the Channel and Rx